

# FOLIA

# VETERINARIA

The scientific journal of the  
UNIVERSITY OF VETERINARY MEDICINE AND  
PHARMACY IN KOŠICE — Slovakia

ISSN 0015-5748  
eISSN 2453-7837



1  
LXI • 2018



**FOLIA VETERINARIA** is a scientific journal issued by the University of Veterinary Medicine and Pharmacy in Košice, Komenského 73, 041 81 Košice, Slovakia. The journal is published quarterly in English (numbers 1—4) and distributed worldwide.

Editor-in-Chief: *Jana Mojžišová*

Deputy/Managing Editor: *Juraj Pistl*

Editorial Advisory Board: *Bíreš, J.* (Košice, Slovakia), *Celer, V.* (Brno, Czechia), *Faix, Š.* (Košice, Slovakia), *Fedoročko, P.* (Košice, Slovakia), *Kolacz, R.* (Wroclaw, Poland), *Novák, M.* (Bratislava, Slovakia), *Paulsen, P.* (Vienna, Austria), *Pechová, A.* (Brno, Czechia), *Večerek, V.* (Brno, Czechia), *Vorlová, L.* (Brno, Czechia)

Editors: *Faixová, Z., Kovalkovičová, N., Kundriková, L., Nagy, J., Nagy, O., Petrovová, E., Ševčíková, Z., Tomko, M., Trbolová, A., Vargová, M.* — technical editor, (Košice, Slovakia)

Contact: tel.: +421 915 984 669  
e-mail: [folia.veterinaria@uvlf.sk](mailto:folia.veterinaria@uvlf.sk)

Electronic Publisher: De Gruyter Open, Bogumila Zuga 32A, 01-811 Warsaw, Poland

ISSN 2453-7837 on-line  
ISSN 0015-5748 print  
EV 3485/09

Publisher's identification number: IČO 00397474

March 2018

# FOLIA VETERINARIA

PUBLISHED BY  
THE UNIVERSITY OF VETERINARY MEDICINE AND PHARMACY IN KOŠICE  
SLOVAKIA



Folia Veterinaria  
Vol. 62, 1, 2018

VYDÁVA  
UNIVERZITA VETERINÁRSKEHO LEKÁRSTVA A FARMÁCIE V KOŠICIACH  
2018

# FOLIA VETERINARIA, 62, 1, 2018

## CONTENTS

<b>FLEŠÁROVÁ, S., MAŽENSKÝ, D.:</b> MACROSCOPIC STUDY OF CELIAC, CRANIAL MESENTERIC AND CAUDAL MESENTERIC ARTERIES IN THE EUROPEAN HARE .....	5
<b>MARETTOVÁ, E., MARETTA, M.:</b> IMMUNOHISTOCHEMICAL STUDY OF THE GOAT <i>DUCTUS DEFERENS</i> .....	11
<b>OKOH, G. R., KAZEEM, H. M., KIA, G. S. N., MAILAFIA, S.:</b> EVALUATION OF ENZYME LINKED IMMUNO-SORBENT ASSAY AND RAPID IMMUNO-DIAGNOSTIC TEST FOR RABIES ANTIGEN DETECTION IN ARCHIVED DOG BRAIN TISSUES .....	18
<b>NOWAKOWICZ-DĘBEK, B., WLAZŁO, Ł., BIS-WENCEL, H., HROMADA, R., ŠMIECH, A., SASAKOVA, N., ZOŇ, A.:</b> ADDITION OF DRIED BLOOD PLASMA TO FEED OF MINKS DURING LACTATION AND REARING OF KITS .....	25
<b>DANIELOVÁ, P., KORYTÁR, L., CSANK, T.:</b> AVIFAUNA OF LAKE GEČA — PILOT FAUNISTIC AND SEROLOGICAL STUDY.....	32
<b>KANTA, M., BEŇOVÁ, K.:</b> MONITORING OF <sup>137</sup> CS AND <sup>40</sup> K IN THE LEVICE DISTRICT, SOUTHERN SLOVAKIA .....	38
<b>TKÁČOVÁ, Z., KÁŇOVÁ, E., JIMÉNEZ-MUNGUÍA, I., ČOMOR, L., ŠIROCHMANOVÁ, I., Bhide, K., Bhide, M.:</b> CROSSING THE BLOOD-BRAIN BARRIER BY NEUROINVASIVE PATHOGENS.....	44
<b>KÁŇOVÁ, E., JIMÉNEZ-MUNGUÍA, I., ČOMOR, L., TKÁČOVÁ, Z., ŠIROCHMANOVÁ, I., Bhide, K., Bhide, M.:</b> THE ROLE OF MENINGOCOCCAL PORIN B IN PROTEIN-PROTEIN INTERACTIONS WITH HOST CELLS.....	52
<b>ŠIROCHMANOVÁ, I., ČOMOR, L., KÁŇOVÁ, E., JIMÉNEZ-MUNGUÍA, I., TKÁČOVÁ, Z., Bhide, M.:</b> PERMEABILITY OF THE BLOOD-BRAIN BARRIER AND TRANSPORT OF NANOBODIES ACROSS THE BLOOD-BRAIN BARRIER .....	59
<b>JIMÉNEZ-MUNGUÍA, I., PULZOVÁ, L., Bhide, K., ČOMOR, L., KÁŇOVÁ, E., TOMEČKOVÁ, Z., ŠIROCHMANOVÁ, I., Bhide, M.:</b> CONTRIBUTION OF PILI OF <i>S. PNEUMONIAE</i> IN THE ONSET OF MENINGITIS .....	67



## MACROSCOPIC STUDY OF CELIAC, CRANIAL MESENTERIC AND CAUDAL MESENTERIC ARTERIES IN THE EUROPEAN HARE

Flešárová, S., Maženský, D.

Department of Anatomy, Histology and Physiology  
University of Veterinary Medicine and Pharmacy, Komenského 73, 041 81 Košice  
Slovakia

slavka.flesarova@uvlf.sk

### ABSTRACT

The aim of this paper was to describe the branching schema of the ventral branches of the abdominal aorta: the *a. celiaca*, the *a. mesenterica cranialis* and the *a. mesenterica caudalis*. The study was carried out on nine adult European hares using the corrosion cast technique. After the euthanasia, the vascular network was perfused with saline. Batson's corrosion casting kit No. 17 was used as a casting medium. After polymerisation of the medium, the maceration was carried out in KOH solution. In all specimens, the first branch originating from the *a. celiaca* was the *a. lienalis*. The *a. hepatica* was present as the second branch in four cases and as the third branch also in four cases. The first branch of the *a. mesenterica cranialis* was the *a. colica media* in seven cases. The second branch was represented by the *a. pancreaticoduodenalis caudalis* also in seven cases. Two *aa. jejunales* originated as the third branch. In seven cases, the fourth branch formed the *truncus jejunalis* and the fifth branch the *a. ileocecalis*. The *a. mesenterica caudalis* had a uniform arrangement in all of the specimens. The results enabled

us to conclude that there was higher variability of the branching pattern of the *a. celiaca* in comparison with the *a. mesenterica cranialis* and the *a. mesenterica caudalis* in the European hare.

**Key words:** *a. celiaca*; *a. mesenterica caudalis*; anatomical study; *a. mesenterica cranialis*; European hare

### INTRODUCTION

Anatomical studies dealing with blood vessels supplying the visceral organs of the abdominal cavity are very important. They help to better understand the arrangement of the principal intraabdominal arteries, their variations and anomalies and to avoid the obstruction of blood vessels in different clinical and pathological conditions as well as in surgical procedures [12].

A detailed knowledge of the variations in the arterial system of the visceral organs inside the abdominal cavity is essential in surgical and radiological anatomy. The high possibility of gastrointestinal disturbances caused by differ-

ent pathological agents requiring rapid diagnosis and surgical intervention, makes the knowledge of vascular variations an especially important factor [11].

The anatomical pattern of the branches arising from the ventral surface of the abdominal aorta in the domesticated rabbit have been described in detail in many different studies [1, 2, 4, 5, 6, 7, 8, 10, 12]. Despite the high occurrence of the European hare as a wild animal in Europe, the detailed knowledge of its arterial system is still lacking in the literature.

The aim of our study was to describe the arrangement and distribution of the branches originating from, the *a. celiaca*, the *a. mesenterica cranialis* and the *a. mesenterica caudalis* in the European hare.

## MATERIALS AND METHODS

This study was carried out on 9 adult European hares (*Lepus Europaeus*, L. 1758, age 140 days). We used hares (obtained from ISFA APRC, Nitra, Slovak Republic) of both sexes (female n=5; male n=4) weighing between 2.5–3.2 kg in an accredited experimental laboratory of the University of Veterinary Medicine and Pharmacy in Košice, Slovakia. The animals were kept in cages under standard conditions (temperature 15–20 °C, relative humidity 45 %, 12-hour light period), and fed with a granular feed mixture (O-10 NORM TYP, Spišské krmne zmesi, Spišské Vlachy, Slovakia). The drinking water was available to all animals *ad libitum*. Thirty minutes before sacrifice by intravenous administered of embutramide (T-61, 0.3 ml.kg<sup>-1</sup>), the animals were injected intravenously with heparin (50 000 IU.kg<sup>-1</sup>). Immediately after euthanasia, the vascular network was perfused with a physiological solution. During manual injection through the ascending aorta, the right heart atrium was opened in order to lower the pressure in the vessels which enabled an optimal injection distribution. 50 ml of Batson's corrosion casting kit No. 17 (Dione, České Budějovice, Czechia) was used as the casting medium. The maceration was carried out in 2–4 % KOH solution for a period of 5 days at 60–70 °C. The study was carried out under the authority decision No. 2647/07-221/5.

## RESULTS

The *a. celiaca*, the first unpaired artery from the ventral surface of the abdominal aorta is intended for the blood supply to the spleen, stomach, liver, pancreas, omentum and partly the duodenum. It was directed to the left and caudolaterally.

The *a. celiaca* gave off three branches in six cases and four branches in three cases (Fig. 1). In all of the cases, the first branch arising from the *a. celiaca* was the *a. lienalis* (Fig. 1). The second branch was represented by the *a. hepatica* in four cases, by the *a. gastrica sinistra* in two cases, by a common trunk for the *a. gastrica dextra* and the *a. gastrica sinistra* in two cases and by the *a. gastrica dextra* in one case (Fig. 1). The *a. hepatica* was the third branch in four cases, a common trunk for the *a. gastrica dextra* and the *a. gastrica sinistra* in three cases, the *a. gastrica dextra* in one case and the *a. gastrica sinistra* also in one case (Fig. 1). A doubled *a. gastrica dextra* was present in one case as the fourth branch. Also, in one case was found as the fourth branch: the *a. hepatica* (Fig. 1) and the *a. gastrica sinistra*.

In four cases, the *a. lienalis* gave off the *r. gastricus dexter* as the first branch. In one case, the *r. gastricus dexter* originated directly from the lateral surface of the *aorta abdominalis* cranially to the origin of the *a. celiaca*. The spleen was supplied by small branches arising from the *a. lienalis*; two branches in three cases, three in four cases and four in two cases. The *aa. gastricae breves* had an opposite direction to the previous branches. They participated on supplying blood to the gastric wall in number of one in one case, of two in four cases, of three in three cases and in number of four in one case. The main continuation of *a. lienalis* was the *a. gastroepiploica sinistra* running along the greater curvature of stomach and anastomosing with the *a. gastroepiploica dextra* from the opposite direction. The *a. gastrica sinistra* supplied the wall of the stomach by small branches which consisted of two branches in one case, three in two cases, four in four cases and five in two cases. The number of small gastric branches arising from the *a. gastrica dextra* was three branches in three cases, two and five in two cases, and four in one case. In the case of the presence of the doubled *a. gastrica dextra*, each of them gave off two branches to the wall of the stomach. In two cases, the *a. hepatica* sent as the first branch, the *a. gastrica dextra*. After the origin of this artery, the *a. hepatica* entered the liver through the *porta hepatis*. Its continuation was represented by the

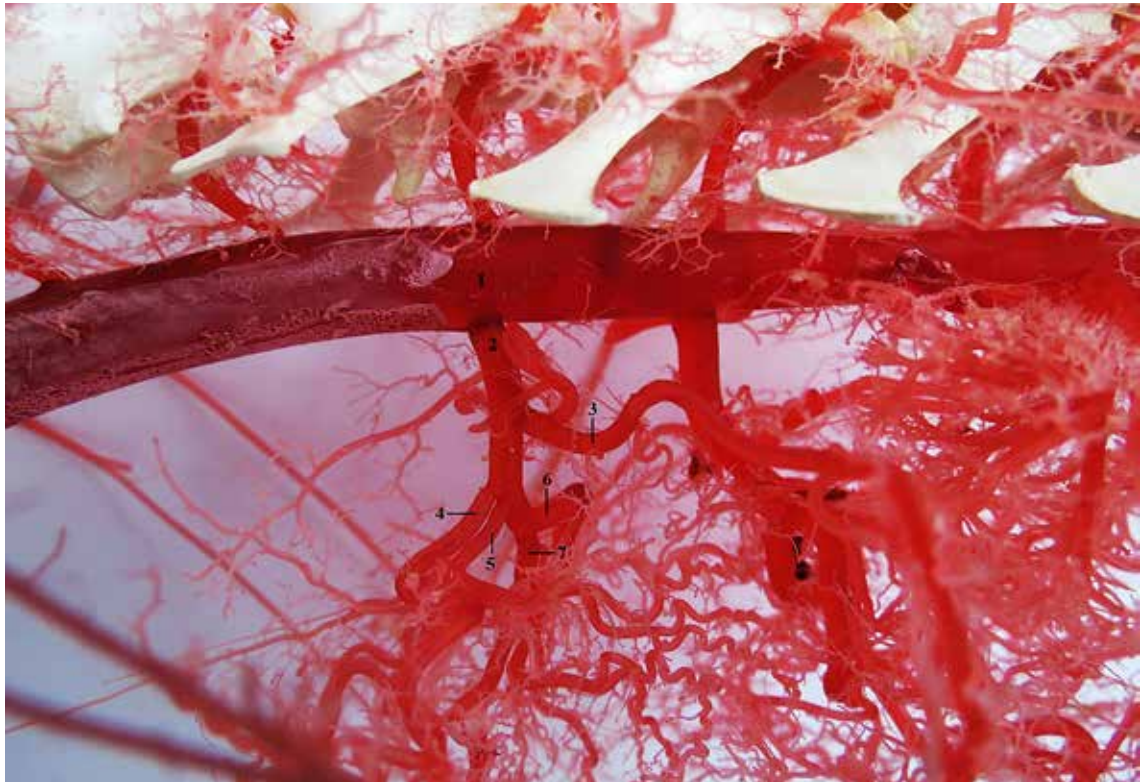


**Fig. 1. Branching pattern of the *a. celiaca***  
 1 — *aorta abdominalis*; 2 — *a. celiaca*; 3 — *a. lienalis*; 4 — *a. gastrica dextra*; 5 — *a. gastrica sinistra*  
 6 — *a. hepatica*; 7 — *a. gastroduodenalis*. Macroscopic image, lateral view

*a. gastroduodenalis* which was divided terminally into the *a. gastroepiploica dextra* and the *a. pancreaticoduodenalis cranialis*. In the rest of the cases, the *a. hepatica* ultimately divided into only two branches: the *a. gastroepiploica dextra* and the *a. pancreaticoduodenalis cranialis*.

The *a. mesenterica cranialis* which supplied the pancreas, small intestine, cecum, ascending colon and transverse colon, had five branches in seven cases (Fig. 2) and six branches in two cases. The first branch was represented by the *a. colica media* in seven cases (Fig. 2) and by the *a. pancreaticoduodenalis caudalis* in two cases. The *a. colica media* originated as the second branch in two cases and the *a. pancreaticoduodenalis caudalis* in seven cases (Fig. 2). The *aa. jejunales* originated as the third branch in different numbers: one in one case (Fig. 2), two in five cases, three in two cases and four in one case. The fourth branch was formed in one case by a single *a. colica dextra* and also in one case by a doubled *a. colica dextra*. In seven cases, the fourth branch was the *truncus jejunalis* which gave off the *aa. jejunales* (Fig. 2). They appeared as ten branches in one case, twelve in two cases and thirteen in four cases. The

*truncus jejunalis* constituted the fifth branch in two cases with ten and thirteen *aa. jejunales*. In seven cases, the fifth branch was represented by the *a. ileocolica* which gave off: *a. cecalis dorsalis*, *a. cecalis ventralis*, *a. appendicularis*, and a single *a. colica dextra* in two cases or doubled *a. colica dextra* in five cases (Fig. 2). The sixth branch was formed by the *a. ileocolica* with branches: *a. cecalis dorsalis*, *a. cecalis ventralis*, *a. appendicularis* and doubled *a. colica dextra*.

The *a. mesenterica caudalis* as the latest unpaired and ventrally originating branch from aorta abdominalis was in all cases divided into two branches. It supplied the descending colon and rectum. The cranially directed *a. colica sinistra* was smaller in diameter than the stouter and caudally directed *a. rectalis cranialis*. The above described arrangement was found in all of the cases (Fig. 3).

## DISCUSSION

The domesticated rabbit is one of the species most frequently used in the study of various diseases associated

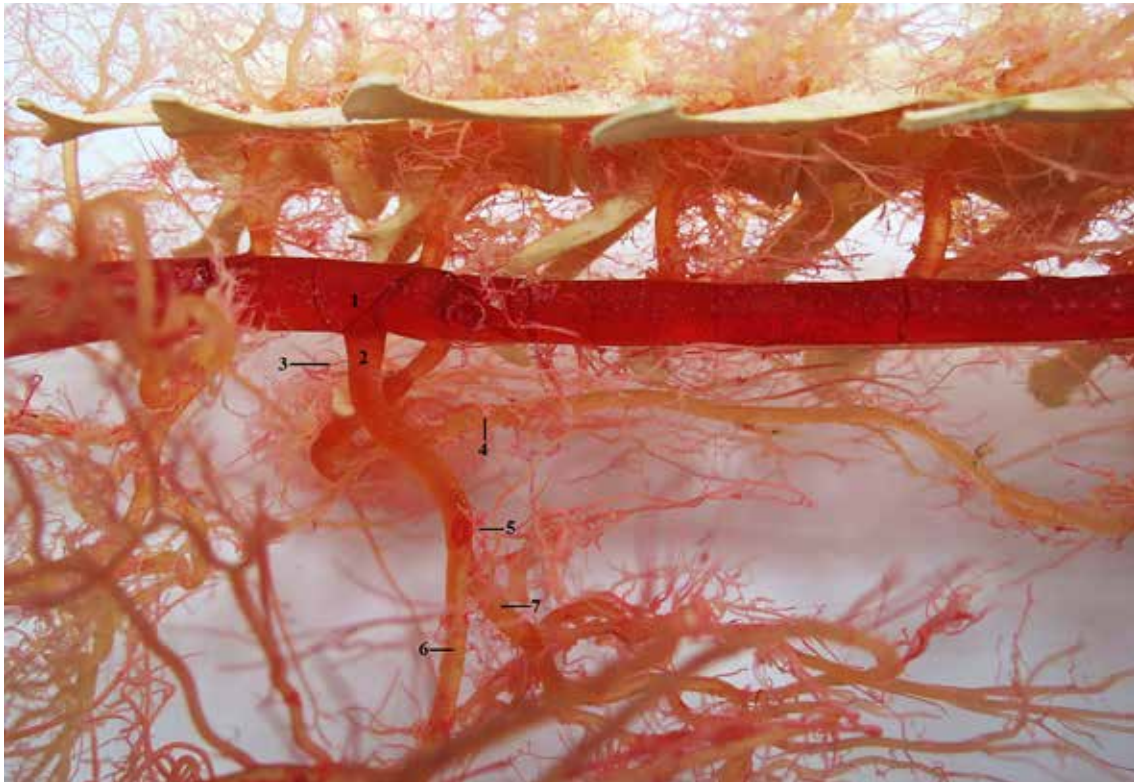


**Fig. 2. A. mesenterica cranialis and its main branches**

1 — *aorta abdominalis*; 2 — *a. mesenterica cranialis*; 3 — *a. colica media*; 4 — *a. pancreaticoduodenalis caudalis*  
5 — *a. jejunalis*; 6 — *truncus jejunalis*; 7 — *a. ileocecalis*. Macroscopic image, lateral view



**Fig. 3. Arrangement of the *a. mesenterica caudalis***

1 — *aorta abdominalis*; 2 — *a. mesenterica caudalis*; 3 — *a. colica sinistra*; 4 — *a. rectalis cranialis*  
Macroscopic image, ventral view

with the gastrointestinal tract as well as in the study of pharmacology, toxicology and surgery [12]. For this reason, the arterial system of its abdominal viscera has been described more in detail [1, 2, 5, 7, 8]. The studies dealing with the variations of the arterial system in the wild European hare are much rarer [3, 9].

In the study of the arterial system of the New Zealand white rabbit, a uniform division of the *a. celiaca* into two trunks was described. The first trunk was common for the *a. hepatica*, the *a. gastroduodenalis* and the *a. gastrica dextra*. The second trunk was divided into the *a. lienalis* and the *a. gastrica sinistra* [10]. Abidu-Figueiredo et al. [1] described in the domesticated rabbit as the first branch in all cases, the *a. lienalis*, which is consistent with our findings. The *a. hepatica* as the first branch of the *a. celiaca* was designated by Popesko et al. [10]. The *a. lienalis* of the domesticated rabbits sends one to five branches to the spleen [1], while in the European hare two to four branches to the spleen. In the hare, we found one to four *aa. gastricae breves*, but in the domesticated rabbit there were one to five [1]. In the hare and rabbit, the number of small branches with origins from the *a. gastrica sinistra* and supplying the wall of the stomach was the same [1]; except in the rabbit, these small branches originated off of the *a. gastroduodenalis* and the *a. hepatica* [1]. In the hare, the *a. gastrica sinistra* was intended only for the lesser curvature of the stomach.

The *a. pancreaticoduodenalis caudalis*, as the first branch originating from the *a. mesenterica cranialis* in the rabbit, was found in all cases [2, 12] or in more than one half of the cases [5, 8]. In 6.7% of the cases, the *a. pancreaticoduodenalis caudalis* was duplicated [8]. A single or doubled *a. pancreaticoduodenalis caudalis* was described by Kigata et al. [7]. In the hare, we found the *a. pancreaticoduodenalis caudalis* as the first branch in two cases. In the hare, the *a. colica media* originated as the second branch in two cases. In the rabbit, the *a. colica media* represented the second branch in all cases [2, 12], in more than one half of cases [5], or it formed the first branch [8]. Kigata et al. [7] found one to three *a. colica media* in the rabbit. In 80% of the male and 86.67% of female rabbits, one single *a. jejunalis* was the third branch [5]. In the hare, there were one to four *a. jejunalis* originating from the *a. mesenterica cranialis* before its terminal division. In the hare, the fourth branch was formed in one case by a single *a. colica dextra*, in one case by a doubled *a. colica dextra* and in seven cases by the *truncus jejunalis*. The terminal division of the *a. mes-*

*enterica cranialis* into the *truncus jejunalis* and the *a. ileocolica* in the rabbit was in the literature more common [2, 8, 12] and was the same as in the hare. In the rabbit, from the *truncus jejunalis* originated the *aa. jejunales* in different numbers: 18—20 [12], 17—18 [5], 11—23 [8] and 11—17 [7]. One to six *aa. jejunales* arose directly from the *a. mesenterica cranialis* [8]. In the hare, the *aa. jejunales* originating from the *truncus jejunalis* were present in number from 10 to 13. The division of the *a. ileocolica* from which originated branches supplying the ileum, cecum, appendix and proximal colon was very variable in the hare and the rabbit [5, 7, 8, 12].

In the hare and rabbit, the arrangement of the *a. mesenterica caudalis* showed the same schema: a slenderer *a. colica sinistra* in the cranial direction and a stouter *a. rectalis cranialis* in the caudal direction [1, 5, 12].

## CONCLUSIONS

There was a higher variability of the branching pattern of the *a. celiaca* in comparison with the *a. mesenterica cranialis* and the *a. mesenterica caudalis* in the European hare. The distribution patterns of the *a. celiaca* and the *a. mesenterica cranialis* in the hare are highly specialized in this species. Such specialization should always be considered when performing abdominal surgery.

## REFERENCES

1. Abidu-Figueiredo, M., Xavier-Silva, B., Cardinot, T.M., Babinski, M.A., Chagas, M.A., 2008: Celiac artery in New Zealand rabbit: Anatomical study of its origin and arrangement for experimental research and surgical practice. *Pesq. Vet. Bras.*, 28, 237—240.
2. Ahasan, A.S.M.L., Islam, M.S., Kabria, A.S.M.G., Rahman, M.L., Hassan, M.M., Uddin M., 2012: Major variation in branches of the abdominal aorta in New Zealand White rabbit (*Oryctolagus Cuniculus*). *Intern. J. Nat. Sci.*, 2, 91—98.
3. Brudnicki, W., Kirkillo-Stacewicz, K., Skoczylas, B., Nowicki, W., Jablonski, R., Brudnicki, A., Wach, J., 2015: The arteries of the brain in hare (*Lepus europaeus Pallas*, 1778). *Anat. Rec.*, 298, 1774—1779.
4. Craigie, E. H., 1948: *Bensley's Practical Anatomy of the Rabbit*. Blakiston Company, Philadelphia, 325—326.

5. Estruc, T. M., Nascimento, R. M., Siston, N. M., Mencialha, R., Abidu-Figueiredo, M., 2015: Origin and main branches of the cranial and caudal mesenteric arteries in the New Zealand rabbit. *J. Morphol. Sci.*, 32, 143—148.
6. Jeican, I. I., Gheban, D., Socaciu, M., Toader, S., Ciuce, C., 2016: Experimental model of mixed intestinal infarction in rabbit. *Rev. Med. Chir. Soc. Med. Nat. Iasi*, 120, 592—603.
7. Kigata, T., Ikegami, R., Shibata, H., 2017: Macroscopic anatomical study of the distribution of the cranial mesenteric artery to the intestine in the rabbit. *Anat. Sci. Int.*, 93, 291—298.
8. Malinovský, L., Bednářová, Z., 1990: Variability of ramification of the *a. mesenterica cranialis* in the domestic rabbit (*Oryctolagus cuniculus f. domestica*). *Folia Morphol.*, 38, 283—292.
9. Mazensky, D., Flesarova, S., 2015: The arterial blood supply to the cervical spinal cord in European hare. *Biologia*, 70, 406—410.
10. Popesko, P., Rajtova, V., Horak, J., 1990: *Anatomic Atlas of Small Laboratory Animals I*. 1st edn., Příroda, Bratislava, 67—78.
11. Šulla, I., Lukáč, I., 2010: *Ischemic Damage of Spinal Cord in Experiment* (In Slovak). P. J. Šafárik University Press, Košice, 125 pp.
12. Uddin, M., Rahman, M. L., Alim, M. A., Ahasan, A. S. M. L., 2012: Anatomical study on origin, course and distribution of cranial and caudal mesenteric arteries in the White New Zealand rabbit (*Oryctolagus cuniculus*). *Intern. J. Nat. Sci.*, 2, 54—59.

Received September 12, 2017

Accepted November 9, 2017



## IMMUNOHISTOCHEMICAL STUDY OF THE GOAT *DUCTUS DEFERENS*

Marettová, E., Mareta, M.

Department of Anatomy, Histology and Physiology,  
University of Veterinary Medicine and Pharmacy, Komenského 73, 041 81 Košice  
Slovakia

elena.marettova@uvlf.sk

### ABSTRACT

*Ductus deferens* plays an important role in sperm transport and participates in the preservation of structure, maturation, and viability of sperm. In this study, we have immunohistochemically examined the *ductus deferens* in the goat. For immunohistochemical study the following monoclonal antibodies were used: cytokeratin 18,  $\alpha$ -smooth muscle actin ( $\alpha$ -SMA), vimentin and elastin. Morphologically, three distinct layers were identified in the goat *ductus deferens* — tunica mucosa, tunica muscularis and tunica adventitia. The epithelium of the mucosa was intensely stained with cytokeratin 18 (CK 18). The fibroblasts in the *lamina propria* and blood capillaries in the muscle layer showed positive reaction for vimentin. A positive reaction for  $\alpha$ -SMA was observed in the smooth muscle cells of the tunica muscularis in the internal, middle and outer sublayers. An intense positive reaction for  $\alpha$ -SMA was observed in the wall of the blood vessels. Elastic fibers in the form of a loose meshwork were present in all three layers. The high density of elastic fibers were found in the tunica adventitia.

**Key words:** *ductus deferens*; goat; immunohistochemical study

### INTRODUCTION

The *ductus deferens* is a channel serving to transport sperm from the epididymis to the ejaculatory duct. Two main structures participate in this transport: epithelium and smooth muscle. Epithelial cells lining the luminal surface provides the environment for the transported sperm, whereas the thick smooth muscle coat, by its peristaltic action, is responsible for the pumping action during ejaculation [20, 22].

Studies relating the the structure of the *ductus deferens* have been made mainly in man [12, 15, 18]. In animals, histological studies have been made in the rat [8] and in the rabbit [6]. Murakami et al. [13] used scanning and transmission electron microscopy to study the ampullary region of the dog vas deferens with special reference to epithelial phagocytosis of spermatozoa. Various components of the wall of the *ductus deferens* were observed to be spe-

cifically arranged, compared with other organs of comparable organization [4, 9, 10]. Immunohistochemically, some studies were made on the *ductus deferens* in the donkey and water buffalo bull [3, 4]. Specific types of cytokeratins in the epithelial cells, and desmin in the muscular layers during the various phases of the development, growth, and involution of the human *ductus deferens* has been defined [18]. Francavilla et al. [7] reported on the distribution of actin, myosin and fibronectin during postnatal development of the epididymis and *ductus deferens* in the rat. In our work we have immunohistochemically examined the components of the wall of the goat *ductus deferens*.

## MATERIALS AND METHODS

Five adult goats, 35–43 kg b. w., age 2–4 years, clinically health were used in this study. The samples of the *ductus deferens* were dissected out in the slaughterhouse. Then, they were fixed in 10% buffered formalin and were processed for paraffin sectioning. Sections of 5 µm thick were stained with Harris haematoxylin and eosin for histological study. For immunohistochemical study the sections were pretreated with 3% H<sub>2</sub>O<sub>2</sub> in methanol to block endogenous peroxidase activity and preincubated with 2% goat serum

to mask unspecific binding sites. The sections were incubated with the primary antibodies [Tab.1] and washed in phosphate-balanced salt solution PBS). Afterwards, the sections were incubated with biotinylated secondary antibody for 45 min, washed in PBS, and finely incubated with avidin-biotin-peroxidase complex (ABC kits, Vector Laboratories, USA). The reaction product formation was achieved by incubating for 10 minutes at room temperature, using a mixture of an equal volume of 0.02% hydrogen peroxide and 0.1% 3,3'-diaminobenzidine tetrahydrochloride made in Tris buffer. For negative controls, the first antibody was substituted by PBS or by normal rabbit serum.

## RESULTS

### Light microscopic observations

In the goat *ductus deferens* three distinct layers were identified: tunica mucosa, tunica muscularis and tunica adventitia. The mucosa was made up of columnar pseudostratified epithelium and the *lamina propria*. The epithelium together with the subjacent *lamina propria* formed flat longitudinal mucosal folds. The tunica muscularis was made up of three sublayers—circular, longitudinal, and oblique layers. Fine inner layer consisted of smooth muscle

Tab. 1. Antibodies used in the study

Antibodies	Donor	Code	Isotype	Dilution	Source
<b>Cytokeratin 18</b>	Mouse	C 04	IgG1	1:20	Exbio
<b>Vimentin</b>	Mouse	1074	IgG1	1:50	Imunotech
<b>α-Smooth muscle actin</b>	Mouse	M 851	IgG2a	1:200	Dako
<b>Elastin</b>	Mouse	E 4013	IgG1	1:5000	Sigma

Table 2. Immunolocalization of different proteins in layers of the goat *ductus deferens*

	CK 18	Vim	SMA	EI
<b>Epithelium</b>	+++	–	–	–
<b>Lamina propria</b>	–	++	–	+
<b>Tunica muscularis</b>	–	+	+++	+
<b>Adventitia</b>	–	++	–	++

Reactivity: – —negative; +—weak; ++—moderate reactivity; +++—strong reactivity

cells arranged circularly. The middle layer contained bundles of smooth muscle cells arranged mainly circularly and helically. The outer longitudinal layer consisted of coarse bundles of smooth muscle cells arranged obliquely. The loose connective tissue of the adventitia diffusely merged with the surrounding supportive tissue of the spermatic cord.

### Immunohistochemical observations

Immunostaining revealed positive reactions for CK 18 in the lining epithelial cells of the mucosa in which differences in the reactivity were found. The apical cell membrane gave strong reaction the resting epithelial body displayed moderate reactivity [Fig. 1], whereas the basal cells were stained less intensely. The loose connective tissue of the mucosa was rich in fibroblasts positive for vimentin. The blood capillaries stained with vimentin, and were perforating the muscular coat and adventitia [Fig. 2]. The muscular coat with smooth muscle cells was stained by  $\alpha$ -SMA. More intense reaction was observed in the inner layer [Fig. 3]. Additionally,  $\alpha$ -SMA staining was seen in the smooth muscle cells of the blood vessels [Fig. 4]. The elastic fibres positively stained with elastin were distributed in all three layers: in the mucosa they formed fine loose net-

works, in the muscular layer elastic fibers surrounded the bundles of smooth muscle cells. A dense layer of elastic fibres was seen on the periphery of the muscular coat and in the tunica adventitia where the elastic fibers formed dense mesh works [Fig. 5]. A higher concentration of elastic fibers was found around the blood vessels.

### DISCUSSION

Comparative histological studies showed that the mucosa of *ductus deferens* from different animal species reveal some species-specific characteristics. The mucosa of the goat *ductus deferens* constitutes folds different from other animal species. In the rat, the mucosal folds are variable while in the rabbit the *ductus deferens* are characterized by a plethora of complex mucosal folds [9]. In the goat the mucosal folds were flat and the number of folds ranged from 2 to 3. Also, differences in the lining epithelium are found in various animal species. In the rabbit, the epithelium is simple cuboidal and columnar, in the donkey, it is high cuboidal, in the buffalo, it is low columnar pseudostratified, in the human it is tall columnar pseudostratified and pseudostratified columnar with stereocilia in the rat [9]. In the



**Fig. 1. Localisation of CK 18.**

The CK reaction was only confined to the the lining epithelium (EP) of the *tunica mucosa* and to basal cells. Intense immunoreaction was in the apical cell membrane

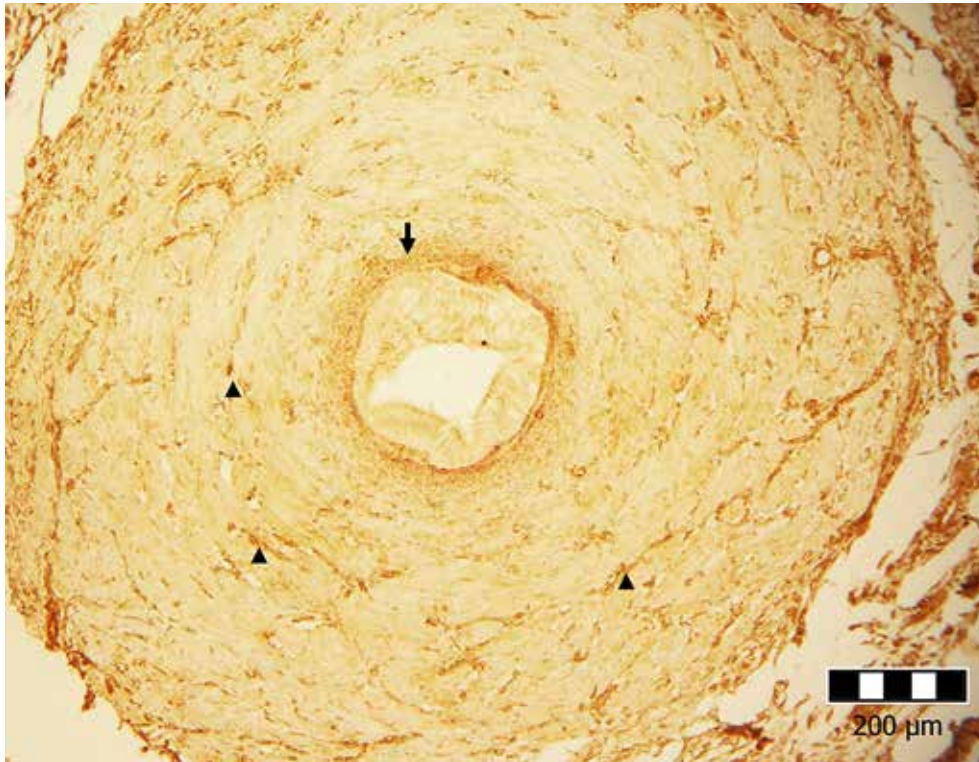


**Fig. 2. Localisation of vimentin**

Fibroblasts with positive reaction were located in the loose connective tissue of the mucosa (arrow). A positive reaction was confined to blood capillaries among the smooth muscle bundles of the muscular coat (arrowheads).

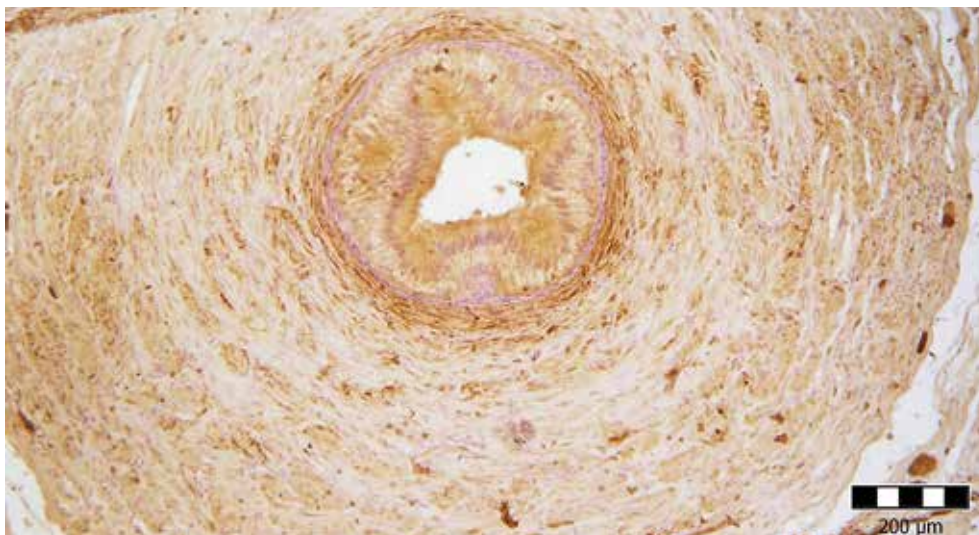


**Fig. 3. Localisation of  $\alpha$ -smooth muscle actin**

Smooth muscle cells of the inner layer of the muscular coat are intensely stained by  $\alpha$ -smooth muscle actin (arrow)

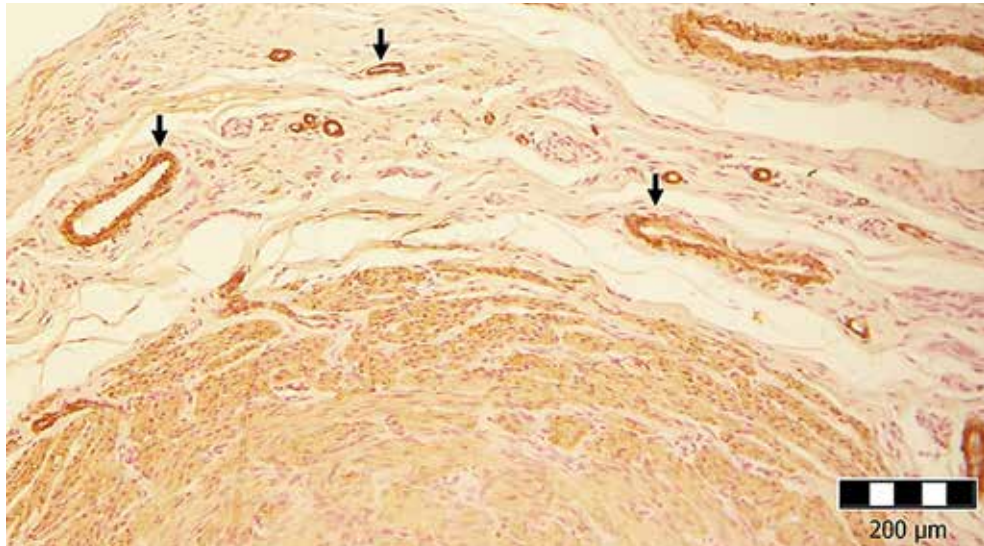


**Fig. 4. Localisation of  $\alpha$ -smooth muscle actin**  
Smooth muscle cells of the outer layer of the muscular coat (MC) and of blood vessels in the adventitia are stained by  $\alpha$ -smooth muscle actin (arrow)



**Fig. 5. Localisation of elastin.**  
Positively stained elastic fibres in the muscular layer are located between bundles of smooth muscle cells (arrow). A higher concentration of elastic fibres were on the periphery of outer muscle sublayer and *tunica adventitia* (EF)

goat the epithelium was found to be high pseudostratified. A three-layered muscularis and a serosa or an adventitia have been found in different mammals [10, 15].

Immunohistochemical studies reveal that most epithelia lining the human male reproductive tract, including those in the epididymis, *ductus deferens*, prostate gland, and seminal vesicle, synthesize CK 5, in addition to cytokeratins 7, 8, 18, and 19 [2]. In the ampulla of the *ductus deferens* of camel, the cytokeratin reaction was found in the pseudostratified columnar epithelium and in the secre-

tory columnar epithelium of the submucosal glands, where strong reaction was seen in the apical cytoplasm of columnar and basal cells of the secretory units [1]. The epithelium of the *ductus deferens* in rodents showed absorptive, synthetic and secretory activities [11, 20], thus providing an appropriate luminal environment for sperm before ejaculation. We found a higher concentration of CK 18 in the epithelial cells which may correspond with these activities. Recent studies suggest that the epithelium might modulate the contractility of smooth muscle. Ru an et al. [19]

reported, that ATP inhibition of the vas deferens smooth muscle contraction is epithelium dependent.

The *lamina propria* of the mucosa of the goat *ductus deferens* contained fibroblasts stained with vimentin and myofibroblasts stained with SMA. The myofibroblasts were found subepithelially in many mucosal surfaces throughout almost the whole of the gastrointestinal and genitourinary tracts. The myofibroblasts in other tubular organs have been identified by their expression of various intracellular cytoskeletal proteins — the microfilament  $\alpha$ -smooth muscle actin, type 3 intermediate filaments such as vimentin or desmin, and by the absence of epithelial cytokeratins [17]. Within the human bladder lamina propria there was found a layer of cells with the cytological characteristics of both fibroblasts and smooth muscle cells. This combination of features is characteristic of the myofibroblast [21].

In the tunica muscularis, a positive reaction to  $\alpha$ -SMA was observed in all three layers. A remarkable intense reaction was found in the inner layer, whereas in the middle layer, the reaction to  $\alpha$ -SMA remained only moderately stained. A positive reaction allowed for us to more easily distinguish the different orientation of the smooth muscle cells (SMC) in the middle layer. In the goat, like in other animal species, the SMCs of the middle layer showed an intermingled pattern of orientation. Some outer longitudinal layers penetrate into the circular layer to reenter the outer longitudinal layer and thus make helically arranged muscle loops as described by Williams et al. [22]. The circular profile predominates in the buffalo [4] and also in the goat *ductus deferens*. The outer longitudinal layer was distinct and consisted of coarse bundles of SMCs, particularly in the donkey [3]. In this animal species the muscularis was nearly two folds thicker than that in the buffalo [4]. The strong positive reaction of smooth muscle cells allowed to be seen the high concentration of blood vessels located mainly in the tunica adventitia.

Elastic tissue is a normal component in the genitourinary region [5, 14]. In the wall of the goat *ductus deferens* we found the elastic fibres in all three layers. Differences were seen in their density and arrangements. While in the *lamina propria*, we found elastic fibres as a loose network in the muscle layer where these were intimately associated with the smooth muscle cells. A similar distribution was observed in the *ductus deferens* of man and monkeys [14]. A high concentration of elastic fibers was seen in the wall of the blood vessels located in adventitia. In these areas, the

elastic fibers were observed also in the adult human *ductus deferens* [16]. The function of elastic fibers in the *ductus deferens* has not been fully explained. The role of elastic fibres in the lamina propria of the human *ductus deferens* has been described as providing elastic recoil of the ductus following contraction and dilatation at ejaculation and as participating in peristaltic movements [16]. We suppose that the elastic fibers in the goat *ductus deferens* play a similar role.

## CONCLUSIONS

The *ductus deferens* consists of three layers corresponding to other tubular organs. Immunohistochemically, CK 18 stained the lining epithelium, vimentin expression has been observed in fibroblasts and blood capillaries,  $\alpha$ -SMA was found in the smooth muscle cells of the muscular layer and blood vessels. Elastic fibers were distributed in all three layers with higher concentrations in the periphery of the organ.

## REFERENCES

1. **Abd-Elmaksoud, A. S., Ebada, S.M. Shoaib, M. B., 2012:** Localisation of cytokeratin and smooth muscle actin in the accessory genital glands of camels (*Camelus dromedarius*) during rutting and non-rutting seasons. *Bulg. J. Vet. Med.*, 15, 213—227.
2. **Achtstatter, T., Moll, R., Moore B., Franke, W.W., 1985:** Cytokeratin polypeptide patterns of different epithelia of the human male urogenital tract: immunofluorescence and gel electrophoretic studies. *J. Histochem. Cytochem.*, 33, 415—426.
3. **Alkafafy, M., 2009:** Some immuno-histochemical studies on the epididymal duct in the donkey (*Equus asinus*). *J. Vet. Anat.*, 2, 1—23.
4. **Alkafafy, M., Attia, H., Rashed, R., Kandiel, M., 2010:** Some comparative immunohistochemical studies on the *ductus deferens* in the Donkey (*Equus asinus*) and Water Buffalo Bull (*Bubalus bubalis*). *J. Vet. Anat.*, 3, 55—69.
5. **Augsburger, H. R., 1997:** Elastic fibres system of the female canine urethra. Histochemical identification of elastic, elaunin and oxytalan fibres. *Anat. Histol. Embryol.*, 26, 297—302.
6. **Flickinger, C. J., 1975:** Fine structure of the rabbit epididymis and vas deferens after vasectomy. *Biol. Reprod.*, 13, 50—60.
7. **Francavilla, S., Moscardelli, S., Properzi, G., DeMatteis, M. A., Scorza Barcellona, P. et al., 1987:** Postnatal develop-

- ment of epididymis and *ductus deferens* in the rat. A correlation between the ultrastructure of the epithelium and tubule wall, and the fluorescence-microscopic distribution of actin, myosin, fibronectin, and basement membrane. *Cell Tiss. Res.*, 249, 257—265.
8. Kennedy, S. W., Heidger, P. M., 1979: Fine structural studies of the rat vas deferens. *Anat. Rec.*, 194, 159—179.
  9. Khan, A. A., Zaidi, M. T., Faruqi, N. A., 2003: *Ductus deferens* — a comparative histology in mammals. *J. Anat. Soc. India*, 52, 163—165.
  10. Lohiya, N. K., Sharma, R. S., Ansari, A. S., Kumar, T. C., 1988: Structure of rete testis, vas efferens, epididymis and vas deferens of langur monkey (*Presbytis entellus entellus Dufresne*). *Acta. Eur. Fertil.*, 19, 167—173.
  11. Manin, M., Lecher, P., Martinez, A., Tournadre, S., Jean, C., 1995: Exportation of mouse vas deferens protein, a protein without a signal peptide, from mouse vas deferens epithelium: A model of apocrine secretion. *Biol. Reprod.*, 52, 50—62.
  12. Mcleod, D. G., Reynolds, D. G., Deamre, G. E., 1973: Some histological characteristics of the human vas deferens. *Invest. Urology*, 10, 338—341.
  13. Murakami, M., Nishida, T., Shiromoto M., Inokuchi, T., 1986: Scanning and transmission electron microscopy study of the ampullary region of the dog vas deferens with special reference to epithelial phagocytosis of spermatozoa. *Anat. Anz.*, 162, 289—296.
  14. Murakumo, M., Ushiki, T., Abe, K., Matsumura, K., Shinno, Y., Koyanagi, T., 1995: Three-dimensional arrangement of collagen and elastin fibers in the human urinary bladder: a scanning electron microscopic study. *J. Urol.*, 154, 251—256.
  15. Paniagua, R., Regadera, J., Nistal, M., Abauerrea, A., 1981: Histological, histochemical and ultrastructural variations along the length of the human vas deferens before and after puberty. *Acta Anat.*, 111, 190—203.
  16. Paniagua, R., Regadera, J., Nistal, M., Santamaria, L., 1983: Elastic fibres of the human *ductus deferens*. *J. Anat.*, 137, 467—476.
  17. Powell, D. W., Mifflin, R. C., Valentich, J. D., Crowe, S. E., Saada, J. I., West, A. B., 1999: Myofibroblasts. I. Paracrine cells important in health and disease. *Am. J. Physiol.*, 277, C 1—9.
  18. Regadera, J., Espana, G., Roias, M. A., Recio, J. A., Nistal, M., Suarez-Quian, C. A., 1997: Morphometric and immunocytochemical study of the fetal, infant, and adult human vas deferens. *J. Androl.*, 18, 623—636.
  19. Ruan, Y. C., Wang, Z., Du, J. Y., Zuo, W. L., Guo, J. H., Zhang, J. et al., 2008: Regulation of smooth muscle contractility by the epithelium in rat vas deferens: role of ATP-induced release of PGE2. *J. Physiol.*, 586, 4843—4857.
  20. Setchell, B. P., Brooks, D. E., 2006: Anatomy, vasculature, innervation, and fluids of the male reproductive tract. Chapter 17, Vol. 1. In Knobil, E., Neill, J. D. (Eds.): *The Physiology of Reproduction*, 3rd edn., Raven press, New York, 770—825.
  21. Wiseman, O. J., Fowler, C. J., Landon, D. N., 2003: The role of the human bladder *laminapropria myofibroblast*. *BJU Int.*, 91, 89—93.
  22. Williams, P. L., Banister, L. H., Berry, M. M., Collins, P., Dyson, M., Dussek, J. E., Ferguson, M. W. J., 1995: Gray's Anatomy. In *Reproductive System*, 38th edn., Churchill Livingstone, New York, 1855—1856.

Received September 18, 2017

Accepted December 5, 2017



## EVALUATION OF ENZYME LINKED IMMUNO-SORBENT ASSAY AND RAPID IMMUNO-DIAGNOSTIC TEST FOR RABIES ANTIGEN DETECTION IN ARCHIVED DOG BRAIN TISSUES

Okoh, G. R.<sup>1</sup>, Kazeem, H. M.<sup>2</sup>, Kia, G. S. N.<sup>3</sup>, Mailafia, S.<sup>1</sup>

<sup>1</sup>Department of Veterinary Microbiology, Faculty of Veterinary Medicine, University of Abuja, Abuja

<sup>2</sup>Department of Veterinary Microbiology

<sup>3</sup>Department of Veterinary Public Health and Preventive Medicine, Ahmadu Bello University, Zaria  
Nigeria

godspower.okoh@uniabuja.edu.ng

### ABSTRACT

Rabies urgently requires strengthening of new and existing diagnostic methodology in order to overcome the threat it poses. We evaluated the Enzyme Linked Immuno-Sorbent Assay (ELISA) and the Rapid Immunodiagnostic Test (RIDT) in detecting rabies viral antigens, comparing both tests with the Direct Fluorescent Antibody Test (DFAT) which is the gold standard in rabies diagnosis. Fifty dog brain tissues collected from the archives of the Central Diagnostic Laboratory, National Veterinary Research Institute, Vom, Nigeria, were utilized for this study. ELISA performed better than RIDT and recorded equivalent result with DFAT as compared with RIDT. There was a 96% agreement between ELISA and DFAT for rabies antigen detection (concordance coefficient 78% : 95% C.I. 0.6366 to 0.8654) while there was a 54% agreement between RIDT and DFAT (concordance coefficient 17% : 95% C.I. 0.05138—0.2752). Compared to DFAT, the sensitivities of ELISA and RIDT were 95.5% and 47.6%, respectively, and the specificities of ELISA and RIDT were 100% and 87.5% respec-

tively. The simple Cohen's kappa coefficient for ELISA related to the DFAT was found to be 0.834 (95% C.I. 0.613—1.0). For RIDT, the Kappa value was 0.170 (95% C.I. 0.003—0.337). The ELISA is as reliable a diagnostic method as the DFAT which is the gold standard for rabies diagnosis. It has an advantage of being able to analyse large number of samples at the same time, making it more suitable for epidemiological studies and for laboratories that cannot perform the DFAT. The unsatisfactory result of RIDT in this study reiterates the need to perform an adequate test validation before it can be used in the laboratory for rabies diagnosis.

**Key words:** Direct Fluorescent Antibody Test; Enzyme Linked Immuno-Sorbent Assay; rabies; Rapid Immunodiagnostic Test; sensitivity; specificity

### INTRODUCTION

Globally, estimates show that human death due to endemic dog-mediated rabies is most prevalent in Asia, with

the highest occurrence and mortalities recorded in India. Next to Asia is Africa; however, the absence of dependable data has led to uncertainty in the estimation of the disease burden [23]. India has the most prevalent rate of human rabies in the world, basically due to large number of stray dogs [18]. Rabies which is known to be endemic in Nigeria has the domestic dog as the primary reservoir of the causative virus [3]. It first occurred in the country in humans in 1912 and was first diagnosed in the laboratory in a dog in 1925 [5], since then, human and animal rabies cases have been reported in all the regions and ecological zones of Nigeria annually [2, 35].

Rabies remains a threat underappreciated by healthcare practitioners in many endemic areas, often owing to lack of rapid diagnostic tools, post-mortem evaluations, and public health reporting. Although most veterinary laboratories in Africa have sufficient personnel capacity to diagnose rabies in animals, routine diagnosis is often limited by a lack of laboratory equipment and reagents [16, 24].

Diagnosing rabies can be demanding sometimes, this is because it is easily confused, especially at the early stages, with other diseases [8]. Proper history taking and clinical signs are very important in the diagnosis of rabies; however, confirmatory diagnosis of rabies depends on the laboratory identification of the virus or its specific components. Microscopic examination of specimens is one of the laboratory routines that allows for the rapid identification of rabies virus-specific antigen, irrespective of geographical location and condition of the host. The Direct Fluorescent Antibody Test (DFAT) is the 'gold standard' method for diagnosing rabies and its use has been recommended by the World Health Organization (WHO) [35]. However, Fooks et al. [13] noted that decomposed samples can affect the sensitivity and specificity of DFAT. To ensure reliable results, the brain tissues to be tested must be preserved by chilling or freezing. The transportation of the tissues to the rabies laboratory often presents difficulties; especially since facilities for refrigeration are usually limited [1, 36]. Even when ice or dry ice and insulated packages are available, the delays involved in transportation often result in deterioration of the tissue in route, which increases the likelihood of false negative results with DFAT. Because of these difficulties, many specimens are not submitted for laboratory examination, even though it is important that decisions on post-exposure prophylaxis should, whenever possible, be based upon the results of laboratory tests [36].

Rabies urgently requires strengthening of new and existing diagnostic methodology in order to overcome the threat it poses [34]. It is pertinent to note that the accurate laboratory diagnosis of rabies in an animal has a direct effect on human treatments [20]. Therefore, rapid and accurate diagnosis of rabies is vital to human post-exposure prophylaxis, steering epidemiologic surveillance and providing adequate information for the design of rabies control programs [12]. The DFAT has been regarded as the 'gold standard' method for rabies diagnosis for many years despite the numerous limitations associated with this technique [10, 13]. The Enzyme Linked Immuno-sorbent Assay (ELISA) is suitable for analysing samples not preserved in good conditions [22]. It is rapid, easy to use, and relatively safe because they do not require the use of infectious virus, making them suitable for use in developing countries [8]. A recently described method for the detection of RABV antigen from post-mortem samples is the Rapid Immuno-Diagnostic Test (RIDT), a useful method for rabies diagnosis without the need for laboratory equipment [11]. This RIDT is a one-step test that facilitates low-cost and rapid identification of viral antigens.

There is a need for more economical and user friendly tests, particularly for use in developing countries. Therefore, this study sought to evaluate the performance of ELISA and RIDT in relation to DFAT for the diagnosis of rabies in frozen dog brain tissues.

## MATERIALS AND METHODS

### Specimen collection

This experiment was conducted at the Rabies laboratory, National Veterinary Research Institute, Vom. Fifty dog brain tissues preserved at  $-20^{\circ}\text{C}$  were collected from the archives of the Central Diagnostic Laboratory, National Veterinary Research Institute, Vom, for this study. The tissues were thawed at room temperature. Approximately 1 g of brain tissue samples were cut and homogenized in 10ml phosphate buffered saline (PBS), pH 8.5. Supernatants were carefully collected after centrifuging at  $3000\times g$  for 20 minutes. All homogenate samples were stored at  $-70^{\circ}\text{C}$  until used.

### Direct Fluorescent Antibody Technique

The direct fluorescent antibody test (DFAT) was performed as described previously [19, 28]. Impression smears

were made on appropriately labelled pre-cleaned slides by turning the slides over the assembled portion of the brain stem, hippocampus, cerebellum, and cerebrum. The slides were air dried at room temperature and fixed by placing them in a coplin jar containing acetone at  $-20^{\circ}\text{C}$  for 30 minutes. The slides were removed from the acetone and then air-dried at room temperature. The fixed slides were transferred to a humidified chamber and a drop of  $150\mu\text{l}$  of fluorescein-labelled monoclonal anti-rabies immunoglobulin (Fujirubio Diagnostics, Inc., USA) was used for staining. These were then incubated at  $37^{\circ}\text{C}$  for 30 minutes. After incubation, the slides were washed three times with PBS (pH 8.5). The slides were then air-dried at room temperature and arranged in a slide carrier. A drop of 50% mounting buffered glycerol and a cover slip were applied on each smear. The slides were visualized under a fluorescent microscope (Zeiss International, Germany). The presence of bright/dull/dim yellow-green, oval or ellipsoid fluorescing intracellular accumulations was considered positive. Fluorescence was scored by two separate individuals using a three-plus scoring system (scores were as follows: 3+++ bright yellow green fluorescence; 2++ dull yellow green fluorescence; + dim but detectable yellow green fluorescence).

#### **Enzyme Linked Immuno-Sorbent Assay**

The test was carried out according to the manufacturer's instruction (MyBioSource, USA). Briefly, in the micro-ELISA strip plate, two wells were left as negative controls and another two wells as positive controls. Negative and positive controls in a volume of  $50\mu\text{l}$  were added to the negative and positive control wells respectively. In the sample wells, a  $10\mu\text{l}$  sample and a  $40\mu\text{l}$  Sample dilution buffer were added.  $100\mu\text{l}$  of HRP-conjugate reagent was added to the positive control, negative control and sample wells and then mixed very well by gentle shaking. The plate was incubated for 60 minutes at  $37^{\circ}\text{C}$  after covering with an adhesive strip. Following incubation, the test wells were washed manually with 1:20 pre-diluted washing buffer solution ( $400\mu\text{l}$ ) by carefully peeling off the adhesive strip and washing 5 times. At each washing step, the wash solution was decanted after resting for one minute. After the last wash and decanting, any remaining wash solution was removed by aspirating. The plate was inverted and blotted against clean paper towels. Fifty microliter of Chromogen Solution A and  $50\mu\text{l}$  Chromogen Solution B were added to each well (shielded from light) and mixed by gently shak-

ing. The plate was then incubated at  $37^{\circ}\text{C}$  for 15 minutes. Fifty microlitres of the stop solution was added to each well to terminate the reaction and the wells were observed for colour changes.

The optical density (OD) of the test wells were then read at 450 nm using a microtitre plate reader ensuring that the bottom of the wells were clean prior to reading. The assay was carried out within 15 minutes after adding the stop solution. The critical value (cut off) was calculated as the average OD value of the negative control +0.15. The sample was canine rabies virus positive if the OD value  $\geq$  cut off. Scoring was done based on the values of the sample OD and cut off.

#### **Rapid Immuno-Diagnostic Test**

The test was done according to the manufacturer's instruction (Quickings, China) and as described previously [11]. Briefly, swab stick was inserted into 10% brain tissue fluid homogenates (prepared as described earlier) until saturated and then placed into the assay buffer tube where it was thoroughly agitated to ensure good sample extraction. The cassette was taken out from the foil pouch and placed horizontally. Gradually, 3 drops of sample extraction were dripped into the sample hole using a disposable dropper. The result was interpreted in 5–10 minutes. The presence of both control band and test band on the strip (whether test band is clear or vague) was considered positive. The test and control lines on the test strips were scored by two separate individuals using a three-plus scoring.

#### **Data analysis**

The intensity of the fluorescence was counted and given one point per cross (+: 1 point; ++: 2 points; +++: 3 points). The concordance coefficient and simple Cohen's kappa coefficient value were used for statistical comparison of the diagnostic tests. The concordance coefficient values were expressed as a percentage. The kappa value of the agreement levels was interpreted as follows: poor agreement  $\leq 0.20$ ; fair agreement 0.20–0.40; moderate agreement 0.40–0.60; good agreement 0.60–0.80; and very good agreement  $\geq 0.80$ . The confidence interval was calculated by assuming a binomial distribution. All statistical procedures were done using the MedCalc Software (MedCalc Software bvba, Version 17.8).

## RESULTS

A total of 50 archived dogs brain tissues were tested with ELISA, RIDT and also with DFAT, which was used as a reference method. Forty four (88%) of the 50 brain samples tested positive by DFAT, 42 (84%) tested positive by ELISA and 21(42%) tested positive by RIDT (Table 1). Two (4%) samples that were negative for rabies antigen by DFAT were positive by ELISA. Twenty two (44%) samples that were positive by DFAT were negative by RIDT while 1 (2%) sample that was negative by DFAT was positive by RIDT (Table 2). However, we found 96% agreement (42 positives and 6 negatives) of ELISA and DFAT and 54% agreement of

RIDT and DFAT (20 positives and 7 negatives). Compared to DFAT, the sensitivities of ELISA and RIDT were 95.5% and 47.6% respectively, while the specificities of ELISA and RIDT were 100% and 87.5% respectively (Table 2).

The simple Cohen's kappa coefficient for ELISA relative to the DFAT was found to be 0.834 (95% C.I. 0.613–1.0). For RIDT, the Kappa value relative to DFAT was 0.170 (95% C.I. 0.003–0.337). The concordant result of the various techniques was shown in Figure 1. The concordance coefficient for ELISA and RIDT relative to DFAT were 78% (0.6366 to 0.8654) and 17% (95% C.I.; 0.05138–0.2752) respectively.

**Table 1. Rabies antigen detection by DFAT, ELISA and RIDT**

	DFAT	[%]	ELISA	[%]	RIDT	[%]
<b>Positive</b>	44	88	42	84	21	42
<b>Negative</b>	6	12	8	16	29	58
<b>Total</b>	<b>50</b>	<b>100</b>	<b>50</b>	<b>100</b>	<b>50</b>	<b>100</b>

DFAT — Direct Immuno-Fluorescent Test; ELISA — Enzyme Linked Immuno-Sorbent Assay; RIDT — Rapid Immuno-Diagnostic Test

## DISCUSSION

The “gold standard” method for diagnosing rabies worldwide is the direct fluorescent antibody test (DFAT), which is recommended by the World Health Organization (WHO) and OIE [27, 38]. The main advantages of DFAT are its high sensitivity and specificity, even on fixed specimen [37] and that results can be obtained within 3~4 hours [9]. Despite the detectable advantages of the DFAT in di-

**Table 2. Sensitivity and Specificity of ELISA and RIDT for rabies antigen detection in archived brain samples**

DFAT	ELISA			RIDT		
	P	N	Total	P	N	Total
P	42	2	44	20	22	42
N	0	6	6	1	7	8
<b>Total</b>	<b>42</b>	<b>8</b>	<b>50</b>	<b>21</b>	<b>29</b>	<b>50</b>
<b>Sensitivity</b>	95.5%			47.6%		
<b>Specificity</b>	100%			87.5%		

DFAT	ELISA			RIDT		
	P	N	Total	P	N	Total
P	42	2	44	20	22	42
N	0	6	6	1	7	8
<b>Total</b>	<b>42</b>	<b>8</b>	<b>50</b>	<b>21</b>	<b>29</b>	<b>50</b>
<b>Sensitivity</b>	95.5%			47.6%		
<b>Specificity</b>	100%			87.5%		

P — positive; N — negative; DFAT — Direct Immuno-Fluorescent Test  
ELISA — Enzyme Linked Immuno-Sorbent Assay; RIDT — Rapid Immuno-Diagnostic Test

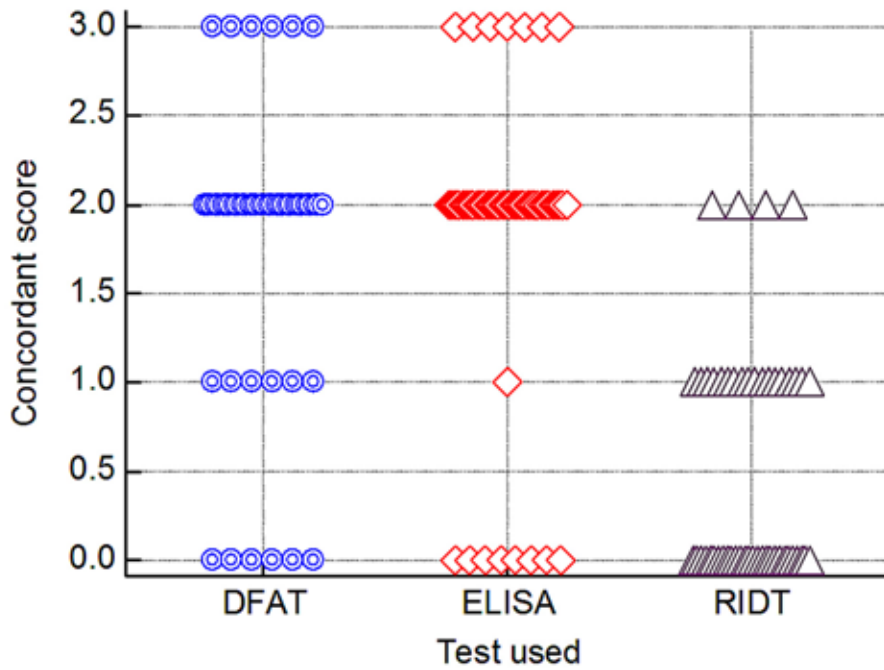


Fig. 1. Concordant results of dog brain tissues preserved at  $-20^{\circ}\text{C}$

agnosing rabies, complementary diagnostic methods that can be more reliable as that of DFAT are needed. Any false negative results may lead to death and widespread under-reporting of the disease while false positive results can lead to unnecessary post exposure prophylaxis [15, 40]. Consequently, the true public health impact of rabies will be greatly underestimated and political commitment for its control would be lacking [7].

In this study, 88 % of the frozen brain specimens tested positive by DFAT, 84 % tested positive by ELISA and 42 % tested positive by RIDT. Similar findings have been recorded by earlier researchers; Whitefield et al. [37] recorded 66.9 % positive result by DFAT in frozen brain specimens. Of the 1253 specimens analysed in a trial by Perrin and Sureau [30], 651 were positive in both the DFAT and the ELISA. Two different studies conducted by Yang et al. [40] and Sharma et al. [33], gave 17 % and 64.7 % positive results respectively by RIDT on fresh samples. Generally, the accuracy of rabies diagnosis is dependent on the quality of the sample [13, 6], the type of anti-rabies conjugate used [31], virus antigen distributions in the brain and areas of the brain tested [4].

The present study evaluated the efficacy of RIDT to be used under laboratory and field condition for rabies diagnosis and obtained sensitivity and specificity of 47.6 % and

87.5 % respectively. This however, contradicts the findings of Nishizono et al. [25] who reported a sensitivity of 95.25 % and a specificity of 88.9 % using a type I RIDT kit which recognizes epitope II and III of the nucleoprotein of rabies virus. Similarly, Kang et al. [14] recorded a high sensitivity and specificity of 91.7 % and 100 % respectively. This variation in the sensitivity and specificity of RIDT was observed by Eggerbauer et al. [11] who compared six commercially available RIDTs for diagnostic and analytical sensitivity, as well as their specificity and concluded that the sensitivity and specificity varied considerably with different test kits. Also, none of the test kits investigated proved to be satisfactory, although the results somewhat contradicted previous studies, indicating batch to batch variations. Therefore, the low sensitivity and specificity of RIDT recorded in our study could be attributed to poor quality control and relatively low detection limit of the test kit used.

The ELISA is usable even on autolysed or partially degraded brain samples. It can be read qualitatively with the naked eyes and a large number of samples can be tested at the same time [9, 17]. However, false positive results due to cross reactivity with other antigens with very similar epitopes had been recorded [30]. In this study, the sensitivity and specificity of ELISA were shown to be 95.45 %

and 100 % respectively. This is in complete agreement with earlier studies [21, 26, 29, 32]. More recently, Xu et al. [39] recorded a sensitivity and specificity of 97 % and 99.9 % respectively using a modified ELISA technique known as WELYSSA. In our study, 96 % agreement was observed between DFAT and ELISA. The very good strength of agreement between the ELISA and DFAT (Concordance coefficient 78 %; Kappa 0.834) implies that ELISA is as reliable as the DFAT and can be used in laboratories that cannot perform DFAT or whenever DFAT results are in doubt.

## CONCLUSIONS

The ELISA is as reliable a diagnostic method as the DFAT which is the gold standard for rabies diagnosis. It has an advantage of being able to analyse large number of samples at the same time, making it more suitable for epidemiological studies and for laboratories that cannot perform DFAT. The unsatisfactory result of RIDT in this study reiterates the need to perform an adequate test validation before it can be used in the laboratory for rabies diagnosis.

## ACKNOWLEDGEMENTS

The authors wish to thank Dr. Yakubu Dashe, the Head of Central Diagnostic Laboratory, National Veterinary Research Institute (NVRI), Vom, for his immense support. We would also like to appreciate Dr. Tekki, I.S and the entire staff of rabies laboratory, NVRI for their contribution and the technical support provided during the course of this work.

## REFERENCES

1. Aguiar, T.D.F., Teixeira, M.F.S., Costa, E.C., Vitaliano, A.B., Teles, C. H. A., Barroso, I.C. et al., 2013: Medium-term cryopreservation of rabies virus samples. *Rev. Soc. Bras. Med. Trop.*, 46, 678—683.
2. Atuman, Y.J., Ogunkoya, A.B., Adawa, D.A. Y., Nok, A. J., Biallah, M. B., 2014: Dog ecology, dog bites and rabies vaccination rates in Bauchi State, Nigeria. *IJVSM*, 2, 41—45.
3. Barecha, C.B, Girzaw, F., Kandi, V., Pal, M., 2017: Epidemiology and public health significance of rabies. *Persp. Med. Res.*, 5, 55—67.
4. Bingham, J., van der Merwe, M., 2002: Distribution of rabies antigen in infected brain material: determining the reliability of different regions of the brain for the rabies fluorescent antibody test. *J. Virol. Methods.*, 101, 85—94.
5. Boulger, L. R., Porterfield, J. S., 1958: Isolation of a virus from Nigerian fruit bats. *Trans. R Soc. Trop. Med. Hyg.*, 52, 421—424.
6. Cliquet, F., Freuling, C., Smreczak, M., van der Poel, W. H. M., Horton, D., Fooks, A. R. et al., 2010: Development of harmonized schemes for monitoring and reporting of rabies in animals in the European Union. *EFSA Sci. Rep.*, 7, 1—60.
7. Coleman, P.G., Fèvre, E.M., Cleaveland, S., 2004: Estimating the public health impact of rabies. *Emerg. Infect. Dis.*, 10, 140—142.
8. Dacheux, L., Wacharapluesadee, S., Hemachudha, T., Meslin, F.-X., Buchy, P., Reynes, J.M. et al., 2010: More accurate insight into the incidence of human rabies in developing countries through validated laboratory techniques. *PLoS Negl. Trop.*, 4, 765.
9. Duong, V., Tarantola, A., Ong, S., Meya, C., Choeng, R., Ly, S. et al., 2016: Laboratory diagnostics in dog-mediated rabies: an overview of performance and a proposed strategy for various settings. *Int. J. Infect. Dis.*, 46, 107—114.
10. Dürr, S., Näissengar, S., Mindekem, R., Diguimbye, C., Niezgodá, M., Kuzmin, I. et al., 2008: Rabies diagnosis for developing countries. *PLoS Negl. Trop.*, 2, 206.
11. Eggerbauer, E., Benedictis, P., Hoffmann, B., Mettenleiter, T. C., Schlottau, K., Ngoepe, E. C. et al., 2016: Evaluation of six commercially available rapid immunochromatographic tests for the diagnosis of rabies in brain material. *PLoS Negl. Trop. Dis.*, 10, 1—16.
12. Ehizibolo, D. O., Nwosuh, C., Ehizibolo, E. E., Kia, G. S. N., 2009: Comparison of the fluorescent antibody test and direct microscopic examination for rabies diagnosis at the National Veterinary Research Institute, Vom, Nigeria. *Afr. J. Biomed. Res.*, 12, 73—74.
13. Fooks, A. R., Johnson, N., Freuling, C. M., Wakeley, P. R., Banyard, A. C., McElhinney, L.M. et al., 2009: Emerging technologies for the detection of rabies virus: challenges and hopes in the 21st century. *PLoS Negl. Trop. Dis.*, 3, 530.
14. Kang, B. K., Oh, J. S., Lee, C. S., Park, B. K., Park, Y. N., Hong, K. S. et al., 2007: Evaluation of a rapid immunodiagnostic test kit for rabies virus. *J. Virol. Methods*, 145, 30—36.
15. Lembo, T., Niezgodá, M., Velasco-Villa, A., Cleaveland, S., Ernest, E., Rupprecht, C. E., 2006: Evaluation of a direct rapid immunohistochemical test for rabies diagnosis. *Emerg. Infect.*

- Dis.*, 12, 310—313.
16. Mallewa, M., Fooks, A.R., Banda, D., Chikungwa, P., Mankhambo, L., Molyneux, E. et al., 2007: Rabies encephalitis in malaria-endemic area, Malawi, Africa. *Emerg. Infect. Dis.*, 13, 136.
  17. Mani, R.S., Madhusudana, S.N., 2013: Laboratory diagnosis of human rabies: Recent advances. *Sci. World. J.*, 2013, 1—10.
  18. Menezes, R., 2008: Rabies in India. *CMAJ*, 178, 564—566.
  19. Meslin, F.X., Kaplan, M.M., Koprowski, H., 1996: *Laboratory diagnosis of rabies*. Geneva, World Health Organisation, 88—95.
  20. Messenger, S.L., Smith, J.S., Orciari, L.A., Yager P.A., Rupprecht, C.E., 2003: Emerging patterns of rabies deaths and increased viral infectivity. *Emerg. Infect. Dis.*, 9, 151—154.
  21. Miranda, N.L., Robles, C.G., 1991: A comparative evaluation of a new immunoenzymatic test (RREID) with currently used diagnostic tests (DME and FAT) for dog rabies. *Southeast Asian J. Trop. Med. Public Health*, 22, 46—50.
  22. Morvan, J., Mouden, J.C., Coulanges, P., 1990: Rapid diagnosis of rabies by the ELISA method. Its application in Madagascar: advantages and disadvantages. *Arch. Inst. Pasteur Tunis*, 57, 193—203.
  23. Mshelbwala, P.P., Audu, S.W., Ogunkoya, A.B., Okaiyeto, S.O., James, A.A., 2013: Detection of rabies antigen in the saliva and brains of apparently healthy dogs slaughtered for human consumption and its public health implications in Abia State, Nigeria. *ISRN Vet. Sci.*, 2013, 468043.
  24. Nel, L.H., 2013: Discrepancies in data reporting for rabies, Africa. *Emerg. Infect. Dis.*, 19, 529—533.
  25. Nishizono, A., Khawplod, P., Ahmed, K., Goto, K., Shiota, S., Mifune, K. et al., 2008: A simple and rapid immunochromatographic test kit for rabies diagnosis. *Microbiol. Immunol.*, 52, 243—249.
  26. Oelofsen, M.J., Smith, M.S., 1993: Rabies and bats in a rabies-endemic area of southern Africa: application of two commercial test kits for antigen and antibody detection. *Onderstepoort J. Vet. Res.*, 60, 257—260.
  27. Office International des Épizooties (OIE), 2008: *Manual of Diagnostic Tests and Vaccines for Terrestrial Animals*. 6th edn., OIE, Paris, 304—322.
  28. Office International des Épizooties (OIE), 2013: Rabies (Infection with rabies virus). *OIE Terrestrial Manual*, 1—28.
  29. Perrin, P., Gontier, C., Lecocq E., Bourhy, H., 1992: A modified rapid enzyme immunoassay for the detection of rabies and rabies-related viruses: RREID-lyssa. *Biol.*, 20, 51—58.
  30. Perrin, P., Sureau, P., 1987: A collaborative study of an experimental kit for rapid rabies enzyme immunodiagnosis (RREID). *Bull. World Health Organ.*, 65, 489—493.
  31. Robardet, E., Andrieu, S., Rasmussen, T.B., Dobrostana, M., Horton, D.L., Hostnik, P. et al., 2013: Comparative assay of fluorescent antibody test results among twelve European National Reference Laboratories using various anti-rabies conjugates. *J. Virol. Methods*, 191, 88—94.
  32. Saxena, S.N., Madhusudana, S.N., Tripathi, K.K., Gupta, P., Ahuja, S., 1989: Evaluation of the new rapid rabies immunodiagnosis technique. *Indian J. Med. Res.*, 89, 445—448.
  33. Sharma, P., Singh, C.K., Narang, D., 2015: Comparison of immunochromatographic diagnostic test with heminested reverse transcriptase polymerase chain reaction for detection of rabies virus from brain samples of various species. *Vet. World*, 8, 135—138.
  34. Singathia, R., Dutta, P., Yadav, R., Gupta, S.R., Gangil R., Gattani, A., 2012: Current update on rabies diagnosis. *IJAVMS*, 6, 229—240.
  35. Tekki, I.S., Ponfa, Z.N., Nwosuh, C.I., Kumbish, P.R., Jonah, C.L., Okewole, P.A. et al., 2016: Comparative assessment of seller's staining test (SST) and direct fluorescent antibody test for rapid and accurate laboratory diagnosis of rabies. *Afr. Health Sci.*, 16, 123—127.
  36. Umoh, J.U., Blendon, D.C., 1981: Immunofluorescent staining of rabies virus antigen in formalin-fixed tissue after treatment with trypsin. *Bull. World Health Organ.*, 59, 737—744.
  37. Whitfield, S.G., Fekadu, M., Shaddock, J.H., Niezgod, M., Warner, C.K., Messenger, S.L., 2001: A comparative study of the fluorescent antibody test for rabies diagnosis in fresh and formalin-fixed brain tissue specimens. *J. Virol. Methods*, 95, 145—51.
  38. World Health Organization (WHO), 1992: WHO expert committee on rabies. *World Health Organ. Tech. Rep. Ser.*, 824, 1—84.
  39. Xu, G., Weber, P., Hu, Q., Xue, H., Audry, L., Li, C. et al., 2007: A simple sandwich ELISA (WELYSSA) for the detection of lyssavirus nucleocapsid in rabies suspected specimens using mouse monoclonal antibodies. *Biol. J. In. Assoc. Biol. Stand.*, 35, 297—302.
  40. Yang, D.K., Shin, E.K., Oh, Y.I., Lee, K.W., Lee, C.S., Kim, S.Y. et al., 2012: Comparison of four diagnostic methods for detecting rabies viruses circulating in Korea. *J. Vet. Sci.*, 13, 43—48.

Received September 18, 2017

Accepted December 6, 2017



## ADDITION OF DRIED BLOOD PLASMA TO FEED OF MINKS DURING LACTATION AND REARING OF KITS

Nowakowicz-Dębek, B.<sup>1</sup>, Wlazło, Ł.<sup>1</sup>, Bis-Wencel, H.<sup>1</sup>, Hromada, R.<sup>2</sup>  
Śmiech, A.<sup>3</sup>, Sasakova, N.<sup>2</sup>, Zoń, A.<sup>1</sup>

<sup>1</sup>Department of Animal and Environmental Hygiene

<sup>3</sup>Department of Pathology, University of Life Sciences in Lublin, Akademicka 13, 20-950 Lublin  
Poland

<sup>2</sup>Department of Environmental Protection

University of Veterinary Medicine and Pharmacy, Komenského 73, 041 81 Košice  
Slovakia

<sup>4</sup>Experimental Institute of Zootechnics Institute in Chorzelów  
Poland

bozena.nowakowicz@up.lublin.pl

### ABSTRACT

Studies on the effects of dried blood plasma on certain health parameters of mink (of the pastel variety) were conducted during lactation and the rearing of the kits. The study included two groups of mink (control group and experimental group). Animals in the experimental group received 0.5% of dry blood plasma and the control group did not receive the plasma supplement. From the whole blood of both groups the direct and indirect haematological indices were recorded. Also, in both groups, the histopathological and immunohistochemical studies were performed on the: liver, kidneys, lymph nodes, spleen, and intestinal segments. From the experimental group some of the organs examined demonstrated slightly altered histopathology.

**Key words:** blood plasma; defensins; haematological markers; histopathological examination; immunohistochemistry; mink

### INTRODUCTION

Birth and lactation are a particular burden for all mammalian females. Inappropriate nutrition during pregnancy and lactation can adversely affect the health of the mother, the offspring and the number of litters. Food and organizational errors can lead to: the loss of foetuses directly before labour; the newborns just after birth; or the death of the young. Breeders are striving for the best reproduction rates because only then can successful breeding be accomplished. Furthermore, the use of growth promoting and therapeutic antibiotics in a piglet's feed may generate antimicrobial resistance which can be transferred to humans. For this reason, the search for other products and alternatives to the use of antibiotics, began. The spray dried plasma seems to be the most promising [18].

In recent years, dried blood plasma has been used in many animal species and these formulas have confirmed their high value as a feed additive [9, 11, 12, 14, 15, 16]. They are rich in specific proteins and consists of about 50% of

the albumin fraction, 25% of globulins, 5% of fibrinogen, and 20 percent of other proteins, including: haptoglobin, transferrin, growth factors and other proteins or peptides [11, 13]. However, they have not been used in the feeding of carnivores; that is why studies were conducted to determine the effects of plasma addition to feed on the histopathological and immunohistochemical image of mink's tissue (*Neovison vison*) during lactation and the rearing of the kits.

## MATERIALS AND METHODS

This study included two groups of mink (*Neovison vison*) of the pastel variety. Each group consisted of 30 mink and all animals were 3 months old. The study was carried out during lactation and the rearing of the kits. During those time frames, dried blood plasma was added to the feed of the mink. The plasma used in the experiment (SDAP) is a ready-to-use product, manufactured using strictly defined procedures. The drying of plasma was carried out in the Anicet's BallTec dryer [13], at 55 °C, and then sterilized by heating to 200 °C. The resulting product in a dusty form was packed in paper bags, ventilated and stored in accordance with the manufacturer's instructions in cool and dark room. The basic composition of the plasma was: protein min. 70.0%, fat max. 2.0%, fibre max. 0.3%, and ash max. 14.0%. The experimental group D received 0.5% of beef-pork plasma dietary additive to a daily feed ration and the control group C received no supplemental dietary plasma. The animals were provided with veterinary and zootechnical care and subjected to appropriate prophylactic treatment throughout the study period. The animals of both groups showed no signs of disease throughout the experiment. Food poisoning, diarrhea or other gastrointestinal symptoms were not observed.

Blood samples for haematological tests were collected from the females twice: during lactation and at the time of rearing. The blood samples were taken from vena saphena, and collected in Sarstedt S-Monovette tubes, in the morning, before the feeding of the animals. The following parameters were recorded: red blood count (RBC), haematocrit (Ht), haemoglobin (Hb), mean red cell volume (MCV) and mean corpuscular haemoglobin (MCH), and the mean corpuscular haemoglobin concentration (MCHC). In addition, the total number of white blood cells (WBC), red blood cell distribution width (RDW), thrombocyte (PLT),

mean platelet volume (MPV), and the platelet anisocyte (PDW) were also recorded. The haematological parameters were determined using the MS-4vet.

After weaning, the females from both groups were slaughtered, according to the Local Ethical Commission (No. 48/2011). Samples of the following organs were collected: liver, kidney, lymph nodes, spleen, and the small intestine. They were subjected to the routine microscopic evaluation and immunohistochemical studies. The sections of the internal organs were collected from both the experimental and control animal groups. The tissue material was fixed in 10% neutral buffered formalin for paraffin block preparation, then sectioned and stained by hematoxylin and eosin. The small intestine and lymph node sections obtained from all mink groups were additionally processed for immunohistochemical assays. The En vision and Dual Link Systems by DAKO were applied. The reagent was visualized with a color reaction by 3,3-diaminobenzidine /DAB/as /DAKO/ chromogene. The anti-rabbit polyclonal antibody CD3/DAKO/ diluted at 1:100 to identify T lymphocytes, anti-mouse monoclonal primary antibody CD 79alpha/DAKO/ at 1:100 dilution that detects B lymphocytes, and finally, monoclonal primary antibody DEF that serves to detect defensins diluted at 1:200 were also applied. The quantitative study of B and T lymphocytes in the small intestinal wall was performed using computer assisted analysis of microscopy images NIS Elements BR-2.20, Laboratory Imaging/ coupled with a digital camera and light microscope. The percentage of positive cells was determined by counting 100 cells in 5 fields of view at 20× magnification of the objective-lens.

Results were statistically calculated using the STATISTICA software, based on the ANOVA test. For comparison of two groups, Wilcoxon signed-rank test was used.

## RESULTS

Statistical analysis did not show any statistically significant differences in the blood haematological parameters of the control C and experimental D groups ( $P > 0.05$ ).

The average number of red blood cells (RBC) was  $9.7 \times 10^{12} \cdot l^{-1}$  in the control group and  $10.5 \times 10^{12} \cdot l^{-1}$  in the experimental group, slightly exceeding the reference values reported by Hunter [10], who gave the range from 5.80 to  $9.73 \cdot 10^{12} \cdot l^{-1}$  and Berestov et al. [3].

The mean haematocrit (Ht) in the study ranged from 0.59 to 0.63 l.l<sup>-1</sup> and was slightly above the reference values of 0.35–0.56 l.l<sup>-1</sup> [3, 10].

The mean haemoglobin (Hb) levels ranged from 6.79 to 11.66 mmol.l<sup>-1</sup> and were within the reference values of 6.206–11.79 mmol.l<sup>-1</sup> given by Hunter [10], with the same upward trend for the females of the experimental group.

The mean red cell volume (MCV) values were 61.57–60.47 fl, and they were compatible with the limits of reference values of 35.1–75.0 fl, same as the mean values for the mean haemoglobin in red blood cells (MCH) of females in the control group (17.93 pg) and experimental group (17.37 pg). They were also compatible with the reference values 12.2–25.4 pg [3, 10].

The mean values of the mean haemoglobin concentration in the red blood cells (MCHC) were also consistent with the reference values of 28.6–38.1 g.dl<sup>-1</sup> [3, 10] and were 29.20 and 28.80 g.dl<sup>-1</sup>, respectively.

The mean white blood cell count (WBC) in the study was 6.85 and 7.22 10<sup>9</sup>.l<sup>-1</sup> and was also consistent with Hunter's [10] reference values, which range from 3.80–12.20 10<sup>9</sup>.l<sup>-1</sup> and with Bis-Wencel et al. [4].

Some of the parameters in the experimental group were slightly higher than in the control group, including erythrocytes, leukocytes, hematocrit, haemoglobin, PLT, MPV and PDW (Table 1).

The histopathological examinations of the internal organs taken from mink of the control group showed their correct microscopic structure. In the liver of mink from the experimental group, small inflammatory infiltrates were found around the vessels and between the lobules (Fig. 1). In the kidneys, deposits of crystalline salts in the kidney tubules and single inflammatory infiltrates were seen (Fig. 2). Slight focal destruction of the intestinal villi and the presence of inflammatory infiltrates located mainly in the mucous membrane were observed in the intestine of a few experimental animals (Fig. 3). No cases of diarrhoea or other gastrointestinal pathologies were reported in our study. The flock resistance was also satisfactory, requiring no additional pharmacological intervention. It seems that the observed changes might be connected with the animal intra-subject variability based on genetic predispositions to obesity. In agreement with the information presented in [7], the body condition score (BCS) correlated with the histopathological changes in the mink.

**Table 1. Levels of selected haematological parameters in the blood of mink from both groups**

Parameters	Control group			Experimental group			Statistical analysis	
	M	Me	SD	M	Me	SD	Z	P
<b>RBC</b> [10 <sup>12</sup> .l <sup>-1</sup> ]	9.70	10.25	0.97	10.50	10.25	0.65	-0.22	0.83
<b>Hb</b> [mmol.l <sup>-1</sup> ]	17.47	18.00	2.05	18.23	18.20	0.25	-0.22	0.83
<b>Ht</b> [l.l <sup>-1</sup> ]	59.77	62.90	7.04	63.23	62.90	1.23	0.22	0.83
<b>MCV</b> [fl]	61.57	61.40	1.36	60.47	61.40	4.67	0.22	0.83
<b>MCH</b> [pg]	17.93	17.70	0.59	17.37	17.50	1.11	0.65	0.51
<b>MCHC</b> [g.dl <sup>-1</sup> ]	29.20	29.40	0.53	28.80	28.60	0.35	0.87	0.38
<b>RDW</b> [%]	10.40	10.20	1.21	9.47	9.30	0.67	0.87	0.38
<b>WBC</b> [10 <sup>9</sup> .l <sup>-1</sup> ]	6.85	3.36	7.40	7.22	7.93	1.62	-0.44	0.66
<b>PLT</b> [G.l <sup>-1</sup> ]	556.33	473.00	343.66	561.00	473.00	168.25	0.22	0.83
<b>MPV</b> [fl]	8.80	9.10	0.52	9.13	9.10	0.35	-0.44	0.66
<b>PDW</b> [fl]	8.70	8.90	1.51	9.57	9.80	0.68	-0.22	0.83

M—Mean; SD—standard deviation; Me—median; Z—Wilcoxon signed-rank test; P—test probability; RBC—red blood count; Hb—haemoglobin; Ht—haematocrit; MCV—mean red cell volume; MCH—mean corpuscular haemoglobin; MCHC—mean corpuscular haemoglobin concentration; RDW—red blood cell distribution width; WBC—the total number of white blood cells; PLT—thrombocyte; MPV—mean platelet volume; PDW—platelet anisocyte

The immunohistochemical studies confirmed the dominance of T lymphocytes in apparent infiltrates (Figs. 4 and 5). The lymph nodes showed T-cell hyperplasia (Fig. 6). The immunohistochemical studies conducted at this stage of research showed a positive reaction to the presence of

defensins in the mink from the experimental group. The expression of defensins was slightly increased in comparison with previous studies in the intestinal epithelium, intestinal crypts and inflammatory cells [16], and the reaction was granular and mainly confined to the cytoplasm of the cell.

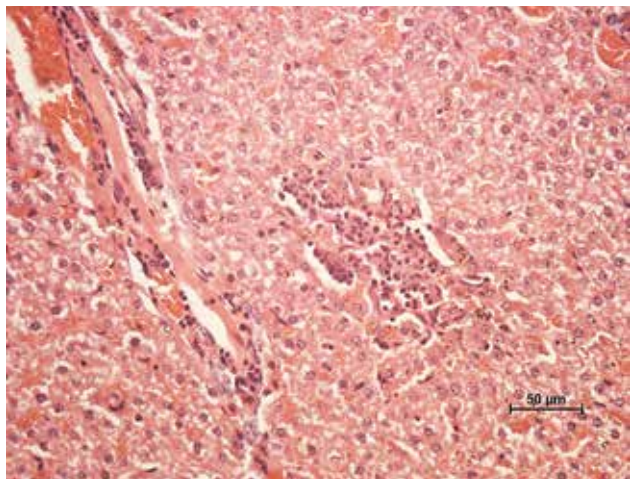


**Fig. 1. Minor inflammatory infiltration in the liver of experimental group, HE stain. Magn. ×200**

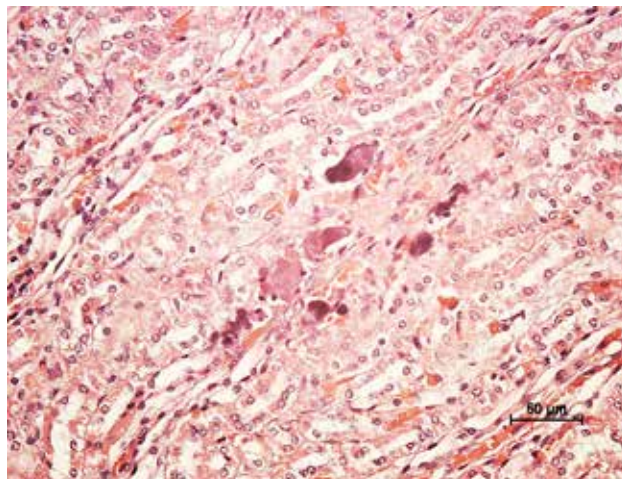


**Fig. 2. Mineral salt deposits in the kidney of experimental group, HE stain. Magn. ×200**

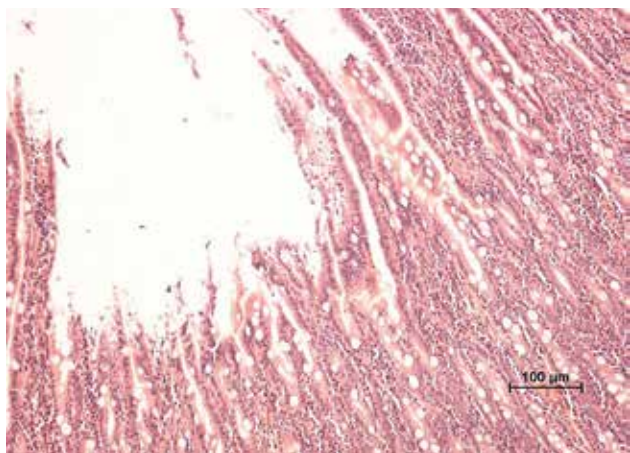


**Fig. 3. Destruction of intestinal villi and presence of inflammatory infiltration in the mucous membrane of experimental group, HE stain. Magn. ×200**

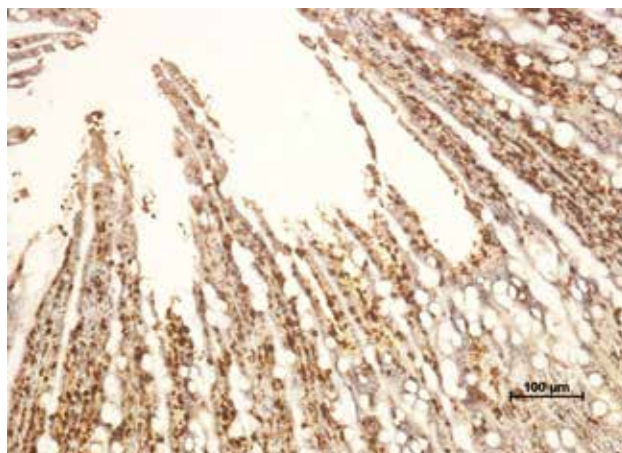


**Fig. 4. Expression of CD3 antigen identifying T lymphocytes in intestinal mucus of experimental group, IHC stain. Magn. ×200**

## DISCUSSION

Commission Regulation (EC) No 1292/2005 amended the ban on the use of blood as a by-product in animal nutrition and therefore, the interest in searching for new sources of animal protein that could be used in animal feed increased. Dried animal blood plasma preparations have

confirmed their unconventional value as a feed additive in growing animals. Dried blood plasma contains specific proteins, nucleotides, and immunoglobulins; therefore, the interest increased in using it as a feed additive in pigs and poultry [11, 12, 15]. Due to the immunoglobulin content, blood preparations can be used in the prevention and treatment of many diseases caused by intestinal pathogens. The

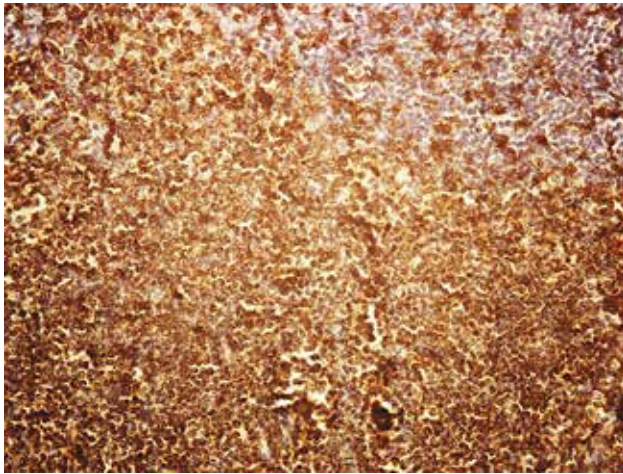


Fig. 5. Expression of CD3 antigen identifying T lymphocytes in the lymph node of experimental grup, IHC stain. Magn. ×200

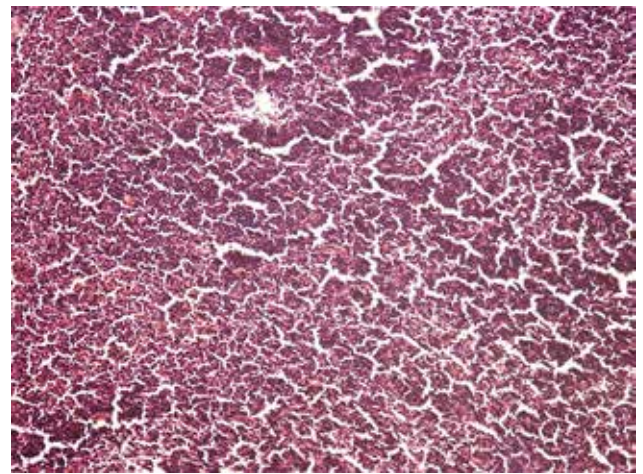


Fig. 6. Obliteration of lumps in the lymph node of experimental grup, IHC stain. Magn. ×200

calves fed before weaning with dried plasma had better weight gain and were characterized by lower morbidity and mortality. Dried blood preparations have also been successfully used in feeding lambs, dogs, foxes, poultry and fish [1].

The basic system of feeding mink in Poland is based on high energy feed. The usage of energy-rich feeds with high levels of energy from fat is a prerequisite for obtaining high quality skins and better reproduction rates [4, 5, 6, 14, 16, 17]. This may adversely affect the health of the animals, especially by threatening the reproductive processes. Such nutrition leads to metabolic abnormalities which result in histopathological changes, especially in the liver and kidneys. Intensive nutrition of this kind can also cause a number of disease processes [6, 7, 8, 17].

The weaning period is a time when the functionality and integrity of the intestinal mucosa deteriorates. Young animals take more feeds to which the digestive tract is not enzymatically prepared [8, 21]. This can increase the amount of undigested feed in the intestines and increase the susceptibility to diseases. These problems are traditionally abolished by the sub-therapeutic use of antibiotics in doses as growth promoters. This can be successfully replaced by immunological modulation with Spray-Dried Animal Plasma (SDAP) bovine serum [23]. Results indicate that SDAP's components possess biological functions that have a positive impact on the digestive system of healthy adult cats. This influence persists even after the sterilization or canning [20]. Positive results of the dried blood plasma usage were obtained in the experiment on pigs and enough evidence supporting the safety of commercial spray dried

porcine plasma in feeding pigs is available [18]. However, such results have not been confirmed in the poultry experiment [9]. The feed additive that can reduce the effects of mycotoxins is also spray dried plasma protein (SDPP). Inclusion of SDPP to pigs has been shown to improve the pig's performance. Weaning is a very stressful event and SDPP can benefit pig growth and decrease intestinal disorders. Evidence suggests that diets supplemented with SDPP have reduced diarrhoea and intestinal barrier dysfunction due to a reduction in inflammation caused by weaning stress [22].

It appears that the addition of plasma to young mink must still be tested with respect to the balanced daily ration of food intake. Protein-rich foods "enhanced" by plasma proteins in the early stages of life can modify the state of homeostasis and be considered a "ballast" for the condition of the internal organs. Nowakowicz-Dębek et al. [18] showed that the addition of 0.5% plasma to adult females during breeding preparation was acceptable to the organism and did not cause important changes in the internal organs. The results confirm the interaction of the defensins produced in Paneth's cells in maintaining intestinal homeostasis, which play an important role in innate and acquired immunity. Among the solutions positively influencing the difficult period of rearing young animals, dried blood plasma should be noted. Defensins, previously known as leucins and phagocytes, are cationic proteins belonging to the group of AMP proteins (antimicrobial peptides). The synthesis of these proteins occurs in many cells, mainly phagocytic in human and other animal intestinal cells. Defensins

as a proinflammatory mediator where dendritic cells participate in signalling from the surface of the mucosa to the basilar membrane in the gastric mucosa [23].

It has been shown that their antibacterial activity is revealed after about 3–4 hours, and that they possess a multistage mode of action. It consists in binding defensins to the membrane of the attacked cell, followed by its endocytosis and apoptosis. Antimicrobial, antiviral, antifungal and antiparasitic effects have been demonstrated and also, defensins induce the production of certain chemokines and activation of the complement, macrophages and mast cells. They bind and neutralize bacterial endotoxins and they participate in wound healing. Furthermore, defensins reduce stress by inhibiting glucocorticoid synthesis, and also act against cancer.

## CONCLUSIONS

In conclusion, it should be stated that the proposed supplementation of blood plasma can contribute to improving the health of the animals and maintaining their good condition during the lactation and perinatal period and the kits' rearing. These studies however, need to be continued in order to determine the precise dosage of plasma supplements.

## REFERENCES

1. **Banach, M., Makara, A., 2011:** Blood and its derivatives (In Polish). *Chemia czasopismo techniczne*, 108, 3–20.
2. **Barabasz B., Bielański P., Niedźwiadek S., Sławoń J., 1994:** Standards for feeding carnivorous and herbivorous fur Animals (In Polish). *IFiZZ PAN*, 28–29.
3. **Berestov, V.A., Blomstedt, L., Brandt, A., Juokslahti, T., Jorgensen, G., Kozhevnikova, L.K., et al., 1989:** Haematology and Clinical chemistry of Fur Animals. Ed. Asbjorn B. (Ed.), *Scientifur*, 10–18.
4. **Bis-Wencel, H., Saba, L., Kopczewski, A., Pyzik-Mołęda, M., Likos-Grzesiak, B., Ondrasovic, O., 2004:** Shaping the reference values of selected white blood cells in the context of high energy diet (In Polish). *Zeszyty Naukowe Przeglądu Hodowlanego*, 72, 75–79.
5. **Bis-Wencel, H., 2006:** Effect of diet on selected mink reproduction indicators (In Polish). *Acta Scientiarum Polonorum, Medicina Veterinaria*, 5, 103–110.
6. **Bis-Wencel, H., Nozdryn-Plotnicki, Z., Saba, L., Zoń, A., Kopczewski, A., Sroka, A., 2006:** Effect of preservatives on histopathological image of internal organs of mink (In Polish). *Medycyna Weterynaryjna*, 62, 70–73.
7. **Bis-Wencel, H., Łopuszyński, W., Saba, L., Bryl, M., Rowicka, A., 2010:** Histopathological examination of selected internal organs of pastel minks in relation to oxidative state parameters. *Bulletin of the Veterinary Institute in Puławy*, 54, 651–654.
8. **Bis-Wencel, H., Bryl, M., Kowaleczko, M., Rowicka, A., Matyjaszczyk, M., 2011:** The bacteriological state of mink's kittening houses in perinatal period, *Annales UMCS, Section EE*, 24, 21–27.
9. **Donkoh, A., Atuahene, C.C., Anang, D.M., Ofori, S.K., 1999:** Chemical composition of solar-dried blood meal and its effect on performance of broiler chickens. *Anim. Feed Sci. Technol.*, 81, 299–307.
10. **Hunter, D.B., 1996:** Mink hematology and clinical biochemistry. In **Hunter, D. B., Lemieux, N., (Eds.):** *Biology, Health and Disease*, 1st edn., Canada Mink Breeders Association. University of Guelph, Ontario, Canada, 7–1 to 7–5.
11. **Jamroz, D., Wiliczekiewicz, A., Orda, J., Kuryszko, J., Stefaniak, T., 2012:** Use of spray-dried porcine blood by-products in diets for young chickens. *J. Anim. Physiol. Anim. Nutr.*, 96, 319–33.
12. **King, M.R., Morel, P.C.H., Pluske, J.R., Hendriks, W.H., 2008:** A comparison of the effects of dietary spraydried bovine colostrum and animal plasma on growth on intestinal histology in weaned pigs. *Livest. Sci.*, 119, 167–173.
13. **Kowalski, Z., Makara, A., Banach, M., 2011:** Production technology for blood plasma and hemoglobin (In Polish). *Chemik*, 65, 5, 466–475.
14. **Langerkvist, G., Johansson, K., Lundeheim, N., 1994:** Selection for litter size, body weight, and pelt quality in mink (*Mustela vison*): correlated responses. *J. Anim. Sci.*, 72, 1126–1137.
15. **Marquez, E., Brancho, M., Archile, A., Rangel, L., Benitez, B., 2005:** Proteins, isoleucine, lysine and methionine content bovine, porcine and poultry blood and their fractions. *Food Chem.*, 93, 503–505.
16. **Nowakowicz-Dębek, B., Śmiech, A., Zoń, A., Bis-Wencel, H., Ondrasovicova, O., Wlazło, Ł., Wnuk, W., 2012:** Tissue pathomorphology and immunohistochemistry in mink (*Neovison vison*) fed blood plasma supplemented diet in the period of preparation for breeding. *Bulletin of the Veterinary Institute in Puławy*, 56, 393–397.

17. Nowakowicz-Dębek, B., Łopuszyński, W., Trawińska, B., Saba, L., 2009: Effect of various management conditions on anatomo-histopathological changes in Arctic fox (*Alopex lagopus*). *Bulletin of the Veterinary Institute in Pulawy*, 53, 105–109.
18. Nowakowicz-Dębek, B., Zoń, A., Jakubczak, A., Wnuk, W., 2013: Haematological parameters of wild and farm mink, red fox and raccoon dog. *Medycyna Weterynaryjna*, 69, 40–42.
19. Pérez-Bosque, A., Polo, J., Torrallardona, D., 2016: Spray dried plasma as an alternative to antibiotics in piglet feeds, mode of action and biosafety. *Porcine Health Management*, 2, 16.
20. Rodríguez, C., Saborido, N., Ródenas, J., Polo J., 2016: Effects of spray-dried animal plasma on food intake and apparent nutrient digestibility by cats when added to a wet pet food recipe. *Anim. Feed Sci. Technol.*, 216, 243–250.
21. Rouvinen-Watt, K., 2007: Mink nursing sickness. *Fur Animal Research*, 15, 157.
22. Weaver, A. C., Campbell, J. M., Crenshaw, J. D., Polo, J., Kim S. W., 2014: Efficacy of dietary spray dried plasma protein to mitigate the negative effects on performance of pigs fed diets with corn naturally contaminated with multiple mycotoxins. *J. Anim. Sci.*, 92, 3878–3886.
23. Żyłowska, M., Wszyńska, A., Jagusztyn-Krynicka, E. K., 2011: Defensins-peptides with antimicrobial activity (In Polish). *Post. Mikrobiol.*, 50, 223–234.

Received July 6, 2017

Accepted December 6, 2017



## AVIFAUNA OF LAKE GEČA — PILOT FAUNISTIC AND SEROLOGICAL STUDY

Danielová, P.<sup>1</sup>, Korytár, L.<sup>1</sup>, Csank, T.<sup>2</sup>

<sup>1</sup>Department of the Environment, Veterinary Legislation and Economy  
University of Veterinary Medicine and Pharmacy, Komenského 73, 04181 Košice

<sup>2</sup>Department of Microbiology and Immunology  
University of Veterinary Medicine and Pharmacy, Komenského 73, 04181 Košice  
Slovakia

lubos.korytar@uvlf.sk

### ABSTRACT

Lake Geča is located in the northern part of the Protected Bird Territory Košická kotlina. With a surface area of 250 ha it is the largest water area in the complex of a number of gravel lake areas located close to the villages Čaña and Geča. From 2014—2016 we used the method of capture and ringing to focus on observations of transigrating passerine birds species. This pilot study included serological testing of selected passerine species for the presence of specific antibodies to Usutu virus (USUV) by the virus neutralization test. During the field research we obtained 1077 data about ringed birds of 43 species. We received one report about the presence of a bird ringed in our study from another location in Slovakia, and 3 long distance (above 100km) reports from Hungary, Czechia and Croatia. No specific antibodies against USUV were detected in the birds tested.

**Key words:** avifauna; Geča; bird-ringing; Usutu virus

### INTRODUCTION

The Important Bird Area (IBA) Košická basin is an important territory from the point of view of the occurrence of many species of free living birds. In this territory there are several valuable locations important for the birds that use these locations throughout the year.

Lake Geča is included in the land registries of the villages Geča, Čaña and Nižná Myšľa, located south of Košice in eastern Slovakia. With a surface area of 250 ha it is the largest water area in the complex of a number of Gravel Lake areas located close to Košice, recorded in the land registries of the above mentioned villages.

In some places, the banks of the lake are bordered with extensive littoral growth with reeds and the important admixture of invasive herbs, particularly Canadian Goldenrod (*Solidago canadensis*) and Giant Goldenrod (*Solidago gigantea*). Such biotopes with dense bank growth provide good shelter and protection for the birds and provide an abundant food supply.

Currently, gravel and sand are extracted actively from Lake Geča by means of extraction boats. The vertical pro-

file of banks that are formed during the extraction is used by numerous populations of Sand Martins (*Riparia riparia*) — hundreds of pairs and European Bee-eater (*Merops apiaster*) — tens of pairs. Bank cavities primarily produced by these two species are used in the breeding period and also by other cavity nesters, such as Eurasian Tree Sparrow (*Passer montanus*), Common starling (*Sturnus vulgaris*), and Northern Wheatear (*Oenanthe oenanthe*).

From the point of view of migration, bird species can be classified as migratory, partially migratory and permanent residents that do not migrate. Climatic seasonality, interspecies and intraspecies competition are among the most important factors responsible for avian migratory behaviour. Abundance of food is characteristic of summer months while in winter the food resources are scarce. Most birds migrate before the nesting period to places where there are relatively sufficient food resources and favourable temperatures [6].

Our nesting species from the families *Sylviidae* and *Acrocephalidae* are long-distance migratory birds and the essential part of their migratory flight takes place at night [2].

Sufficient knowledge about migratory birds is important from the point of view of protection of the health of humans and other animals as they may serve as reservoirs and natural hosts of pathogens and thus play an important role in epizootic cycles [10]. With regard to evolution, humans are less closely related to birds than to mammals and because of that, birds are less responsible for the transmission of zoonotic pathogens [4]. However, due to their active flying abilities and migration they are able to transfer pathogens over long distances [7].

Usutu virus (USUV) belongs the family *Flaviviridae*, causing flavivirus infections.

The life cycle of USUV is very similar to other members of the Japanese encephalitis serocomplex [1].

In Africa USUV circulates among birds and mosquitoes while mammals serve as occasional hosts. It has a zoonotic character and humans become infected after being bitten by an infected mosquito. Humans are dead-end hosts of this virus [3, 8].

Arthropods, particularly mosquitoes (*Culex*), are vectors of USUV. Free living birds have a high potential to distribute pathogenic micro-organisms [12].

Recently, USUV has been isolated also from bats in Germany. Detection of USUV in bats raises a question of the potential role of bats as a reservoir of the virus in Africa

and its transmission by mosquitoes, which merits further research [1].

In the past, USUV was not considered a potential threat to humans as it has not been associated with death or severe disease in humans or other animals and has not been detected outside of tropical and subtropical Africa [12].

In 2001, the USUV caused the deaths of a large number of Blackbirds (*Turdus merula*) in Vienna, Austria. Bird watchers also reported clinically sick blackbirds exhibiting signs of apathy and ruffled feathers. A massive mortality of Barn Swallows (*Hirundo rustica*) was observed in Austria too. [13].

Up to now, no systematic research has been carried out in the area of Lake Geča that focused on observations of individual bird species and the dynamics of migration of small passerine birds. The aim of our study was to obtain relevant information about species spectrum of migrating passerine birds and thus contribute to the knowledge of the migration of birds in the IBA Košická basin. Another aim was to carry out serological testing for the presence of antibodies to USUV.

## MATERIALS AND METHODS

### Capture of birds and sample collection

The capture of birds and collection of samples were carried out on the basis of exemption from the Act No. 543/2002 of the Code on protection of nature and countryside, granted to trained members of the Slovak Ornithological Society/Bird Life Slovakia by the Ministry of the environment of the Slovak Republic.

The birds were trapped only by the permitted method using mist-nets.

We tested the method of night trapping of migrating passerines focusing on the species of the genera: *Acrocephalus*, *Locustella*, *Luscinia* and *Sylvia*. The night trapping was conducted during spring and autumn migrations.

During the night migration flight, the birds were attracted by means of a high performance MP3 players.

The samples of blood used for obtaining serum from the selected group of passerine birds were obtained from the *vena jugularis*.

### Serological examination

Serological examination of blood serum for the pres-

ence of antibodies to USUV was carried out by the microtitration serum-virus neutralization test. The avian sera were inactivated at 56°C for 30 min and diluted 1 : 10 with Eagle's Minimum Essential Medium (EMEM). Duplicate dilutions of samples in EMEM were prepared in 25 µl volumes. To each sample we added the equivalent volumes of 100 TCID<sub>50</sub> viral strains WNV 578/10 and USUV 939/01 (kindly provided by Prof. Norbert Nowotny, University of Veterinary Medicine in Vienna, Austria). Each serum sample was subjected to cytotoxicity checking by adding 25 µl of EMEM medium instead of the virus. After a 1-hour incubation at 37°C, we added to each sample, 50 µl of 10% EMEM solution with antibiotics, containing 1×10<sup>4</sup> Vero E6 cells. Microtitration plates were incubated at 37°C for 5 days under 5% CO<sub>2</sub>.

## RESULTS

During 2014, we obtained information about 556 trapped and ringed birds belonging to 36 species (Table 1).

In the years 2015 and 2016, we trapped and recorded 284 and 232 birds, mostly passerines (Tables 2 and 3).

Of the number we ringed 229 birds that belonged to 24 species, 3 of them were local birds that were retrapped after the previous marking.

We received four retrospective reports about birds ringed within our study from other locations. A Western Yellow Wagtail (*Motacilla flava*), ringed in 2014, was trapped by a bird ringer in the location of Perín ponds in the same year; Sedge Warbler (*Acrocephalus schoenobaenus*), ringed in the autumn of 2014, was checked by a ringer in the following season in Szeged, Hungary, 277 km away from lake Geča. Savi's Warbler (*Locustella luscinioides*),

**Table 1. Birds ringed in 2014**

Species	Ringed	Species	Ringed
<i>Acrocephalus arundinaceus</i>	1	<i>Motacilla flava</i>	21
<i>Acrocephalus palustris</i>	43	<i>Parus major</i>	96
<i>Acrocephalus scirpaceus</i>	25	<i>Passer domesticus</i>	7
<i>Acrocephalus schoenobaenus</i>	30	<i>Passer montanus</i>	83
<i>Aegythals caudatus</i>	11	<i>Phoenicurus ochruros</i>	2
<i>Carduelis cannabina</i>	12	<i>Phylloscopus collybita</i>	50
<i>Carduelis carduelis</i>	9	<i>Phylloscopus sibilatrix</i>	6
<i>Cyanistes caeruleus</i>	51	<i>Phylloscopus trochilus</i>	2
<i>Emberiza schoeniclus</i>	8	<i>Prunella modularis</i>	8
<i>Erithacus rubecula</i>	1	<i>Remiz pendulinus</i>	2
<i>Ficedula albicollis</i>	1	<i>Riparia riparia</i>	17
<i>Hippolais icterina</i>	1	<i>Serinus serinus</i>	3
<i>Hirundo rustica</i>	1	<i>Sturnus vulgaris</i>	1
<i>Chloris chloris</i>	3	<i>Sylvia atricapilla</i>	24
<i>Lanius collurio</i>	3	<i>Sylvia borin</i>	4
<i>Locustella luscinioides</i>	2	<i>Sylvia communis</i>	16
<i>Luscinia megarhynchos</i>	2	<i>Sylvia curruca</i>	4
<i>Merops apiaster</i>	7	<i>Sylvia nisoria</i>	1

Source: An original table

**Table 2. Birds ringed in 2015**

<b>Species</b>	<b>Ringed</b>	<b>Species</b>	<b>Ringed</b>
<i>Acrocephalus arundinaceus</i>	15	<i>Merops apiaster</i>	1
<i>Acrocephalus palustris</i>	93	<i>Parus major</i>	3
<i>Acrocephalus scirpaceus</i>	34	<i>Passer montanus</i>	14
<i>Acrocephalus schoenobaenus</i>	35	<i>Phylloscopus collybita</i>	5
<i>Carduelis cannabina</i>	1	<i>Phylloscopus sibilatrix</i>	2
<i>Carduelis carduelis</i>	2	<i>Phylloscopus trochilus</i>	4
<i>Coturnix coturnix</i>	1	<i>Remiz pendulinus</i>	11
<i>Cyanistes caeruleus</i>	10	<i>Riparia riparia</i>	1
<i>Emberiza schoeniclus</i>	3	<i>Sylvia atricapilla</i>	13
<i>Ficedula albicollis</i>	1	<i>Sylvia borin</i>	2
<i>Chloris chloris</i>	1	<i>Sylvia communis</i>	15
<i>Ixobrychus minutus</i>	1	<i>Sylvia curruca</i>	4
<i>Lanius collurio</i>	1	<i>Sylvia nisoria</i>	3
<i>Locustella fluviatilis</i>	2	<i>Turdus merula</i>	1
<i>Locustella luscinioides</i>	3	<i>Turdus philomelos</i>	1
<i>Luscinia megarhynchos</i>	1		

Source: An original table

**Table 3. Birds ringed in 2016**

<b>Species</b>	<b>Ringed</b>	<b>Species</b>	<b>Ringed</b>
<i>Acrocephalus arundinaceus</i>	1	<i>Passer montanus</i>	4
<i>Acrocephalus palustris</i>	37	<i>Phylloscopus collybita</i>	4
<i>Acrocephalus scirpaceus</i>	17	<i>Phylloscopus sibilatrix</i>	1
<i>Acrocephalus schoenobaenus</i>	14	<i>Phylloscopus trochilus</i>	1
<i>Cyanistes caeruleus</i>	13	<i>Remiz pendulinus</i>	3
<i>Emberiza schoeniclus</i>	2	<i>Sturnus vulgaris</i>	1
<i>Ixobrychus minutus</i>	1	<i>Sylvia atricapilla</i>	74
<i>Locustella luscinioides</i>	5	<i>Sylvia borin</i>	22
<i>Locustella naevia</i>	3	<i>Sylvia communis</i>	9
<i>Luscinia luscinia</i>	2	<i>Sylvia curruca</i>	5
<i>Luscinia megarhynchos</i>	4	<i>Turdus merula</i>	1
<i>Parus major</i>	2	<i>Turdus philomelos</i>	3

Source: An original table

ringed in the autumn of 2015, was found alive in the following year during nesting season in Březina, Czech Republic, location, 500 km away. A Great Reed Warbler (*Acrocephalus arundinaceus*), ringed at lake Geča in 2015, was trapped by ornithologists during a direct migration flight in Croatia, at Vransko jezero lake, 686 km from Geča, only 14 days following the ringing.

A selected group of passerine birds trapped during 2016 was tested for the presence of antibodies to USUV: Great Reed Warbler (*Acrocephalus arundinaceus*) (n = 1); Marsh Warbler (*Acrocephalus palustris*) (n = 10), Eurasian Reed Warbler (*Acrocephalus scirpaceus*) (n = 10); Sedge Warbler (*Acrocephalus schoenobaenus*) (n = 3); Eurasian Blackcap (*Sylvia atricapilla*) (n = 31); Thrush Nightingale (*Luscinia luscinia*) (n = 2); Common Nightingale (*Luscinia megarhynchos*) (n = 3); Eurasian Tree Sparrow (*Passer montanus*) (n = 1); Garden Warbler (*Sylvia borin*) (n = 6); Whitethroat (*Sylvia communis*) (n = 5); Lesser Whitethroat (*Sylvia curruca*) (n = 2); and Song Thrush (*Turdus obscurus*) (n = 2).

## DISCUSSION

The primary results of trapping and ringing obtained in 2014 indicated that the investigated location plays an important role in the migration of diverse species and spectrum of passerine birds.

It is well known that the European species of the genera *Acrocephalus*, *Sylvia* and *Locustella*, wintering in sub-Saharan Africa, belong primarily to night migrants [9, 11]. The species of these genera may be attracted during their migratory night flights by strong light sources (reflectors, lighthouses and similar) and identically, during the day, by playing the recordings of the corresponding bird species [5].

The second of the above mentioned phenomena was tested successfully, as it attracted birds flying over our location and allowed us to trap them in impact nets at selected trapping points.

We gained primary experience with such night trapping focusing specifically on acrocephalid warblers (*A. palustris*, *A. scirpaceus*, *A. schoenobaenus* and *A. arundinaceus*) and *Locustella* (*L. fluviatilis*, *L. luscinioides*) at lake Geča during the 2015 trapping season.

An interesting experience was the entrapment of an adult female of Little Bittern (*I. minutus*). On the basis of this and related visual observation we can confirm the view that birds of this species can be successfully attracted during night hours by sounds of *Acrocephalus* spectrum.

We consider it a success that we were able to confirm assumption from the previous season (2014) that the investigated location is a part of a migration corridor of our rare species of the Barred Warbler (*S. nisoria*), as indicated by successful trapping and ringing of 3 juvenile specimens.

In 2016, we successfully used *Acrocephalus* sounds to trap in complete darkness another juvenile Little Bittern.

USUV has not yet been isolated from birds in the Slovak territory. A part of our survey was the serological testing of lake Geča avifauna for the presence of specific antibodies to USUV. For this purpose we subjected the selected group of birds to virus neutralisation test and confirmed the absence of this virus in the investigated location.

Recently, USUV was isolated from bats in Germany. This detection of USUV in bats raises a question that should be addressed in future research including the potential role of bats as reservoirs in Africa and the transmission of USUV by mosquitoes [1]. Our examination failed to confirm seropositivity of birds from the selected group of passerine birds.

## CONCLUSIONS

During 2014–2016 we carried out the first systematic monitoring of avifauna so far of the ontologically non-investigated lake Geča location. During field investigation we obtained 1077 data about trapped and ringed birds belonging to 43 species.

We received four retrospective reports from other locations about birds ringed during our study.

The presence of specific antibodies to USUV was not confirmed in any of the samples of passerine birds.

## ACKNOWLEDGEMENT

*The study was carried out within the work on the project VEGA 1/0729/16.*

## REFERENCES

1. Ashraf, U., Ye, J., Ruan, X., Wan, S., Zhu, B., Cao, S., 2015: Usutu virus: An emerging flavivirus in Europe. *Viruses*, 7, 219–238.
2. Berthold, P., 1993: *Bird Migration: A General Survey*. Oxford University Press, Oxford, 239 pp.
3. Buckley, A., Dawson, A., Moss, R. S., Hinsley, S. A., Bellamy, P. E., Gould, E. A., 2003: Serological evidence of West Nile virus, Usutu virus and Sindbis virus infection of birds in the UK. *Journal of General Virology*, 84, 2807–2817.
4. Cleaveland, S., Laurenson, M. K., Taylor, L. H., 2001: Diseases of humans and their domestic mammals: pathogen characteristics, host range and the risk of emergence. *Philos. Trans. Roy. Soc. Lond., B, Biol. Sci.*, 356, 1411.
5. Kennerley, P., Pearson, D., 2010: *Reed and Bush Warblers*. London, Helm, 28–30.
6. Klvaňa, P., 2008: Bird migration (In Czech). In Cepák, J., et al. (Eds.): *Atlas of Migration of Birds of Czech and Slovak Republics* (In Czech). Aventinum, Prague, 8–15.
7. Kruse, H., Kirkemo, A. M., Hendeland, K., 2004: Wildlife as source of zoonotic infections. *Emerg. Infect. Dis.*, 10, 2067–2072.
8. Mackenzie, J. S., Gubler, J. D., Peterson, L. R., 2004: Emerging flaviviruses: the spread and resurgence of Japanese encephalitis, West Nile and dengue viruses. *Nature Medicine Supplement*, 10, 98–109.
9. Newton, I., 2008: *The Migration Ecology of Birds*. London, Academic Press, 976 pp.
10. Reed, K. D., Meece, J. K., Henkel, J. S., Shukla, S. K., 2003: Birds, migration and emerging zoonoses: West Nile Virus, Lyme disease, influenza A and enteropathogens. *J. Clin. Med. Res.*, 1, 5–12.
11. Shirihai, H., Gargallo, G., Helbig, A. J., 2015: *Sylvia Warblers. Identification, Taxonomy and Phylogeny of the Genus Sylvia*. London, Christopher Helm, 576 pp.
12. Vázquez, A., Jiménez-Clavero, M. A., Franco, L., Donoso-Mantke, O., Sambri, V., Niedrig, M., et al., 2011: Usutu virus — potential risk of human disease in Europe. *EuroSurveillance*, 16, 5 pp.
13. Weissenböck, H., Mannsberger, S. CH., Bakonyi, T., Nowotny, N., 2007: Emergence of Usutu virus in Central Europe: diagnosis, surveillance and epizootiology. In Takken, W., Knols, B. G. J. (Eds.): *Emerging Pests and Vector-borne Diseases in Europe*. Wageningen Academic Publishers, The Netherlands 153–168.

Received, October 3, 2017

Accepted, December 12, 2017



## MONITORING OF $^{137}\text{Cs}$ AND $^{40}\text{K}$ IN THE LEVICE DISTRICT, SOUTHERN SLOVAKIA

Kanta, M., Beňová, K.

Department of Biology and Genetics, Institute of biology, zoology and radiobiology  
University of Veterinary Medicine and Pharmacy, Komenského 73, 04181 Košice  
Slovakia

katarina.benova@uvlf.sk

### ABSTRACT

The contamination of the environment, soil and meat of wild animals with radionuclides can negatively affect human health. The aim of our study was to analyse the risk arising from post-Chernobyl contamination of the meat of wild boars (*Sus scrofa*) originating from the district Levice, southern Slovakia, with the radioactive artificial element  $^{137}\text{Cs}$ . The level of natural radionuclide  $^{40}\text{K}$  was also determined. We examined altogether 45 samples obtained from 9 wild boars hunted in this area during the period of 2013—2015. From each animal we collected and analysed samples from the thigh, stomach contents, stomach muscles and skin. We also examined samples of soil from the locations where these animals were shot. The activity values of radioactive caesium  $^{137}\text{Cs}$  determined in this study were very low and therefore the consumption of wild boar meat originating from this location presents no risk to human health.

**Key words:** contamination;  $^{137}\text{Cs}$ ;  $^{40}\text{K}$ ; radionuclides; soil; wild boar

### INTRODUCTION

The natural environment is exposed to various chemical contaminants, including the radioactive elements; some of them long-lived naturally occurring radionuclides. There are approximately 60 natural radionuclides and one of the most abundant elements in the Earth's crust is  $^{40}\text{K}$  that remains to this point of time [9]. Another source of radioactivity has a cosmogenic origin and is the result of interaction between certain gases in the atmosphere and cosmic rays. Besides such sources of naturally occurring radiation exposure, the natural environment may be subjected to radioactive contamination caused by human activity including nuclear weapon tests, the accidents of nuclear power plants, and processing or storage of nuclear fuel and waste. Such contamination can have long term effects on some biocenoses [1].

Of the several catastrophic nuclear accidents that happened in the nuclear energy era, the Chernobyl was probably the worst. Due to the explosion and fire at the Chernobyl power plant on April 26, 1986, about  $3.8 \times 10^{16}$  Bq of radioactive caesium was released to the atmosphere. The

ratio of the escaped radioactive caesium  $^{137}\text{Cs}$  and  $^{134}\text{Cs}$  was approximately 2:1 [16]. The radioactive cloud released during the accident reached even very distant places all over Europe. With regard to the distance of the former Czechoslovakia from Chernobyl, the estimated 1986 effective dose for children was 0.36 mSv and for adults 0.22 mSv. The most affected regions of Europe included for example Norway where the  $^{137}\text{Cs}$  activity reached levels as high as  $500\text{ kBq}\cdot\text{m}^{-2}$  [13].

With regard to the time lapse and the character of the nuclear accident, of all artificial radionuclides only  $^{137}\text{Cs}$ , with a physical half-life decay of 30 years, occurs in the soil in Slovakia [6]. Generally, radionuclides show a very high mobility in soil [2]. The  $^{137}\text{Cs}$  and  $^{40}\text{K}$  isotopes belong to the same group of alkali metals, have similar chemical properties and are strong reducing agents. This is an explanation for competitive-sorption behaviour between  $^{40}\text{K}$  and  $^{137}\text{Cs}$  in mountain soils [8]. It was observed that with an increase in the soil density, which is related to the amount of organic matter, the concentration of  $^{137}\text{Cs}$  decreased and at the same time the amount of natural  $^{40}\text{K}$  increased. The features of upper soil layers including the content of organic matter and resulting concentration and immobilization of  $^{137}\text{Cs}$  in soil may be affected also by other factors, such as altitude [9].

Plant uptake is the major pathway for the migration of radiocaesium from soil to animal and human diets. Caesium has a high mobility within plants. Although radiocaesium is most likely taken up by the K transport systems within the plant, differences in internal Cs concentration (on a dry matter basis) may vary by a factor of 20 between different plant species grown under similar conditions [17]. Uptake of  $^{137}\text{Cs}$  from the environment by some plants is very high so these plants serve as bioindicators of contamination with this radionuclide [11]. Mosses are capable of taking up as much as 93 % of the incident radionuclides [3]. Other organisms that are able to accumulate  $^{137}\text{Cs}$  to the largest extent are mushrooms [4]. Because radioactive caesium is continuously taken up and passed on by organisms in forest ecosystems, the animals and vegetation in the affected forests and mountains are especially contaminated. The level of radiopotassium in soil affects the absorption of radiocaesium by plants which then serve as food for wild boars and radiocaesium in wild boar meat which is a potential source of exposure of people to this radionuclide.

With raw materials, semi-products and final products originating totally or partially from forest ecosystems one must consider the presence of increased levels of radioactive caesium. Under central European conditions, the Chernobyl accident resulted in the highest contamination of game meat. With regard to the still persisting limit-exceeding levels of radioactive caesium in the meat of wild boars recorded in Germany and Czechia, this meat can act as the main source of radiation exposure to humans [1].

The aim of our study was to monitor the level of the radionuclides  $^{40}\text{K}$  and  $^{137}\text{Cs}$  in the meat of wild boars hunted in the Levice district in Slovakia, and in the soil from the locations where these animals were hunted.

## MATERIALS AND METHODS

The samples were collected from 8 wild boars shot in the hunting grounds PZ Svätý Bartolomej Hontianske Trst'any in November-December of the 2013–2015 hunting season and from 1 male wild boar killed in August at the airport in PZ Hokovce. Altogether 45 samples were obtained from the boars, 5 samples from each animal: thigh muscle (0.5 kg); skin with hair ( $10\times 10\text{ cm}$ ); the whole stomach with its contents. We also collected one sample from the surface horizon of soil (0.5 l) from the location where each animal was shot. Information about the boars (*Sus scrofa*) is presented in Table 1.

After removing twigs and leaves from soil samples, the samples were transferred to Marinelli vessels to a volume of 450 ml. Thigh and stomach muscles and skin were cut to small pieces of approximately  $1\text{--}2\text{ cm}^3$ . The stomach contents were used for measurements without any processing.

All samples were transferred to Marinelli vessels and measurements of the individual radionuclides were performed using a gamma spectrometer equipped with HPGe detector (HPGeGC2020, 20 % effectiveness; 1.8 resolution) and an interpretation unit desktop Inspektor, validated by Czech Metrological Institute. The analysis of all spectra was performed using the software system Genie 2000 (Canberra). All measurements were carried out at the Veterinary and Pharmaceutical University in Brno, Czechia. The presented relative standard uncertainties  $u_a$  were determined according to IOS Geneve [7].

**Table 1. Information about the wild boars (*Sus scrofa*)**

Boar number	Gender	Age	Weight [kg]	Hunting range	Location	Date of sampling
1	Male	7 years	140	Hontianske Trstany	Ďapúš	30th Nov., 2013
2	Female	1 month	10	Hontianske Trstany	Koryto	7th Dec., 2013
3	Female	8 months	60	Hontianske Trstany	Stará hora	7th Dec., 2013
4	Male	2 months	15	Hokovce	Letisko	30th Aug., 2015
5	Male	3 months	30	Hontianske Trstany	Hopkov	2nd Nov., 2015
6	Female	14 months	60	Hontianske Trstany	Hopkov	11th, Nov., 2015
7	Female	4 months	20	Hontianske Trstany	Nad baňou	12th Nov., 2015
8	Female	3 years	80	Hontianske Trstany	Nad baňou	24th Nov., 2015
9	Female	4 years	90	Hontianske Trstany	Slaný bok	24th Nov., 2015

## RESULTS AND DISCUSSION

Results of measurements of the activity of radiocaesium  $^{137}\text{Cs}$  and radiopotassium  $^{40}\text{K}$  in Becquerel per kg are presented as relative standard means in Table 2.

Soil is the first link in the food chain. Soil is one of the few components of the environment in which the  $^{137}\text{Cs}$  can be detected even today. This radionuclide is best retained by clayey materials [2]. Kubica et al. [9] investigated the radioactivity of artificial  $^{137}\text{Cs}$  and natural  $^{40}\text{K}$  in the soils collected from the main Ridge of the Flysh Carpathians and observed high variations with respect to individual regions and layers of soil cores. The lowest concentration of  $^{137}\text{Cs}$  was  $16\text{ Bq.kg}^{-1}$  and the highest reached was  $1,127\text{ Bq.kg}^{-1}$ . They reported that fluctuation of the radionuclides concentrations in the soils could strongly depend also on the meteorological conditions. All sampling sites with high level of  $^{40}\text{K}$  showed low concentration of  $^{137}\text{Cs}$ .

Of the radiation emitted from the Chernobyl disaster, only  $^{137}\text{Cs}$  is detected in the soil in the Slovak territory. The soil relief in the district Levice, southern Slovakia, is affected considerably by natural conditions. Despite the presence of illimerised soil, the radiocaesium activity in the soil samples measured in our study was low and did not exceed  $68.7 \pm 4.6\text{ Bq.kg}^{-1}$ . Except for the samples of soil related to wild boar No. 5, we did not observe relationship between the level of  $^{40}\text{K}$  and  $^{137}\text{Cs}$ .

In Central Europe, game meat showed the highest degree of radioactive contamination after the Chernobyl nuclear accident [13]. Radionuclides pass to the meat of

wild boars particularly by consumption of mushrooms *Elaphomyces granulatus*, which are favoured by these animals. Dvořák et al. [1] investigated activities of various diet components of wild boars and reported that the activity of fruiting body of the above mushroom collected in location Šabrava, situated in the Odry Highlands and partly in the Nízký Jeseník mountains, was the highest and reached  $4743\text{ Bq.kg}^{-1}$  and  $2858\text{ Bq.kg}^{-1}$ . However, most components of food found in the stomach contents manifested specific activities lower than the minimum detectable activity [1].

While during the study conducted in Germany (1986—2003) the level of radiocaesium in the meat of roe deer gradually decreased, it persisted at relatively stable level in the meat of wild boars. In the period of 1998—2008, muscles from 656 wild boars hunted in the Ravensburg district (southern Germany) were analysed for  $^{137}\text{Cs}$ . The activity varied from less than 5 up to  $8\,266\text{ Bq.kg}^{-1}$  in dependence on season, atmospheric conditions and the related feeding habits of wild boars and availability of feed [14]. Hohman and Huckschlag [5] observed that the highest concentration of  $^{137}\text{Cs}$  in the muscles was detected in winter. The authors examined also stomach contents and found out that they were usually less contaminated compared to muscles; the median of the stomach content was  $22\text{ Bq.kg}^{-1}$ , the maximum  $1749\text{ Bq.kg}^{-1}$ , while the median of muscle was  $129\text{ Bq.kg}^{-1}$ , and the maximum  $5,573\text{ Bq.kg}^{-1}$ . No difference in the specific activities of female and male muscles was proved.

After a gradual decrease in the activity of radiocaesium in game meat in the 90s in north-eastern Moravia, its levels unexpectedly increased after floods [12]. The  $^{137}\text{Cs}$  ac-

**Table 2. The level of activity of radiocaesium and radiopotassium (relative standard uncertainties  $u_r$ ) in the samples**

		Thigh muscle	Skin + hair	Stomach muscle	Stomach content	Soil
Boar 1	$^{137}\text{Cs}$ [Bq.kg <sup>-1</sup> ]	< 3.1 ± 8.0	< 3.6 ± 7.8	< 0.56 ± 4.6	3.54 ± 25.0	45.2 ± 3.8
	$^{40}\text{K}$ [Bq.kg <sup>-1</sup> ]	< 80.0 ± 7.8	< 90 ± 7.8	11.6 ± 4.7	30.8 ± 7.9	389 ± 3.8
Boar 2	$^{137}\text{Cs}$ [Bq.kg <sup>-1</sup> ]	< 14.0 ± 7.5	< 5.0 ± 7.8	0.23 ± 20.4	0.61 ± 10.5	39.2 ± 3.9
	$^{40}\text{K}$ [Bq.kg <sup>-1</sup> ]	< 330 ± 7.8	< 120 ± 8.1	62.3 ± 2.46	58.7 ± 3.9	409 ± 3.8
Boar 3	$^{137}\text{Cs}$ [Bq.kg <sup>-1</sup> ]	3.14 ± 25	< 4.2 ± 7.8	0.7 ± 23.3	0.87 ± 17.9	68.7 ± 4.6
	$^{40}\text{K}$ [Bq.kg <sup>-1</sup> ]	< 76 ± 7.9	< 100 ± 7.8	16.6 ± 4.8	20.4 ± 4.8	341 ± 3.7
Boar 4	$^{137}\text{Cs}$ [Bq.kg <sup>-1</sup> ]	< 11.0 ± 7.5	< 29 ± 7.8	< 3.4 ± 0.27	< 3.4 ± 0.27	41.5 ± 3.9
	$^{40}\text{K}$ [Bq.kg <sup>-1</sup> ]	< 260 ± 7.9	< 740 ± 7.8	32.1 ± 8.0	< 86 ± 7.8	375 ± 3.8
Boar 5	$^{137}\text{Cs}$ [Bq.kg <sup>-1</sup> ]	< 13 ± 7.8	< 6.3 ± 7.8	< 3.7 ± 7.8	0.33 ± 13.9	27 ± 3.9
	$^{40}\text{K}$ [Bq.kg <sup>-1</sup> ]	< 320 ± 7.9	< 160 ± 7.9	< 91 ± 7.8	63.9 ± 3.9	30.7 ± 4.5
Boar 6	$^{137}\text{Cs}$ [Bq.kg <sup>-1</sup> ]	2.0 ± 61.3	< 7.1 ± 7.9	< 0.76 ± 4.8	0.51 ± 10.9	65.3 ± 3.9
	$^{40}\text{K}$ [Bq.kg <sup>-1</sup> ]	< 130 ± 10.1	< 180 ± 7.9	23.3 ± 4.8	73.1 ± 3.9	170 ± 3.9
Boar 7	$^{137}\text{Cs}$ [Bq.kg <sup>-1</sup> ]	< 8.5 ± 7.8	< 6.7 ± 7.9	< 3.7 ± 7.8	0.86 ± 8.5	51.2 ± 3.8
	$^{40}\text{K}$ [Bq.kg <sup>-1</sup> ]	< 210 ± 7.9	< 170 ± 7.7	< 95 ± 7.8	60.8 ± 3.9	358 ± 13.7
Boar 8	$^{137}\text{Cs}$ [Bq.kg <sup>-1</sup> ]	< 6.7 ± 7.8	0.66 ± 34.2	0.12 ± 25.0	0.69 ± 10.1	59.6 ± 3.8
	$^{40}\text{K}$ [Bq.kg <sup>-1</sup> ]	105 ± 7.8	30.7 ± 1.47	53.1 ± 4.0	57.6 ± 3.9	292 ± 3.8
Boar 9	$^{137}\text{Cs}$ [Bq.kg <sup>-1</sup> ]	1.5 ± 44.0	0.59 ± 15.9	0.11 ± 20.5	0.47 ± 12.1	63.7 ± 4.6
	$^{40}\text{K}$ [Bq.kg <sup>-1</sup> ]	21.9 ± 7.9	22.9 ± 4.5	41.2 ± 4.0	49.4 ± 3.9	243 ± 4.7

tivities in wild boar meat exceeded the acceptable limit of 600 Bq.kg<sup>-1</sup>. This involved particularly the animals younger than 1 year. By year 2000, radiocaesium activity decreased again down to the levels measured before the flooding. Latini [10] called attention to the limit exceeding levels in wild boar meat in the region of Šumava where the level in the muscles reached 10 699 Bq.kg<sup>-1</sup>.

Šprem et al. [15] investigated the  $^{137}\text{Cs}$  and  $^{40}\text{K}$  load in large mammal game species (10 brown bear, 9 wild boar, 7 roe deer, 21 red deer and 2 chamois) in the mountain forest region of Gorski Kotar in Croatia. The results indicated that herbivore game species show significantly lower  $^{137}\text{Cs}$  concentrations than omnivore species (brown bear, wild boar), thereby confirming the hypothesis that

different dietary strategy impact caesium concentration in meat. The measured caesium load in brown bear meat was in the range of two orders of magnitude, while caesium load in wild boar meat was found in the range of one order of magnitude. The estimated effective equivalent dose showed that the highest caesium uptake would be with the consumption of brown bear and wild boar meat and much lower doses could be taken in by the consumption of the meat from herbivore species. In this study, the measured  $^{40}\text{K}$  concentrations were uniformly distributed among the sampled species and none of the species stood out in terms of measured concentrations. A 7-year old male brown bear had significantly lower  $^{40}\text{K}$  concentrations ( $83.0\text{ Bq}\cdot\text{kg}^{-1}$ ) and also the lowest load of  $^{137}\text{Cs}$  ( $1.88\text{ Bq}\cdot\text{kg}^{-1}$ ), showing a similar parallel trend of the two radionuclides.

Our study showed considerable variation of results of both radionuclides in individual boars. The load of both  $^{137}\text{Cs}$  and  $^{40}\text{K}$  in the thigh of wild boar 2 was the highest; so was the  $^{40}\text{K}$  soil load in the area where this boar was shot, but not the concentration of  $^{137}\text{Cs}$  in the soil. The lowest load of  $^{137}\text{Cs}$  was determined in the thigh, skin and hair, and stomach muscle of boar No. 9, but the  $^{137}\text{Cs}$  level in the soil in its home range was close to the maximum level determined in our study.

In the study by Šprem et al. [15] the concentration of  $^{137}\text{Cs}$  found in muscles of wild boar ( $n=9$ ) ranged from  $6.34$  to  $58.7\text{ Bq}\cdot\text{kg}^{-1}$  ( $25.0 \pm 19.6\text{ Bq}\cdot\text{kg}^{-1}$ ) and of  $^{40}\text{K}$  from  $104$  to  $117\text{ Bq}\cdot\text{kg}^{-1}$  ( $113 \pm 4.01\text{ Bq}\cdot\text{kg}^{-1}$ ). These levels were not far from those determined in our study. The highest level of  $^{137}\text{Cs}$  determined in our study in thigh muscle was  $<14 \pm 7.5\text{ Bq}\cdot\text{kg}^{-1}$ , which is much lower than the acceptable limit of  $600\text{ Bq}\cdot\text{kg}^{-1}$ .

We observed no relationship between the stomach contents and meat contamination with Cs contrary to observations reported by Hohmann and Huckschlag [5], however the latter authors examined samples from much higher number of animals (2433).

Wild boars as non-specific omnivores are capable of adapting their eating habits to local and seasonal conditions. According to Hohmann and Huckschlag [5] the radiocaesium is more readily available to the organisms in the forest ecosystems than in agricultural areas owing to the differences in soil characteristics. Wild boars in the district Levice fed during the year on agricultural crops and in winter they were provided concentrate or bulk feed through game feeding. This is probably one of the reasons

why the measured activity of  $^{137}\text{Cs}$  in meat from wild boars living in district Levice was so low.

## CONCLUSIONS

Despite considerable diversity of natural conditions in the district Levice, southern Slovakia, the consumption of meat from game living in this area poses no risk to humans as far as the activity of  $^{137}\text{Cs}$  is concerned. This is indicated by our measurements of this radionuclide in samples from wild boars and soil. None of the samples exceeded or even approached the maximum acceptable level of  $600\text{ Bq}\cdot\text{kg}^{-1}$ . However, monitoring of the risk related to this radionuclide is still important as values exceeding this limit can be measured even today in some Germany and Czechia territories.

## REFERENCES

1. Dvořák, P., Snášel, P., Beňová, K., 2010: Transfer of radiocesium into wild boar Meat. *Acta Veterinaria Brno*, 79, 85–91.
2. Gadd, G. M., 1996: Influence of microorganisms on the environmental fate of radionuclides. *Endeavour*, 20, 150–156.
3. Heinrich, G., Müller, H. J., Oswald, K., Griesa, 1989: Natural and artificial radionuclides in selected styrian soils and plants before and after the reactor accident in Chernobyl. *Biochem. Physiol. Pflanzen*, 185, 55–67.
4. Henrich, G., 1991: Uptake and transfer factors of  $^{137}\text{Cs}$  by mushrooms. *Radiat. Environ. Biophys.*, 31, 39–49.
5. Hohmann, U., Huckschlag, D., 2005: Investigations on the radiocaesium of wild boar (*Sus scrofa*) meat in Rhineland-Palatine: a stomach content analysis. *European Journal of Wildlife Research*, 51, 263–270.
6. IHE, 1987: *Report on Radiation Situation in Czechoslovak Territory after Chernobyl Nuclear Accident* (In Czech). Institute of Hygiene and Epidemiology — Radiation Hygiene Centre. The main nuclear programme information centre, Prague, 168 pp.
7. IOS Geneve, 1993: *Guide to the Expression of Uncertainty in Measurement for Standardization*, 1st edn., corrected and reprinted in 1995, International Organization for Standardization, Geneva, Switzerland.
8. Kubica, B., Skiba, S., Drewnik, M., Stobinski, M., Kubica, M., Golas, J., Misiak, R., 2010: The radionuclides ( $^{137}\text{Cs}$  and  $^{40}\text{K}$ ) in soil samples taken from Tatra National Park (TPN, Poland). *Nukleonika*, 55, 377–387.

9. Kubica, B., Szarlowicz, K., Stobinski, M., Skiba, S., Reczynski, W., Golas, J., 2014: Concentrations of  $^{137}\text{Cs}$  and  $^{40}\text{K}$  radionuclides and some heavy metals in soil samples from the eastern part of the Main Ridge of the Flysch Carpathians. *J. Radioanal. Nucl. Chem.*, 299, 1313—1320.
10. Latini, T., 2011: Occurrence of radioactivity in wild boars (In Czech). *Maso (Meat)*, 5, 24—26.
11. Nimis, P.L., 1996: Radiocesium in plants of forest ecosystems. *Studia Geobotanica*, 15, 3—49.
12. Obzina, J., 2002: Radiocaesium Findings in Meat of Game Shot in the Period of 1992—2002 in the Districts Šumperk and Jeseník (In Czech). Attestation thesis. Veterinary and Pharmaceutical University in Brno, 35 pp.
13. Pedersen, Ch. S., Nyb, S., Varskog, P., 1998: Seasonal variation in radiocesium concentration in Willow Ptarmigan and Rock Ptarmigan in Central Norway after the Chernobyl fallout. *Journal of Environmental Radioactivity*, 41, 65—81.
14. Semizhon, T., Putyrskaya, V., Zibold, G., Klemt, E., 2009: Time-dependency of the  $^{137}\text{Cs}$  contamination of wild boar from a region in Southern Germany in the years 1998 to 2008. *Journal of Environmental Radioactivity*, 100, 988—992.
15. Šprem, N., Babic, I., Barišić, D., Barišić, D., 2013: Concentration of  $^{137}\text{Cs}$  and  $^{40}\text{K}$  in meat of omnivore and herbivore game species in mountain forest ecosystems of Gorski Kotar, Croatia. *J. Radioanal. Nucl. Chem.*, 298, 513—517.
16. UNSCEAR, 1988: *Source, Effects and Risk of Ionizing Radiation*. Report to the General Assembly with Scientific Annexes, Vol. 1, Scientific Annex A, New York, UN.
17. Zhu, Y.-G., Smolders, E., 2000: Plant uptake by radiocaesium: a review of mechanisms, regulation and application. *Journal of Experimental Botany*, 51, 1635—1645.

Received October 11, 2017

Accepted December 14, 2017



## CROSSING THE BLOOD-BRAIN BARRIER BY NEUROINVASIVE PATHOGENS

Tkáčová, Z.<sup>1</sup>, Kaňová, E.<sup>1</sup>, Jiménez-Munguía, I.<sup>1</sup>  
Čomor, L.<sup>1</sup>, Širochmanová, I.<sup>1</sup>, Bhide, K.<sup>1</sup>, Bhide, M.<sup>1,2</sup>

<sup>1</sup>Laboratory of Biomedical Microbiology and Immunology  
University of Veterinary Medicine and Pharmacy, Kosice

<sup>2</sup>Institute of Neuroimmunology, Slovak Academy of Sciences, Bratislava  
Slovakia

[zuzana.tkacova17@gmail.com](mailto:zuzana.tkacova17@gmail.com)

### ABSTRACT

The penetration of the blood-brain barrier (BBB) and invasion of the central nervous system (CNS) are important steps for all neuroinvasive pathogens. All of the ways of pathogens passing through the BBB are still unclear. Among known pathways, pathogen traversal can occur paracellularly, transcellularly or using a “Trojan horse” mechanism. The first step of translocation across the BBB is the interactions of the pathogen’s ligands with the receptors of the host brain cells. Lyme disease, the most common vector-borne disease in the temperate zones of Europe and North America, are caused by *Borrelia* species (former *Borrelia burgdorferi sensu lato*) that affects the peripheral and the CNS. In this review, we have presented various pathogen interactions with endothelial cells, which allow the disruption of the BBB so that the pathogens can pass across the BBB.

**Key words:** blood-brain barrier; *Borrelia*; paracellular and transcellular passage; “Trojan horse” mechanism

### INTRODUCTION

Infections of the CNS, with associated high morbidity often cause serious permanent damage to the CNS [20]. Despite the availability of antimicrobial treatment, in the last two decades, an increase in the incidence of bacterial neuroinfections has been recorded. A large number of bacterial pathogenic species have the potential to infect the CNS. Nevertheless, it is not clear why a relatively small number of pathogens are responsible for infections of the CNS. Among various bacterial pathogens which cause infections of the CNS, *Neisseria meningitidis*, *Borrelia*, *Streptococcus pneumoniae* and *Listeria monocytogenes* are the most important ones in central Europe [30]. These pathogens are capable of crossing the BBB, where they invade the CNS, which further leads to damaged cells of the neurovascular unit (NVU). The neurovascular unit includes the brain microvascular endothelial cells (BMEC), glial cells, astrocytes and neurons [13] (Fig. 1).

## Blood-brain barrier

The BBB is a regulatory interface between the peripheral circulation and the CNS [30]. The BBB regulates the passage of blood-borne substances and cells into the brain and thus maintains the homeostasis of the neural microenvironment that is crucial for normal neuronal activity and function [1]. It is a specialized system which has a unique role in the protection of the brain from toxic substances in blood and filters harmful compounds from the brain back to the bloodstream. The BBB allows the passage of water, some gases, and lipid-soluble molecules by passive diffusion, as well as the selective transport of molecules such as glucose and amino acids [1]. The unique property of the BBB is primarily determined by the presence of endothelial junctional complexes made up of adherens junctions (AJs) and highly specialized tight junctions (TJs). Apart from the presence of specialized TJs, other unique properties of the BBB are the absence of fenestrae, reduced level of fluid-phase endocytosis and asymmetrically localized enzymes [2]. An intact BBB prevents the transfer of macromolecules to the brain tissue. The penetration of substances into the brain, also avoids enzymatic barriers, which are composed of enzyme systems located in the walls of the cerebral blood vessels (e.g. aminopeptidase or monoaminoxidase).

## Cells of blood-brain barrier

The BBB is formed by the brain microvascular endothelial cells (BMECs) that line the cerebral microvessels. The periendothelial structures of the BBB include pericytes (related to smooth muscle cells, surrounding the endothelium, reduced endothelial apoptosis and the stabilization of

the endothelium), astrocytes (induce many BBB features and support the tissue of the CNS) and a basal membrane (Fig. 1). Astrocytes are glial cells that vastly outnumber the neurons in the brain. Astrocytes are involved in metabolic interactions with neurons, and also form close associations with endothelia and fibroblasts [52]. Less is known about the role of the pericytes in the BBB. The characteristic shape of astrocytes is a stellate appearance with long cytoplasmic processes. They are specialized cells within the capillary basement membrane, which help to maintain structural integrity and the function of the blood vessels [13]. The basal lamina of cerebral microvessels provides a scaffold upon which the endothelial and the glial compartments interact [2]. The BMECs interact dynamically with neighboring cells, astroglia, pericytes, and microglia that contribute to their unique characteristics. Despite the fact that astrocytes envelop more than 99% of the BBB endothelium, they are not directly involved in the physical properties of the BBB [23]. Interaction of astrocytes with the BMECs induces and modulates the development of the unique properties of the BBB which is the reduction in the adhesional and tight junctional gap areas [52].

Polarized cells have functions such as: the transport of ions and nutrients; secretion of protein products; and protection of the interior of the organism from pathogens. Cell polarity is observed in the functionally distinct portions of the plasma membrane known as the apical domain and the basolateral domain [35]. The apical domain contains anion channels,  $H^+/K^+$  ATPase and transporters, whereas the lateral portion of the basolateral domain contains proteins involved in attachment to neighboring cells and cell-

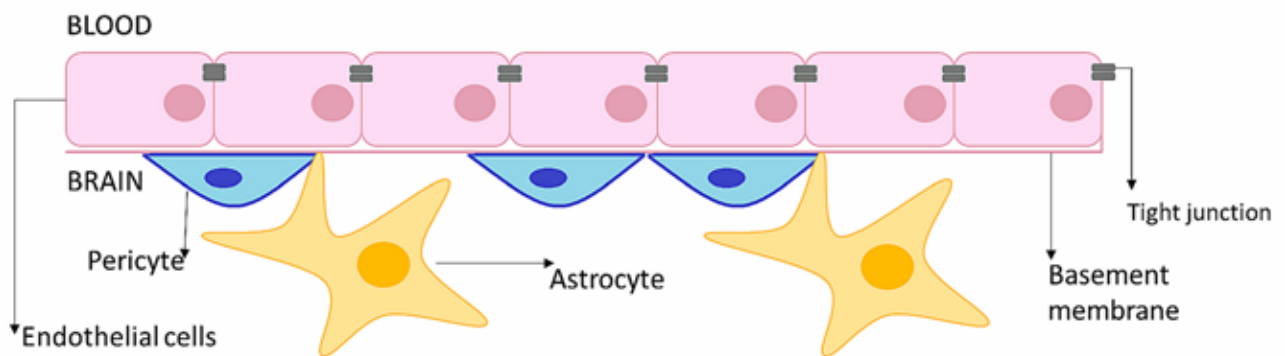


**Fig. 1. Structure of the blood brain barrier**

BBB consists mainly of brain microvascular endothelial cells (BMEC), pericytes, astrocytes and basement membrane. An original drawing

cell communication. The basal portion of the basolateral domain contains the binding sites for constituents of the basal lamina, receptors for hormones and other signaling molecules that regulate the function of the cell [35]. The TJs, which are localized in the apical end of the basolateral membrane, play a key role in establishing endothelial polarity. The TJs of the cerebral microvasculature are composed of four integral membrane proteins — occludin [17], claudins [18], junctional adhesion molecules (JAM) [34] and the recently discovered endothelial cell-selective adhesion molecule [36] (Fig. 2).

### Traversal of the BBB by pathogens

One of the basic steps in the invasion of a pathogen into the CNS is crossing through the BBB. Several pathogens are able to penetrate physiologically impermeable barriers such as the BBB. There are two main types of passing through the BBB, paracellular and transcellular [30] (Fig. 3). Crossing through the BBB is associated with protein-protein interactions between the pathogen and cells of the BBB. Some pathogens have developed an array of complex types of BBB disruptions. One of the most perfect mechanism of translocation, without mechanical damage to the BBB is the “Trojan horse“ mechanism or mimicry of surface ligands on the host cells. Some neuroinvasive pathogens express the ligand of the surface receptors of the host proteases, which break down the extracellular matrix or components of the basal membrane.

1. Transcellular passage involves penetration of the patho-

gens through the BMECs. This crossing is initiated by adherence of the pathogen to the ECs leading to the entry of the bacterium into the CNS across the BBB using pinocytosis or receptor-mediated mechanisms. Transcellular traversal of the BBB has been demonstrated for *Escherichia coli* [30], Group B *Streptococcus* [40], *Listeria monocytogenes* [21], *Mycobacterium tuberculosis* [27], *Citrobacter freundii* [3], *Haemophilus influenzae* [41], *Streptococcus pneumoniae* [45] and *Candida albicans* [28].

2. The paracellular route is defined as microbial infiltration between the cells. This traversal involves loosening of the TJs or disturbing the supporting components of TJs, i.e. basement membrane and glial cells [55]. The paracellular transmigration of the BBB has been suggested for the *Trypanosoma* [24] and *Treponema pallidum* [22].

Both routes have also been suggested for *Cryptococcus neoformans* [11, 12], *Neisseria meningitidis* [38, 10], and the Lyme disease pathogen *Borrelia burgdorferi* [9].

3. In the case of the “Trojan horse” mechanism, the first step is infection of leukocytes, primary lymphocytes, and/or mononuclear leukocytes by pathogens. Then these infected immune cells carry the pathogen through the BBB. This way of crossing is mainly used by bacteria that are able to survive in the host immune cells [30]. Passing the BBB by the “Trojan horse” mechanism has been suggested for bacteria such as *Listeria monocytogenes* and *Mycobacterium tuberculosis* [15].

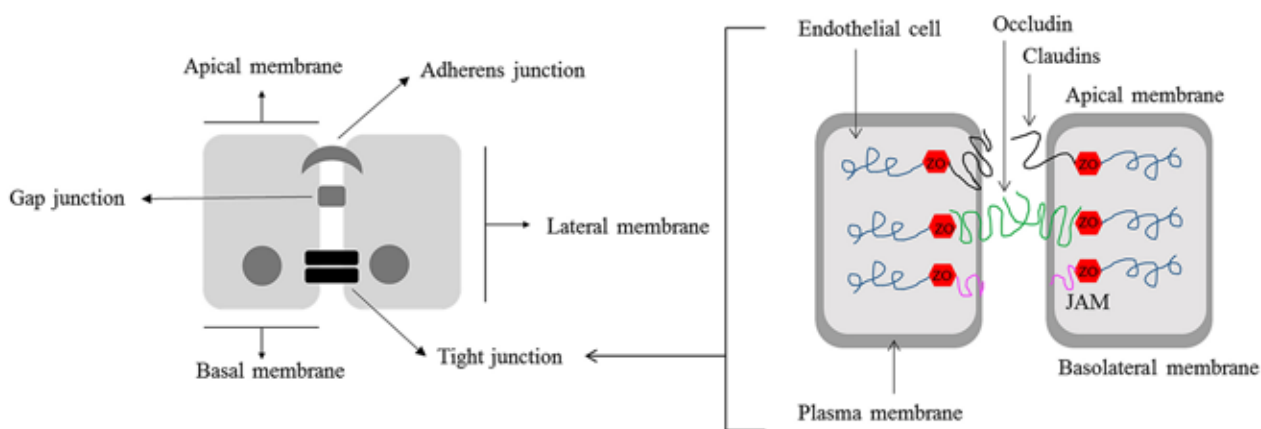


**Fig. 2. Organization of intracellular junctions**

BMEC attached to each other via adherens junctions, tight junctions and gap junctions. The TJs are composed of integral proteins: occludin, claudins, junctional adhesion molecules (JAM) and the recently discovered endothelial cell-selective adhesion molecule. Edited according to [35]

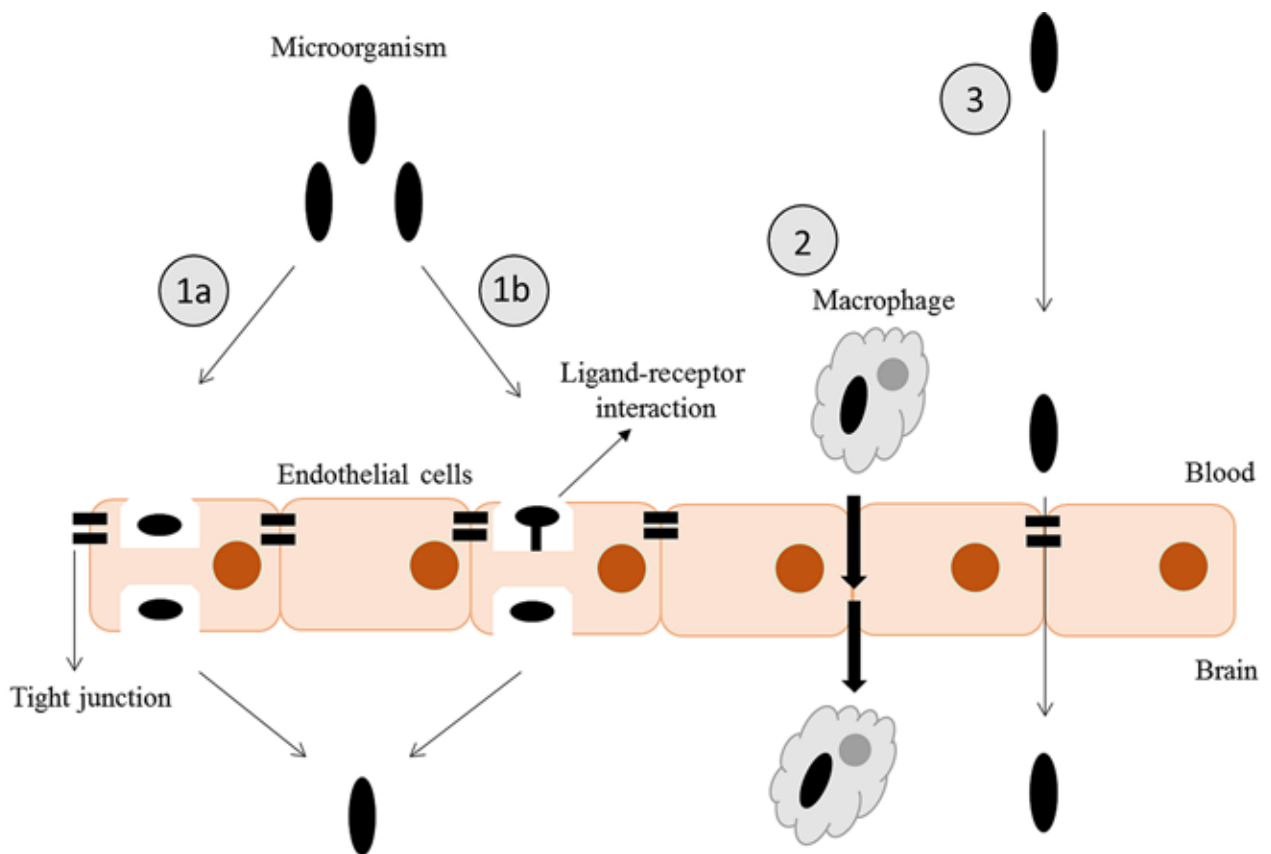


**Fig. 3. Mechanisms of crossing through the BBB**

- 1a) Transcellular penetration-pinocytosis (ligands are brought into endothelial cell, forming an invagination and they are released into brain);  
 1b) Transcellular penetration-ligand-receptor interaction (pathogen ligand interacts with host receptor and it allows the pathogen to cross the BBB);  
 2) The “Trojan horse” mechanism (Infected phagocytes to carry the pathogen through the BBB); 3) Paracellular penetration (Passage through the endothelial cells with or without disrupted tight and adherens junction). An original drawing

In recent years, the interest of researchers has been aimed at the cell signaling pathway, which is triggered after infection in the cells of the NVU. Neuroinvasive pathogens infect host cells through ligand-receptor interactions. Pathogens ligands interact with receptors, which are bound to the brain microvascular endothelial cells. These interactions are described in a variety of pathogens (Table 1).

### Transversal of the BBB by *Borrelia*

Lyme disease is an infectious bacterial disease caused by the microaerophilic spirochete *Borrelia* species, which affects the peripheral and CNS. It is one of the most common tick-borne diseases in Europe and in North America [49]. Neurological complications, collectively termed neuroborreliosis, can occur in up to 15% of untreated patients. Typical symptoms of the damage of the CNS are headache, flu-like symptoms, fatigue, memory loss and depression. In the case of the infection of the peripheral nervous system,

typical symptoms are the malfunction of the facial nerve and muscle weakness [49].

Several bacteria express their own proteases that digest the extracellular matrix in order to invade tissues, however, *B. burgdorferi* appear to utilize the fibrinolytic system of the host to disseminate [7]. *B. burgdorferi* does not produce any collagenase, elastase, hyaluronidase or plasminogen activators [31]. It is a well-known fact that *Borrelia* can bind plasminogen and promotes degradation of the ECM [7]. On the other hand, fibrinolytic system also initiates other proteases, including the matrix metalloproteinases (MMPs), which are predicted to be essential for borreliosis invasion into the brain [16]. Plasminogen bound on the bacterial surface can be converted into plasmin by host activators [4]. Plasmin bound to the surface of the bacterial cell is stabilized and protected against inactivation by  $\alpha$ 1- and  $\alpha$ 2-antiplasmin [42]. *Borrelia* induces the expression and secretion of the urokinase-type plasminogen activa-

**Table 1. Protein-protein interactions during translocation of pathogen across the BBB**

Pathogen	Predicted ways of BBB penetration	Ligand (pathogen)	Receptor (host)	References
<i>E.coli</i>	Transcellular	CNF1 FimH OmpA IBEA	37 LRP, 67 LRP CD48 Gp96 45-kDa protein	[14], [29] [44] [26]
<i>S. pneumoniae</i>	Transcellular	Phosphorylcholin	Platelet-activating factor receptor	[45]
<i>L. monocytogenes</i>	Transcellular	Internalin B	gC1q-R (receptor for the globular head of the complement component C1q)	[21], [5], [47]
	"Trojan horse" mechanism	Vip ND	Met receptor tyrosine kinase gp96 ND	[6] [15]
<i>Neisseria meningitidis</i>	Transcellular	Opc (outer membrane protein)	Fibronectin (anchoring to the integrin- $\alpha$ 5 $\beta$ 1 receptor)	[56], [37]
		Pili (Pil A and Pil B)	CD46	[43]
<i>Group B Streptococci</i>	Transcellular	Glycosyltransferase	ND	[53]
		LTA	Laminin	[53]
		Lmb	Fibrinogen	
		FbsA	ND	[33]
		Pili (PilA and PilB)	ND	[33]
<i>Treponema pallidum</i>	Paracellular	ND	ND	[54]
<i>Borrelia burgdorferi s.l.</i>	Transcellular	ND	ND	[9]
			Proteoglycans	[51]
	Paracellular	Vsp1	Platelet integrins	[12]
			Glycosaminoglycans	[46]
		OspA	Glycosphingolipids	[46]
		70-kDa PBP	Plasmin(ogen) proteoglycans	[25]
		Plasmin(ogen)	[25]	
<i>Mycobacterium tuberculosis</i>	Transcellular	Upregulation of genes	ND	[27]
	"Trojan horse" mechanism	Rv0980c	ND	[39]
		Rv0987c	ND	[39]
		Rv0989c	ND	[39]
		Rv1801	ND	[39]

N.D. — not detected (unknown)

tor (uPA) and the expression of the uPA receptor (uPAR; CD87) by a variety of cell types, including monocytes [8]. The protection of cell surface-bound plasmin from physiological inhibitors may allow the spirochete to traverse normal tissue barriers, to colonize organs and to propagate pathological processes within the affected tissues. *Borrelia* is able to activate and upregulate proinflammatory cells of human MMPs [19] and induce the release of MMP9 (gelatinase), and MMP1 (collagenase). These molecules are subsequently exploited for penetration through different host barrier, including the BBB [19].

Another alternative, which is used by *Borrelia* to translocate through the BBB, is the exploitation of CD40. OspA of *Borrelia* binds CD40 expressed on brain endothelial cells of the host. This binding induces the expression

of various types of integrins and the expression of matrix metalloproteinases (MMP3 and MMP9). Activation of CD40 in endothelial cells mediates downstream signaling that leads to the production of pro-inflammatory cytokines [35] and enhanced expression of ICAM-1, E-selectin, VCAM-1 with the consequent increase in cell binding, vascular endothelial growth factor (VEGF) and vascular permeability factor (VPF), and finally creates fenestrations [50, 48, 32] that leads to a weakening of the barrier. OspA is undoubtedly a multifunctional protein that is absolutely necessary in the various stages of borrelial lifecycle and pathogenesis. It is also well known that *Borrelia* can bind plasminogen via OspA on their surface [12]. Plasminogen can be activated to plasmin [12, 8] leading to degradation of the extracellular matrix and translocation across the BBB.

## CONCLUSIONS

Passing through the BBB is an important step in the invasion of pathogens. This summary explains different ways of passages of pathogens across the BBB. The identification of pathogenic ligands and the understanding of ligand-receptor interactions helps us to unfold the basic principles of neuroinvasion and increases the probability of creating a suitable vaccine against such neuroinfections.

## ACKNOWLEDGEMENTS

*The study was supported by APVV-14-0218 and INFEK-TZOOON (Center of excellence for infections in animals and zoonoses, ITMS code: 26220120002, co-financed from the European structural funds) for the support of this study.*

## REFERENCES

1. **Abbott, N.J., Ronnback, L., Hansson, E., 2006:** Astrocyte-endothelial interactions at the blood-brain barrier. *Nat. Rev. Neurosci.*, 7, 41–53.
2. **Archer, D.P., Ravussin, P.A., 1994:** Role of blood-brain barrier in cerebral homeostasis. *Ann. Fr. Anesth. Reanim.*, 13, 57–61.
3. **Badger, J.L., Stins, M.F., Kim, K.S., 1999:** *Citrobacter freundii* invades and replicates in human brain microvascular endothelial cells. *Infect. Immunol.*, 67, 4208–4215.
4. **Berge, A., Sjobring, U., 1993:** PAM, a novel plasminogen-binding protein from *Streptococcus pyogenes*. *J. Biol. Chem.*, 268, 25417–25424.
5. **Braun, L., Ohayon, H., Cossart, P., 1998:** The InIB protein of *Listeria monocytogenes* is sufficient to promote entry into mammalian cells. *Mol. Microbiol.*, 27, 1077–1087.
6. **Cabanes, D., Sousa, S., Cebria, A., Lecuit, M., Garcia-del Portillo, F., Cossart, P., 2005:** Gp96 is a receptor for a novel *Listeria monocytogenes* virulence factor, Vip, a surface protein. *EMBO J.*, 24, 2827–2838.
7. **Coleman, J.L., Roemer, E.J., Benach, J.L., 1999:** Plasmin-coated *Borrelia burgdorferi* degrades soluble and insoluble components of the mammalian extracellular matrix. *Infect. Immunol.*, 67, 3929–3936.
8. **Coleman, J.L., Gebbia, J.A., Benach, J.L., 2001:** *Borrelia burgdorferi* and other bacterial products induce expression and release of the urokinase receptor (CD87). *J. Immunol.*, 166, 473–480.
9. **Comstock, L.E., Thomas, D.D., 1991:** Characterization of *Borrelia burgdorferi* invasion of cultured endothelial cells. *Microb. Pathog.*, 10, 137–148.
10. **Coureuil, M., Mikaty, G., Miller, F., Bourdoulous, S., Duménil, G., Mège, R.M., et al., 2009:** Meningococcal type IV pili recruit the polarity complex to cross the brain endothelium. *Science*, 325, 83–87.
11. **Chang, Y.C., Stins, M.F., McCaffery, M.J., Miller, G.F., Pare, D.R., Dam, T., et al., 2004:** Cryptococcal yeast cells invade the central nervous system via transcellular penetration of the blood-brain barrier. *Infect. Immunol.*, 72, 4985–4995.
12. **Charlier, C., Chretien, F., Baudrimont, M., Mordelet, E., Lortholary, O., Dromer, F., 2005:** Capsule structure changes associated with *Cryptococcus neoformans* crossing of the blood-brain barrier. *Am. J. Pathol.*, 166, 421–432 C.
13. **Chauhan, V.S., Kluttz, J.M., Bost, K.L., Marriott, I., 2011:** Prophylactic and therapeutic targeting of the neurokinin-1 receptor limits neuroinflammation in a murine model of pneumococcal meningitis. *J. Immunol.*, 186, 7255–7263.
14. **Chung, J.W., Hong, S.J., Kim, K.J., Goti, D., Stins, M.F., Shin, S., et al., 2003:** 37-kDa laminin receptor precursor modulates cytotoxic necrotizing factor 1-mediated RhoA activation and bacterial uptake. *J. Biol. Chem.*, 278, 16857–16862.
15. **Drevets, D.A., Dillon, M.J., Schawang, J.S., Van Rooijen, N., Ehrchen, J., Sunderkotter, C., et al., 2004:** The Ly-6Chigh monocyte subpopulation transports *Listeria monocytogenes* into the brain during systemic infection of mice. *J. Immunol.*, 172, 4418–4424.
16. **Fuchs, H., Wallich, R., Simon, M.M., Kramer, M.D., 1994:** The outer surface protein A of the spirochete *Borrelia burgdorferi* is a plasmin(ogen) receptor. *Proc. Natl. Acad. Sci. USA*, 91, 12594–12598.
17. **Furuse, M., Itoh, M., Hirase, T., Nagafuchi, A., Yonemura, S., Tsukita, S., 1994:** Direct association of occludin with ZO-1 and its possible involvement in the localization of occludin at tight junctions. *J. Cell Biol.*, 127, 1617–1626.
18. **Furuse, M., Fujita, K., Hiiiragi, T., Fujimoto, K., Tsukita, S., 1998:** Claudin-1 and -2: novel integral membrane proteins localizing at tight junctions with no sequence similarity to occludin. *J. Cell Biol.*, 141, 1539–1550.
19. **Gebbia, J.A., Coleman, J.L., Benach, J.L., 2001:** *Borrelia spirochetes* upregulate release and activation of matrix metalloproteinase gelatinase B (MMP-9) and collagenase 1 (MMP-1) in human cells. *Infect. Immunol.*, 69, 456–462.

20. Grab, D. J., Nikolskaia, O., Kim, Y. V., Lonsdale-Eccles, J. D., Ito, S., Hara, T., et al., 2004: African trypanosome interactions with an *in vitro* model of the human blood-brain barrier. *J. Parasitol.*, 90, 970—979.
21. Greiffenberg, L., Goebel, W., Kim, K. S., Weiglein, I., Buber, A., Engelbrecht, F., et al., 1998: Interaction of *Listeria monocytogenes* with human brain microvascular endothelial cells: InlB-dependent invasion, long-term intracellular growth, and spread from macrophages to endothelial cells. *Infect. Immunol.*, 66, 5260—5267.
22. Haake, D. A., Lovett, M. A., 1994: Interjunctional invasion of endothelial cell monolayers. *Methods Enzymol.*, 236, 447—463.
23. Hawkins, B. T., Davis, T. P., 2005: The blood-brain barrier/neurovascular unit in health and disease. *Pharmacol. Rev.*, 57, 173—185.
24. Hoffman, O., Weber, R. J., 2009: Pathophysiology and treatment of bacterial meningitis. *Advances in Neurological Disorders*, 2, 1—7.
25. Hu, L. T., Pratt, S. D., Perides, G., Katz, L., Rogers, R. A., Klempner, M. S., 1997: Isolation, cloning, and expression of a 70-kilodalton plasminogen binding protein of *Borrelia burgdorferi*. *Infect. Immunol.*, 65, 4989—4995.
26. Huang, S. H., Wass, C., Fu, Q., Prasadarao, N. V., Stins, M., Kim, K. S., 1995: *Escherichia coli* invasion of brain microvascular endothelial cells *in vitro* and *in vivo*: molecular cloning and characterization of invasion gene *ibe10*. *Infect. Immunol.*, 63, 4470—4475.
27. Jain, S. K., Paul-Satyaseela, M., Lamichhane, G., Kim, K. S., Bishai, W. R., 2006: Mycobacterium tuberculosis invasion and traversal across an *in vitro* human blood-brain barrier as a pathogenic mechanism for central nervous system tuberculosis. *J. Infect. Dis.*, 193, 1287—1295.
28. Jong, A. Y., Stins, M. F., Huang, S. H., Chen, S. H., Kim, K. S., 2001: Traversal of *Candida albicans* across human blood-brain barrier *in vitro*. *Infect. Immunol.*, 69, 4536—4544.
29. Khan, N. A., Kim, Y., Shin, S., Kim, K. S., 2007: FimH-mediated *Escherichia coli* K1 invasion of human brain microvascular endothelial cells. *Cell Microbiol.*, 9, 169—178.
30. Kim, K. S., 2008: Mechanisms of microbial traversal of the blood-brain barrier. *Nat. Rev. Microbiol.*, 6, 625—634.
31. Klempner, M. S., Noring, R., Epstein, M. P., McCloud, B., Hu, R., Limentani, S. A., et al., 1995: Binding of human plasminogen and urokinase-type plasminogen activator to the Lyme disease spirochete, *Borrelia burgdorferi*. *J. Infect. Dis.*, 171, 1258—1265.
32. Mach, F., Schonbeck, U., Bonnefoy, J. Y., Pober, J. S., Libby, P., 1997: Activation of monocyte/macrophage functions related to acute atheroma complication by ligation of CD40: induction of collagenase, stromelysin, and tissue factor. *Circulation*, 96, 396—9.
33. Maisey, H. C., Hensler, M., Nizet, V., Doran, K. S., 2007: Group B streptococcal pilus proteins contribute to adherence to and invasion of brain microvascular endothelial cells. *J. Bacteriol.*, 189, 1464—1467.
34. Martin-Padura, I., Lostaglio, S., Schneemann, M., Williams, L., Romano, M., Fruscella, P., et al., 1998: Junctional adhesion molecule, a novel member of the immunoglobulin superfamily that distributes at intercellular junctions and modulates monocyte transmigration. *J. Cell Biol.*, 142, 117—127.
35. Miyoshi, J., Takai, Y., 2005: Molecular perspective on tight-junction assembly and epithelial polarity. *Advances Drug Delivery Reviews*, 57, 815—855.
36. Nasdala, I., Wolburg-Buchholz, K., Wolburg, H., Kuhn, A., Ebnet, K., Brachtendorf, G., et al., 2002: A transmembrane tight junction protein selectively expressed on endothelial cells and platelets. *J. Biol. Chem.*, 277, 16294—16303.
37. Nassif, X., Pujol, C., Morand, P., Eugene, E., 1999: Interactions of pathogenic *Neisseria* with host cells. Is it possible to assemble the puzzle? *Mol. Microbiol.*, 32, 1124—1132.
38. Nassif, X., Bourdoulous, S., Eugene, E., Couraud, P. O., 2002: How do extracellular pathogens cross the blood-brain barrier? *Trends Microbiol.*, 10, 227—232.
39. Nguyen, L., Pieters, J., 2005: The Trojan horse: survival tactics of pathogenic mycobacteria in macrophages. *Trends Cell Biol.*, 15, 269—276.
40. Nizet, V., Kim, K. S., Stins, M., Jonas, M., Chi, E. Y., Nguyen, D., et al., 1997: Invasion of brain microvascular endothelial cells by group B streptococci. *Infect. Immunol.*, 65, 5074—5081.
41. Orihuela, C. J., Mahdavi, J., Thornton, J., Mann, B., Wooldridge, K. G., Abuseada, N., et al., 2009: Laminin receptor initiates bacterial contact with the blood brain barrier in experimental meningitis models. *J. Clin. Invest.*, 119, 1638—1646.
42. Perides, G., Noring, R., Klempner, M. S., 1996: Inhibition of *Borrelia burgdorferi*-bound fibrinolytic enzymes by alpha2-antiplasmin, PAI-1 and PAI-2. *Biochem. Biophys. Res. Comm.*, 219, 690—695.
43. Plant, L., Sundqvist, J., Zughaier, S., Lovkvist, L., Stephens, D. S., Jonsson, A. B., 2006: Lipooligosaccharide structure contributes to multiple steps in the virulence of *Neisseria meningitidis*. *Infect. Immunol.*, 74, 1360—1367.

44. Prasadarao, N. V., Srivastava, P. K., Rudrabhatla, R. S., Kim, K. S., Huang, S. H., Sukumaran, S. K., 2003: Cloning and expression of the *Escherichia coli* K1 outer membrane protein A receptor, a gp96 homologue. *Infect. Immunol.*, 71, 1680—1688.
45. Ring, A., Weiser, J. N., Tuomanen, E. I., 1998: Pneumococcal trafficking across the blood-brain barrier. Molecular analysis of a novel bidirectional pathway. *J. Clin. Invest.*, 102, 347—360.
46. Rupprecht, T. A., Koedel, U., Heimerl, C., Fingerle, V., Paul, R., Wilske, B., et al., 2006: Adhesion of *Borrelia garinii* to neuronal cells is mediated by the interaction of OspA with proteoglycans. *J. Neuroimmunol.*, 175, 5—11.
47. Shen, Y., Naujokas, M., Park, M., Ireton, K., 2000: InIB-dependent internalization of *Listeria* is mediated by the Met receptor tyrosine kinase. *Cell*, 103, 501—510.
48. Schonbeck, U., Mach, F., Sukhova, G. K., Murphy, C., Bonney, J. Y., Fabunmi, R. P., Libby, P., 1997: Regulation of matrix metalloproteinase expression in human vascular smooth muscle cells by T lymphocytes: a role for CD40 signaling in plaque rupture? *Circ. Res.*, 81, 448—54.
49. Steere, A. C., 2001: Lyme disease. *N. Engl. J. Med.*, 345, 115—125.
50. Sukhova, G. K., Schönbeck, U., Rabkin, E., Schoen, F. J., Poole, A. R., Billingham, R. C., Libby, P., 1999: Evidence for increased collagenolysis by interstitial collagenases-1 and -3 in vulnerable human atheromatous plaques. *Circulation*, 99, 2503—2509.
51. Szczepanski, A., Furie, M. B., Benach, J. L., Lane, B. P., Fleit, H. B., 1990: Interaction between *Borrelia burgdorferi* and endothelium *in vitro*. *J. Clin. Invest.*, 85, 1637—1647.
52. Tao-Cheng, J. H., Brightman, M. W., 1988: Development of membrane interactions between brain endothelial cells and astrocytes *in vitro*. *Int. J. Dev. Neurosci.*, 6, 25—37.
53. Tenenbaum, T., Bloier, C., Adam, R., Reinscheid, D. J., Schrotten, H., 2005: Adherence to and invasion of human brain microvascular endothelial cells are promoted by fibrinogen-binding protein FbsA of *Streptococcus agalactiae*. *Infect. Immunol.*, 73, 4404—4409.
54. Thomas, D. D., Navab, M., Haake, D. A., Fogelman, A. M., Miller, J. N., Lovett, M. A., 1988: *Treponema pallidum* invades intercellular junctions of endothelial cell monolayers. *Proc. Natl. Acad. Sci. USA*, 85, 3608—3612.
55. Tuomanen, E., 1996: Entry of pathogens into the central nervous system. *FEMS Microbiol. Rev.*, 18, 289—299.
56. Unkmeir, A., Latsch, K., Dietrich, G., Wintermeyer, E., Schinke, B., Schwender, S., 2002: Fibronectin mediates Opc-dependent internalization of *Neisseria meningitidis* in human brain microvascular endothelial cells. *Mol. Microbiol.*, 46, 933—946.

Received, December 4, 2017

Accepted January 17, 2018



## THE ROLE OF MENINGOCOCCAL PORIN B IN PROTEIN-PROTEIN INTERACTIONS WITH HOST CELLS

Káňová, E.<sup>1</sup>, Jiménez-Munguía, I.<sup>1</sup>, Čomor, L.<sup>1</sup>, Tkáčová, Z.<sup>1</sup>  
Širochmanová, I.<sup>1</sup>, Bhide, K.<sup>1</sup>, Bhide, M.<sup>1,2</sup>

<sup>1</sup>Laboratory of Biomedical Microbiology and Immunology  
University of Veterinary Medicine and Pharmacy, Kosice

<sup>2</sup>Institute of Neuroimmunology, Slovak Academy of Sciences, Bratislava  
Slovakia

evelinakanova31@gmail.com

### ABSTRACT

*Neisseria meningitidis* is a Gram-negative diplococcus responsible for bacterial meningitis and fatal sepsis. Ligand-receptor interactions are one of the main steps in the development of neuroinvasion. Porin B (PorB), neisserial outer membrane protein (ligand), binds to host receptors and triggers many cell signalling cascades allowing the meningococcus to damage the host cells or induce immune cells responses via the TLR2-dependent mechanisms. In this paper, we present a brief review of the structure and function of PorB.

**Key words:** *Neisseria meningitidis*; PorB; protein; Toll-like receptor

### INTRODUCTION

*N. meningitidis* is an exclusive human pathogen, and the leading worldwide cause of meningitis and fatal sepsis. In the development of the meningococcal disease an inter-

action of several pathogen's ligands with receptors located on the endothelial cells surface in the brain microvesicles is essential. In this paper we have focused on Porin B (PorB), one of the important ligands of *Neisseria*, that binds to the brain microvascular endothelial cells. Unfortunately, there is a lack of consistent information available on the function of the porin of *Neisseria meningitidis*. Thus, in this paper we review the role of PorB of *Neisseria* and presented it in a consistent manner. Reviewing the multifaceted functions of PorB, (e.g. selective sugar binding, role in nonselective ions translocation, role in the activation of human B cells, induction of the release of cytokines, etc.) we will show that this protein is one of the major ligands of *Neisseria* that govern its crucial role in pathogenesis.

### Porin B (PorB)

Approximately 60% of the outer membrane proteins of *Neisseria* species consist of porins, which belong to the Gram-negative porin superfamily [14, 18]. In the case of gonococcus, porins are termed protein IA (PIA, PorBIA, 35 kDa) or IB (PIB, PorBIB, 37 kDa), while in the case of meningococcus they are designated as PorA (class 1 pro-

tein, ~45 kDa) or PorB (class 2 or 3 protein, ~33 kDa) [9, 12, 18]. Porins from *N. meningitidis* and *N. gonorrhoeae* share 60–70% amino acid sequence homology [7, 27] and moderate antigenic variability, which is the basis of the *neisserial* serotyping system [9].

### Structure of PorB

PorB is in trimeric form (Figure 1). Each monomer (~35 kDa) contains a high proportion (~36%) of  $\beta$ -pleated sheets [7, 28]. Each unit forms a 16-stranded (S)  $\beta$ -barrel with eight short periplasmic turns connecting the strands on the periplasmic side of the channel, and eight long interstrand loops (L1-L8) on the extracellular side of the channel (Figure 2). L2 was located as an interface among monomers, and contributes to the trimeric formation. In particular, the extracellular loop 3 (L3) protrudes into the pore and forms a  $\alpha$ -helix, which constricts the pore to 8 Å by 10 Å at its narrowest point. This region is often referred to as a constriction zone for controlling the pathway for solute transport. This topology is similar to that observed for other outer membrane proteins (OMPs), with sequence insertions and variability in the region exposed to the host immune system. The  $\beta$ -barrel regions share a high level of sequence homology among the different strains, while the amino acid sequence variability characterizes the surface-exposed loops [15, 39, 40].

### Function of PorB

Neisserial porins act as pores and are essential for bacterial survival because they modulate the ion exchange between the bacteria and its surrounding environment [44]. The physiological function of porins is to bind sugars selectively. It has been shown that PorB transports small sugars more quickly than larger sugars [28]. On the extracellular side of the channel, the funnel approaching the pore is strongly electronegative, whereas on the periplasmic side of the channel, the funnel is strongly electropositive. Although PorB has previously been characterized as a nonselective channel, these electrostatic charges differ from those of other nonselective porins of known structure, which have consistent, intermediate charge [6, 29]. It was found that glucose has the highest rate of substrate translocation. Similarly, galactose and arabinose showed fast transport through PorB, whereas sucrose and maltose displayed much slower transport rates [40]. Co-crystallization of PorB with sugar substrates revealed a specific binding site for both galactose and sucrose at the same location within the positively charged funnel. This indicates that PorB contains multiple selective mechanisms for substrate selection [40].

The second function involves putative non-selective translocation pathways. PorB translocate cations since it has been electrophysiologically characterized as weakly an-

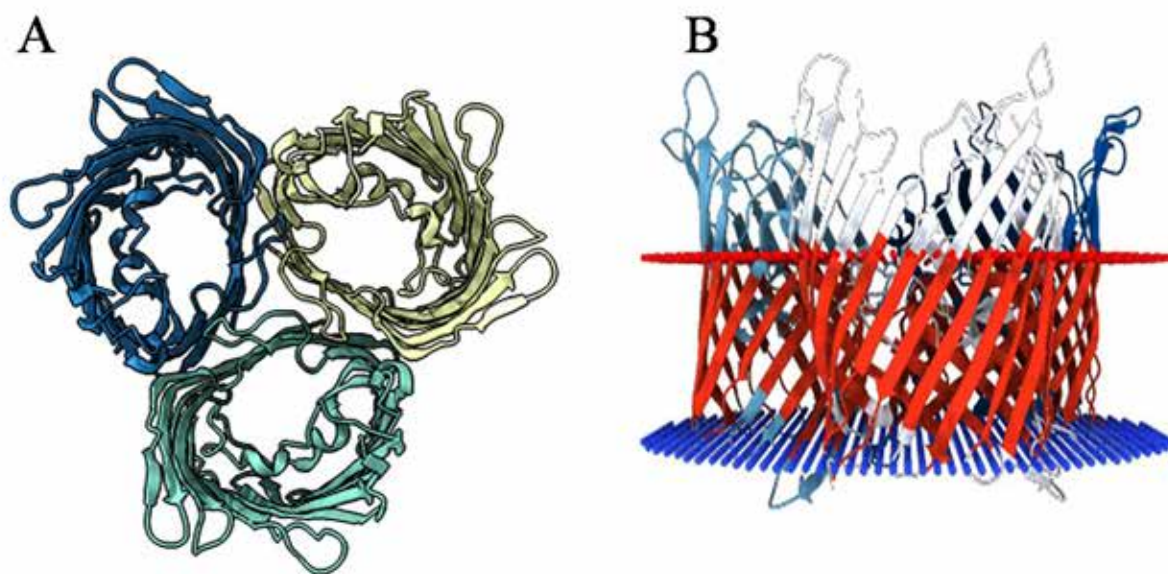


Fig. 1. Transmembrane regional views of the trimeric form [40]: structure of the PorB trimer (A); cartoon model of the PorB trimer (B).

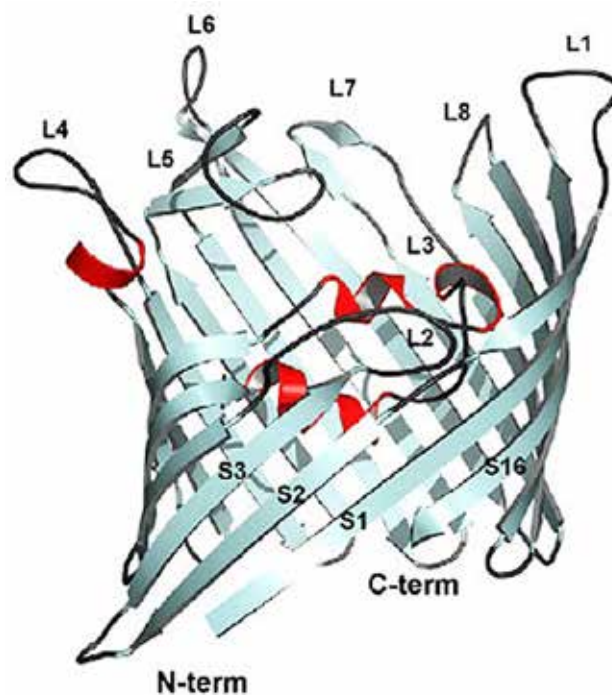


Fig. 2. A cartoon model of the lateral view of the PorB monomer structure. S1—S16 represent strands of amino acids which form the beta barrel, L1—L8 are loops of amino acids (grey), and L3 forms a helical structure (red) that lies across the pore [40].

ion selective [38], suggesting that an anion pathway must be available. Examination of the electrostatic surface representation identifies a putative pathway on the pore face nearest to the crystallographic 3-fold axis that is lined with positively charged residues. A similar feature has been identified in the *E. coli* OmpF [5, 13], the Delfita acidovorans Omp32 [45, 46], and the *E. coli* OmpC [3], which share structural similarity to PorB in the transmembrane  $\beta$ -barrel region of the protein [40].

The regulation of conductance by purine nucleotide triphosphates (pNTP) is a characteristic of PorB, which likely occur physiologically during infection when the channel is inserted into the host mitochondrial membrane. The binding site for pNTP is surrounded by the side chains of Lys9, Lys42, Arg77, Asn96, Lys100, Arg130 and it is adjacent to L3 near to the pore constriction [40]. A previous hypothesis claimed that 16-stranded  $\beta$ -barrel OMPs is non-specific [45]. However, current research shows that porins contain multiply selective and sophisticated mechanisms for substrate selection [40].

#### PorB as a ligand

Neisserial porins play a role in: the induction of in-

flammation; activation of human and murine B cells with a mitogenic effect; release of cytokines from human cells; and stimulation of platelet-activating factor production by human endothelial cells [10, 41]. However, the effect on T cells has not been directly observed. Moreover, neisserial porins have host cell-associated functions, including those that facilitate bacterial/host cell interaction, modulation of host cell survival, and induction of immune stimulation [24, 42]. It was found that porins interact with host cell receptors associated with bacterial adhesion/invasion processes (e.g. the laminin receptor LamR, the gp96 and Scavenger receptor SREC) [1, 33]. Porins promote epithelial cell invasion, especially their critical residues in the surface-exposed loops result in invasion of epithelial cells and direct the interaction of PorB with host cell receptors. Then, they are able to react with host receptors involved on complement activation [21, 32] and with members of the Toll-like receptor family (TLR2 and TLR1) [22, 25]. Toll-like receptors are a set of innate immune receptors that recognize common structures to many different pathogens and to some endogenous molecules. Currently, 11 human TLRs have been discovered, of which TLR4 was the first described mammalian TLR [2, 34].

Neisserial porins are potent immune adjuvants and induce antigen-presenting cell (APC) activation, increase MHC II and CD86 surface expression, which leads to the induction of the B cells proliferation, maturation of dendritic cells (DCs) and activation of macrophages [37, 43]. This immune adjuvant effect is due to the induction of CD86 surface expression [19]. It was found that *Neisseria meningitidis* PorB induces signal transduction events in murine B cells such as upregulation of CD86 and proliferation. Consequently, PorB can induce protein tyrosine kinase (PTK) activity, phosphorylation of Rrk1, Erk2 (serine/threonine kinase) and I $\kappa$ B- $\alpha$ , leading to nuclear factor (NF)- $\kappa$ B nuclear translocation in B cells in a TLR2-dependent manner. PorB-induced NF- $\kappa$ B nuclear translocation was not dependent on either PTK or Erk1/2 activities. Moreover, it was demonstrated that PorB acts through TLR2 as a B-cell mitogen [20]. PorB is able to activate other cell types, including the induction of CD86 expression, cytokines production and other signal transduction events involved in such phenomena [42]. Increased expression of CD86, MHC class I and II and induced DC maturation are caused by PorB. In addition, PorB stimulates T cells in an antigen-specific dependent manner through the activated DC. During *N. meningitidis* infection, many cytokines, mainly IL-6, are produced. Regularly, IL-6 is involved in the inflammatory process observed during infection or disease and is secreted by PorB-maturated DCs [37]. It has been observed that the maturation of DCs, macrophages activation, participation of TLR2 and myeloid differentiation primary response gene 88 (MyD88) are important for PorB-induced B cells [22]. The direct binding of PorB to TLR2 described by Wetzler in 2010, is directly related to cellular activation [42]. This activation via TLR2 occurs in association with TLR1 [11]. It has been described that murine B cells from WT mice respond to PorB by upregulating of costimulatory surface molecules CD86, CD40 and MHC II [22]. IL-6 failed to be induced by PorB in the absence of TLR2, although the co-receptors TLR1 and TLR6 were expressed on B cells [42]. Therefore, the induction of cytokine IL-6 production by PorB requires the presence of TLR2 but it maybe does not depend on the presence of TLR1. It is still unclear whether a TLR2 homodimer or a TLR2 heterodimer connected with another TLR for PorB-induced IL-6 is needed [42]. In general terms, PorB interacting with TLR2 and TLR1 is able to induce immune stimulation because of the evidence of the actual adjuvant activity of PorB and its

ability to enhance the humoral immune response against bacterial capsular polysaccharide (CPS) has been already been described [19]. An increased CD86 expression of APCs, the presence of TLR2 and MyD88 are required for the enhancement of PorB immune activity [19, 22, 43]. *In vivo* it was confirmed that TLR2 plays a role in the adjuvant activity of PorB [42].

A closer similarity in the surface charges of L1, L2, L4, L6 and L7 was observed when electrostatic surface charges of PorB from invasive meningococci serogroups B and C were analysed, finding that all of them were negatively charged. Surface charges of L5, L6 and L7 could be important for mediating TLR2-dependent activation of intracellular signalling cascades that regulate host immune responses. It is still not clear however, whether PorB variants from different strains may modulate TLR2-dependent host cell responses [39].

Many processes of the apoptotic cascade take place in mitochondria in response to several pro- apoptotic signals. PorB binds to the mitochondrial porin (i.e. a voltage dependent anionic channel, VDAC), which is part of the mitochondrial permeability transition pore (PT) and triggers the induction of apoptosis in which mitochondrial depolarization and opening of the PT with cytochrome c releasing into the cytosol are carried out [16, 31, 36]. PorB and VDAC, two different classes of porins, share common functional and structural characteristics such as a high proportion of  $\beta$ - sheets, a  $\beta$ -barrel 3-D structure and regulation of pore size by nucleotides [4, 7, 35]. It seems that modulation of the mitochondrial potential is caused by its association with PorB [23].

In the case of *N. gonorrhoeae*, PorBIA possesses the ability to interact with the scavenger receptor expressed on endothelial cells (SREC-I). This connection is important for the mediation of bacterial uptake into endothelial or epithelial cells in a phosphate sensitive manner [17, 33]. The interaction between PorBIA and SREC-I leads to the re-localization of SREC-I to membrane rafts, caveolin-1 activation and the recruitment of signalling molecules PI3 kinase (PI3K) and phosphoinositol phospholipase C gamma 1 (PLCy1). Activation of PI3K and PLCy1 leads to the phosphorylation of polycystin1 (PKD1) and to the activation of Rac-1, which finally triggers cytoskeletal rearrangements and bacterial uptake [8]. PKD1 is an integral membrane protein that regulates calcium permeable cation channels and the intracellular calcium homeostasis. Moreover, PKD1 plays

a role in cell-cell/matrix interactions and may modulate G-protein-coupled signal-transduction pathways. Members of Rac-1 superfamily regulate a diverse array of cellular events, including the control of cell growth, cytoskeletal reorganization, and activation of protein kinases.

Laminin receptor (LamR), capable of interacting with PorB/A, allows cell adhesion to the basement membrane and it is also involved in tumour cell metastasis [26]. Furthermore, LamR plays a role in the intracellular signalling, ribosomal activity and cell viability [1]. Interestingly, many neurotropic bacteria and viruses use LamR in the binding process to human brain microvascular endothelial cells [30]. It was discovered the LamR-binding domain of PorA lies within the amino acids 171–240 and was localized on the L4. These findings provide an opportunity to produce antibodies recognizing this sequence or a peptide corresponding to LamR residues 263–282, which could inhibit bacterial binding to microvascular endothelial cells [1].

## CONCLUSIONS

All these findings show that neisserial porins play an important role in the stimulation of B-cell proliferation and following an increase of immunoglobulin secretion, as well as they can bind to several described receptors and thereby initiate cascades causing cells reorganization and bacterial uptake.

## ACKNOWLEDGEMENTS

*The study was supported by APVV-14-0218 and INFEK-TZOOM (Center of excellence for infections in animals and zoonoses), ITMS code: 26220120002, co-financed from the European structural funds) for support of this study.*

## REFERENCES

1. Abouseada, N.M., Assafi, M.S.A., Mahdavi, J., Oldfield, N.J., Wheldon, L.M., Wooldridge, et al., 2012: Mapping the laminin receptor binding domains of *Neisseria meningitidis* PorA and *Haemophilus influenzae* OmpP2. *PLoS One*, 7, 46233.
2. Anderson, K.V., Jurgens, G., Nusslein-Volhard, C., 1985: Establishment of dorsal-ventral polarity in the *Drosophila*

embryo: genetic studies on the role of the Toll gene product. *Cell*, 42, 779–789.

3. Basle, A., Rummel, G., Storici, P., Rosenbusch, J.P., Schirmer, T., 2006: Crystal structure of osmoporin OmpC from *E. coli* at 2.0 Å. *J. Mol. Biol.*, 362, 933–942.
4. Colombini, M., Blachly-Dyson, E., Forte, M., 1996: VDAC, a channel in the outer mitochondrial membrane. *Ion Channels*, 4, 169–202.
5. Cowan, S. W., Schirmer, T., Rummel, G., Steiert, M., Ghosh, R., Pauptit, R. A., et al., 1992: Crystal structures explain functional properties of two *E. coli* porins. *Nature*, 358, 727–733.
6. Delcour, A. H., 2009: Outer membrane permeability and antibiotic resistance. *Biochim. Biophys. Acta*, 1794, 808–816.
7. Derrick, J.P., Urwin, R., Suker, J., Feavers, I.M., Maiden, M.C., 1999: Structural and evolutionary inference from molecular variation in *Neisseria* porins. *Infect. Immun.*, 67, 2406–2413.
8. Faulstich, M., Böttcher, J.P., Meyer, T.F., Fraunholz, M., Rudel, T., 2013: Pilus phase variation switches gonococcal adherence to invasion by caveolin-1-dependent host cell signaling. *PLoS Pathog.*, 9, e1003373.
9. Frasch, C.E., Zollinger, W.D., Poolman, J.T., 1985: Serotype antigens of *Neisseria meningitidis* and a proposed scheme for designation of serotypes. *Rev. Infect. Dis.*, 7, 504–510.
10. Galdiero, F., de L'ero, G. C., Benedetto, N., Galdiero, M., Tufano, M. A., 1993: Release of cytokines induced by *Salmonella typhimurium* porins. *Infect. Immun.*, 61, 155–161.
11. Galdiero, M., Galdiero, M., Finamore, E., Rossano, F., Gambuzza, M., Catania, M. R., et al., 2004: *Haemophilus influenzae* porin induces Toll-like receptor 2-mediated cytokine production in human monocytes and mouse macrophages. *Infect. Immun.*, 72, 1204–1209.
12. Gotschlich, E. C., Seiff, M. E., Blake, M. S., Koomey, M., 1987: Porin protein of *Neisseria gonorrhoeae*: cloning and gene structure. *Proc. Natl. Acad. Sci. USA*, 84, 8135–8139.
13. Im, W., Roux, B., 2002: Ion permeation and selectivity of OmpF porin: a theoretical study based on molecular dynamics, Brownian dynamics, and continuum electrodiffusion theory. *J. Mol. Biol.*, 322, 851–869.
14. Jeanteur, D., Lakey, J. H., Pattus, F., 1991: The bacterial porin superfamily: sequence alignment and structure prediction. *Mol. Microbiol.*, 5, 2153–2164.
15. Kattner, C., Toussi, D. N., Zaucha, J., Wetzler, L. M., Ruppel, N., Zachariae, U., et al., 2014: Crystallographic analysis of *Neisseria meningitidis* PorB extracellular loops potentially implicated in TLR2 recognition. *J. Struct. Biol.*, 185, 440–447.

16. Kluck, R. M., Bossy-Wetzler, E., Green, D. R., Newmeyer, D. D., 1997: The release of cytochrome c from mitochondria: a primary site for Bcl-2 regulation of apoptosis. *Science*, 275, 1132—1136.
17. Kuhlewein, C., Rechner, C., Meyer, T. F., Rudel, T., et al., 2006: Low-phosphate-dependent invasion resembles a general way for *Neisseria gonorrhoeae* to enter host cells. *Infect. Immun.*, 74, 4266—4273.
18. Lytton, E. J., Blake, M. S., 1986: Isolation and partial characterization of the reduction-modifiable protein of *Neisseria gonorrhoeae*. *J. Exp. Med.*, 164, 1749—1759.
19. Mackinnon, F. G., Ho, Y., Blake, M. S., Michon, F., Chandraker, A., Sayegh, M. H., Wetzler, L. M., 1999: The role of B/T costimulatory signals in the immunopotentiating activity of neisserial porin. *J. Infect. Dis.*, 180, 755—761.
20. MacLeod, H., Bhasin, N., Wetzler, L. M., 2008: Role of protein tyrosine kinase and Erk1/2 activities in the Toll-like receptor 2-induced cellular activation of murine B cells by neisserial porin. *Clin. Vaccine Immunol.*, 15, 630—637.
21. Madico, G., Ngampasutadol, J., Gulati, S., Vogel, U., Rice, P. A., Ram, S., 2007: Factor H binding and function in sialylated pathogenic neisseriae is influenced by gonococcal, but not meningococcal, porin. *J. Immunol.*, 178, 4489—4497.
22. Massari, P., Henneke, P., Ho, T., Latz, E., Golenbock, D. T., Wetzler, L. M., 2002: Cutting edge: Immune stimulation by neisserial porins is toll-like receptor 2 and MyD88 dependent. *J. Immunol.*, 168, 1533—1537.
23. Massari, P., Ho, Y., Wetzler, L. M., 2000: *Neisseria meningitidis* porin PorB interacts with mitochondria and protects cells from apoptosis. *Proc. Natl. Acad. Sci. USA*, 97, 9070—9075.
24. Massari, P., Ram, S., Macleod, H., Wetzler, L. M., 2003: The role of porins in neisserial pathogenesis and immunity. *Trends Microbiol.*, 11, 87—93.
25. Massari, P., Visintin, A., Gunawardana, J., Halmen, K. A., King, C. A., Golenbock, D. T., et al., 2006: Meningococcal porin PorB binds to TLR2 and requires TLR1 for signaling. *J. Immunol.*, 176, 2373—2380.
26. Menard, S., Castronovo, V., Tagliabue, E., Sobel, M. E., 1997: New insights into the metastasis-associated 67 kD laminin receptor. *J. Cell. Biochem.*, 67, 155—165.
27. Minetti, C. A., Blake, M. S., Remeta, D. P., 1998: Characterization of the structure, function, and conformational stability of PorB class 3 protein from *Neisseria meningitidis*. A porin with unusual physicochemical properties. *J. Biol. Chem.*, 273, 25329—25338.
28. Minetti, C. A., Tai, J. Y., Blake, M. S., Pullen, J. K., Liang, S., Remeta, D. P., 1997: Structural and functional characterization of a recombinant PorB class 2 protein from *Neisseria meningitidis*. Conformational stability and porin activity. *J. Biol. Chem.*, 272, 10710—10720.
29. Nikaido, H., 2003: Molecular basis of bacterial outer membrane permeability revisited. *Microbiol. Mol. Biol. Rev.*, 67, 593—656.
30. Orihuela, C. J., Mahdavi, J., Thornton, J., Mann, B., Wooldridge, K. G., Abouseada, N., et al., 2009: Laminin receptor initiates bacterial contact with the blood brain barrier in experimental meningitis models. *J. Clin. Invest.*, 119, 1638—1646.
31. Petit, P. X., Gubernb, M., Dolezc, P., Susina, S. A., Zamzamia, N., Kroemera, G., 1998: Disruption of the outer mitochondrial membrane as a result of large amplitude swelling: the impact of irreversible permeability transition. *FEBS Lett.*, 426, 111—116.
32. Ram, S., McQuillen, D. P., Gulati, S., Elkins, C., Pangburn, M. K., Rice, P. A., 1998: Binding of complement factor H to loop 5 of porin protein 1A: a molecular mechanism of serum resistance of nonsialylated *Neisseria gonorrhoeae*. *J. Exp. Med.*, 188, 671—680.
33. Rechner, C., Kuhlewein, C., Müller, A., Schild, H., Rudel, T., 2007: Host glycoprotein Gp96 and scavenger receptor SREC interact with PorB of disseminating *Neisseria gonorrhoeae* in an epithelial invasion pathway. *Cell Host Microbe*, 2, 393—403.
34. Roach, J. C., Glusman, G., Rowen, L., Kaur, A., Purcell, M. K., Smith, K. D., et al., 2005: The evolution of vertebrate Toll-like receptors. *Proc. Natl. Acad. Sci. USA*, 102, 9577—9582.
35. Rudel, T., Schmid, A., Benz, R., Kolb, H., Lang, F., Meyer, T. F., 1996: Modulation of Neisseria porin (PorB) by cytosolic ATP/GTP of target cells: parallels between pathogen accommodation and mitochondrial endosymbiosis. *Cell*, 85, 391—402.
36. Scarlett, J. L., Sheard, P. W., Hughes, G., Ledgerwood, E. C., Ku, H., Murphy, M. P., 2000: Changes in mitochondrial membrane potential during staurosporine-induced apoptosis in Jurkat cells. *FEBS Lett.*, 475, 267—272.
37. Singleton, T. E., Massari, P., Wetzler, L. M., 2005: Neisserial porin-induced dendritic cell activation is MyD88 and TLR2 dependent. *J. Immunol.*, 174, 3545—3550.
38. Song, J., Minettib, C. A. S. A., Blakeb, M. S., Colombinia, M., 1998: Successful recovery of the normal electrophysiological properties of PorB (class 3) porin from *Neisseria men-*

- ingitidis* after expression in *Escherichia coli* and renaturation. *Biochim. Biophys. Acta*, 1370, 289—298.
39. **Stefanelli, P., Neri, A., Tanabe, M., Fazio, C., Massari, P., 2016:** Typing and surface charges of the variable loop regions of PorB from *Neisseria meningitidis*. *IUBMB Life*, 68, 488—495.
40. **Tanabe, M., Nimigean, C.M., Iverson, T.M., 2010:** Structural basis for solute transport, nucleotide regulation, and immunological recognition of *Neisseria meningitidis* PorB. *Proc. Natl. Acad. Sci. USA*, 107, 6811—6816.
41. **Tufano, M. A., Biancone, L., Rossano, F., Capasso, C., Baroni, A., de Martino, A., et al., 1993:** Outer-membrane porins from gram-negative bacteria stimulate platelet-activating-factor biosynthesis by cultured human endothelial cells. *Eur. J. Biochem.*, 214, 685—693.
42. **Wetzler, L. M., 2010:** Innate immune function of the neisserial porins and the relationship to vaccine adjuvant activity. *Future Microbiol.*, 5, 749—758.
43. **Wetzler, L. M., Ho, Y., Reiser, H., 1996:** Neisserial porins induce B lymphocytes to express costimulatory B7-2 molecules and to proliferate. *J. Exp. Med.*, 183, 1151—1159.
44. **Young, J. D., Blake, M., Mauro, A., Cohn, Z. A., 1983:** Properties of the major outer membrane protein from *Neisseria gonorrhoeae* incorporated into model lipid membranes. *Proc. Natl. Acad. Sci. USA*, 80, 3831—3835.
45. **Zachariae, U., Klühspies, T., De, S., Engelhardt, H., Zeth, K., 2006:** High resolution crystal structures and molecular dynamics studies reveal substrate binding in the porin Omp32. *J. Biol. Chem.*, 281, 7413—7420.
46. **Zeth, K., Diederichs, K., Welte, W., Engelhardt, H., 2000:** Crystal structure of Omp32, the anion-selective porin from *Comamonas acidovorans*, in complex with a periplasmic peptide at 2.1 Å resolution. *Structure*, 8, 981—992.

Received December 4, 2017

Accepted January 26, 2018



## PERMEABILITY OF THE BLOOD-BRAIN BARRIER AND TRANSPORT OF NANOBODIES ACROSS THE BLOOD-BRAIN BARRIER

Širochmanová, I.<sup>1</sup>, Čomor, E.<sup>1</sup>, Káňová, E.<sup>1</sup>, Jiménez-Munguía, I.<sup>1</sup>  
Tkáčová, Z.<sup>1</sup>, Bhide, M.<sup>1,2</sup>

<sup>1</sup>Laboratory of Biomedical Microbiology and Immunology  
University of Veterinary Medicine and Pharmacy, Košice

<sup>2</sup>Institute of Neuroimmunology, Slovak Academy of Sciences, Bratislava  
Slovakia

sirochmanova.ivana@gmail.com

### ABSTRACT

The presence of a blood-brain barrier (BBB) and a blood-cerebrospinal fluid barrier presents an immense challenge for effective delivery of therapeutics to the central nervous system. Many potential drugs, which are effective at their site of action, have failed due to the lack of distribution in sufficient quantity to the central nervous system (CNS). In consequence, many diseases of the central nervous system remain undertreated. Antibodies, IgG for example, are difficult to deliver to the CNS due to their size (~155 kDa), physico-chemical properties and the presence of Fc receptor on the blood-brain barrier. Smaller antibodies, like the recently developed nanobodies, may overcome the obstacle of the BBB and enter into the CNS. The nanobodies are the smallest available antigen-binding fragments harbouring the full antigen-binding capacity of conventional antibodies. They represent a new generation of therapeutics with exceptional properties, such as: recognition of unique epitopes, target specificity, high affinity, high solubility, high stability and high expression yields in cost-effective recombinant

production. Their ability to permeate across the BBB makes them a promising alternative for central nervous system disease therapeutics. In this review, we have systematically presented different aspects of the BBB, drug delivery mechanisms employed to cross the BBB, and finally nanobodies — a potential therapeutic molecule against neuroinfections.

**Key words:** blood-brain barrier; carrier; nanobody; permeability; shuttle; transport

### Barriers of the brain

Signalling within the central nervous system (CNS) is carried out by neurons that communicate with each other using a combination of chemical and electrical signals. For reliable neural signalling, regulation of the ionic microenvironment is critical [2]. There are three major interfaces (barriers) in the brain and spinal cord of mammals that keep the microenvironment stable (homeostasis) [3]. The principal barrier sites between blood and brain are listed below:

- A) The blood-brain barrier (BBB) is created by tight junction (TJ) formation at the level of the cerebral capillary endothelial cells. It is by far the largest surface area for blood — CNS exchange, and it covers between 12 and 18 m<sup>2</sup> in an average human adult [36]. No brain cell lies further than about 25 μm from a capillary, so once the solutes or drugs cross the BBB, diffusion distances to neurons and glial cell bodies are short. For that reason, drugs with the ability to cross the BBB are currently the most used method for global delivery of drugs to all brain cells.
- B) The blood-cerebrospinal fluid barrier (BCSFB) located at the choroid plexuses in the lateral, third and fourth ventricles of the brain.
- C) The arachnoid barrier enveloping the brain, which is avascular and lying under the dura.

A combination of physical barrier (TJs between cells reducing flux), transport barrier (specific transport barrier mediating solute flux) and metabolic barrier (enzymes metabolizing molecules in transit) represents the function of the barrier at all three interfaces. Modulation and regulation of the barrier function is possible both physiologically and pathologically [4].

### The blood-brain barrier in brief

A close inductive association of several cell types, especially the end feet of astrocytic glial cells, maintain the differentiation of the endothelium into a barrier layer [4, 49]. The supporting roles in barrier induction, maintenance and function are performed by pericytes, microglia and neural terminals, which are also closely associated with the endothelium [4, 37]. The hyperaemia of brain is accomplished by a group of cells, closely related to each other, called the neurovascular unit (NVU). The NVU is composed of neurons, astrocytes, endothelial cells of the BBB, myocytes, pericytes and extracellular matrix components [32].

The role of TJs (zonulae occludentes) is a significant reduction of the permeation of ions and polar solutes, primary to maintain the ionic homeostasis in the brain. This permeation is carried through paracellular diffusional pathways between the endothelial cells from the blood plasma to the brain extracellular fluid [7, 49].

TJs consist of a complex of proteins spreading across the intercellular cleft, such as occludin and claudins, and junctional adhesion molecules (JAM) [48, 49]. Cytoplasmic scaffolding and regulatory proteins ZO-1, ZO-2, ZO-3

link the junctional molecules occludin and claudins to intracellular actin and the cytoskeleton via cingulin [31, 48, 49]. As Abbott and colleagues [3] reviewed, the disappearance of either claudin-3 or claudin-5 from the tight junctional complexes might result in a compromised BBB.

Adherent junctions (AJs) and TJs are part of the junctional complexes between endothelial cells. In AJs, cadherin proteins spread across the intercellular cleft and are linked into the cell cytoplasm by alpha, beta and gamma scaffolding proteins. The AJs give structural support to the tissue by holding the cells together, and are essential for formation of TJs. The disruption of AJs gradually leads to the disruption of the barrier [48].

### Permeability of the BBB

As Saunders et al. [44] reviewed, several studies observed that parenteral injections of trypan blue and other acidic dyes in animal models stained almost all tissues except the brain. These experiments were followed by subsequent studies, which were using embryos or the newborn of various species. Most of them gave the same result as in adults, whereas most of the brain was not stained aside from the circumventricular organs, which led to the concept of the brain being protected by the BBB. Despite similar results both in embryos and adults, it is still widely believed that the BBB is immature and poorly formed in embryos, foetus and the newborn, leaving the developing brain more vulnerable to drugs or toxins entering the foetal circulation from the mother. However, new evidence shows that many adult mechanisms, such as functionally effective TJs, are present in the embryonic brain. Furthermore, some transporters are even more active during development than in the adult.

The TJs block the penetration of macromolecules by restriction of paracellular diffusional pathways between the endothelial cells to ions and other polar solutes. The restriction of ion movement results in the high *in vivo* electrical resistance of the BBB, which is estimated to be 8000 Ω cm<sup>2</sup> [45]. The BBB keeps optimal ionic composition for synaptic signalling function by a combination of specific ion channels and transporters, and thus provides a stable environment for the function of neurons [4, 10]. Since the central and peripheral nervous system both use many of the same neurotransmitters, separating the neurotransmitter pools controls “cross-talk” interference between the two signalling networks [1]. As a typical example serves gluta-

mate, a neuroexcitatory amino acid which blood plasma levels significantly fluctuate after the ingestion of food [4, 10]. Similar to neurotransmitter levels, the protein content in the cerebrospinal fluid (CSF) is much lower than that of the plasma, with a different protein composition. Plasma proteins such as albumin, plasminogen or prothrombin are damaging to neural tissue, which in the final analysis can lead to apoptosis [23, 35]. If the BBB is damaged, these large serum proteins are able to leak into the brain and can cause serious pathological consequences.

The BBB also contributes to the brain homeostasis by protecting the CNS from various neurotoxic substances circulating in the blood, such as endogenous metabolites, xenobiotics or exogenous substances otherwise acquired from the environment. The level of neurogenesis is relatively low compared to the continuous steady rate of neuronal cell death throughout life, therefore any acceleration in the natural rate of cell death resulting from an increased access of neurotoxins into the brain would become prematurely impairing [27].

The neural tissue requires a low passive permeability of the BBB to many essential water-soluble nutrients and metabolites, while lipid soluble substances are able to cross the barrier passively by diffusion. Therefore, to ensure an adequate supply of water soluble substances, specific transport systems are expressed in the BBB [4, 49]. In addition to the unidirectional and bidirectional transport of small molecules, some substances are able to enter the brain tissue from the blood by other ways, e.g. facilitated diffusion (glucose via GLUT-1) or a receptor-mediated endocytosis (transferrin or insulin) [25].

### Changes in BBB permeability

The BBB as a dynamic system, is capable of responding to local changes and requirements. Its regulation serves for the adjustment of nutrient supply, protection from circulating agents, or modification to ease local repairs [4]. A number of mechanisms and cell types are able to regulate the BBB in both physiological and pathological conditions. For example, apical cell-cell junction interactions participate in the regulation of gene expression, cell proliferation, polarity and apoptosis using different types of proteins. The TJs are one type of such cell-cell junctions and associate with several signalling complexes. Expression of TJ components allows cell differentiation by suppressing proliferation. These components affect several signalling and tran-

scriptional pathways, and changes in the expression of TJ proteins are associated with several disease conditions. The aforesaid regulation includes changes in the function of TJs [6], and in the expression and activity of many transporters and enzymes [4, 17]. It appears that intracellular scaffold proteins ZO-1, ZO-2 and ZO-3 regulate the effectiveness of the TJs [48, 49]. Furthermore, many of the cell types associated with brain microvessels, such as astrocytes and microglia, release cytokines and vasoactive agents, which can modify the TJ assembly and barrier permeability [4, 41]. Also, alterations in both intracellular and extracellular calcium concentration can modulate the electrical resistance across the cell layer, thus modifying the effectiveness of the TJs as a barrier. A rise in intracellular calcium may initiate activation of the actin cytoskeleton and may change the configuration of claudins and occludin [3].

### Physiological ways of transport across the BBB

There are several potential routes for permeation across the BBB. The majority of large blood-borne molecules are physically prevented from entering the brain by the presence of the BBB and TJs. To ensure the supply of essential substances into the brain, there are specific and some non-specific transcytotic mechanisms used. Transport of macromolecules across the BBB *via* transcytosis allows solutes with large molecular weight, such as proteins and peptides, to enter the CNS intact. Transcytosis may be either receptor-mediated (RMT) or adsorptive-mediated (AMT) [3].

The BBB endothelium must contain a number of specific solute carriers (transporters) to supply the CNS with essential polar substances, such as amino acids and glucose necessary for metabolism. When penetration of the BBB is considered, bases which carry a positive charge have an advantage over acids. It is probably caused by the cationic nature of these molecules, and their interaction with the negatively charged glycocalyx and phospholipid head groups of the outer leaflet of the cell membrane that ease their entry [3]. Many polar essential molecules such as glucose, amino acids and nucleosides are transported by carrier mediated influx via solute carriers (SLCs), which may be passive, or active. Active transport is further differentiated to primarily active (energy is derived directly from the breakdown of ATP) or secondarily active (energy comes from the electrochemical gradient created by pumping ions out of the cell) [3]. The solute carriers may be unidirectional either into or out of the cell, bi-directional, they may involve an exchange

of one substrate for another, or be driven by an ionic gradient. In the last case, the direction of transport is reversible depending upon the electrochemical gradient [3].

A large spectrum of lipid-soluble molecules are able to passively diffuse through the BBB and enter the brain [28]. There is a general interrelation between the rate at which a solute enters the CNS and its lipid solubility. It is usually defined as a distribution coefficient expressed in terms of  $\log D$  ( $\log D$  octanol/buffer partition coefficient at pH 7.4) [14]. These passively penetrating solutes are captured by ATP-binding cassette (ABC) transporters, multidomain integral membrane proteins, and translocated across the endothelial cells. Some of the more important ABC transporters are Pgp (transporter P-glycoprotein) and BCRP (breast cancer resistance protein), which are placed in the luminal membrane of the BBB endothelium, and MRP (Multidrug resistance-associated protein) placed in either luminal or abluminal membranes [8, 9].

The movement of the blood gases, oxygen and carbon dioxide, across the BBB is diffusive as well, and the dissolved gases move down their concentration gradients [3].

Mononuclear cells appear to be able to penetrate directly through the cytoplasm of the endothelial cells by a process of diapedesis, which enables them to cross the BBB without disruption of TJs [19, 50]. During diapedesis, the fluid-filled channel through the cell is never created. The leukocyte enters the endothelial cell with the luminal membrane closing over it before it creates an opening in the abluminal membrane [12, 50].

### **Nanobodies**

Antibodies or immunoglobulins are glycoproteins produced by B-cells, which play a central role in the host immune defense. Conventional antibodies are multimers of heavy (H) and light (L) chains, each chain consisting of constant (C) and variable (V) domains [28, 40]. In a conventional antibody, the variable region of the heavy chain (VH) and the variable region of the light chain (VL) combine to make the antigen binding site, although it was discovered that the heavy chain alone can also bind antigens [46].

Immunoglobulin G fragmented by proteolytic enzyme papain produce 3 fragments of similar molecular weight (50 kDa), but of different charge. Two out of three fragments are identical and keep their antigen binding ability, which is why they are called fragments of antigen-binding

(Fab). The third fragment does not bind the antigen and crystallizes, therefore it's called fragment crystallisable (Fc) [18, 38].

Since the constant domains of antibodies are not involved in the recognition of antigen, a range of smaller antibody fragments such as Fab, F(ab')<sub>2</sub>, Fv and scFv have been designed. In comparison with the conventional antibodies, smaller antibody formats are more cost-effective to produce, have a faster organ clearance [30, 51], penetrate the solid tumours more efficiently [53], and are more suitable for structural analysis [29, 42].

In the early 1990s it was discovered that the antibody repertoire of camelids contains antibodies consisting of heavy chains only, which are referred to as heavy-chain antibodies (HCABs) [24]. Despite the absence of light chains in camelid HCABs, these antibodies display an extensive antigen-binding repertoire and their binding affinities for their cognate antigens are comparable to conventional antibodies. Structurally, the antigen-binding domains of camelid HCABs are composed of the antigen-binding variable domain termed VHH (variable domain of the HCABs), followed by a hinge region and two constant domains CH2 and CH3, while the CH1 domain known from conventional antibodies is missing [24]. With approximately 15 kDa VHHs are the smallest naturally derived antigen-binding antibody fragments. Recombinantly produced VHH fragments are also called "nanobodies" [34]. The advantages of nanobodies include: small size (2.5 nm in diameter and about 4 nm height), recognition of unique epitopes, high affinity, high solubility, high stability, and high expression yields in heterologous expression systems [15, 22].

As Ghassabeh et al. [22] reviewed, HCABs have also been described in humans as a pathological disorder termed "heavy chain disease." However, these human HCABs devoid of light chain fail to bind antigen, and are consequently non-functional. Camelid HcABs, on the other side, have evolved to be fully functional even in the absence of light chains, while harbouring the full antigen-binding capacity of the conventional antibodies.

### **Transport of nanobodies across the BBB**

The BBB is only permeable to lipophilic molecules of up to 400 Da in size [39], therefore conventional antibodies are unable to spontaneously cross, given their average size is approximately 155 kDa [13]. The delivery of conventional antibodies to the brain is especially tiresome, due to

Fc-receptor mediated efflux to the blood [16], thus nanobodies lacking an Fc-part represent a promising alternative to brain targeting antibodies. Therapeutic application of nanobodies to CNS is difficult because the BBB restrain the delivery of intravenously injected nanobodies to the brain. Various strategies have been developed and tested to overcome the BBB; for example, antibodies against receptors that undergo transcytosis across the BBB have been used as vectors to target drugs or therapeutic peptides into the brain [5].

In a therapeutic experiment using the Hargreaves model of inflammatory pain (injection of inflammatory agents into the rat or mouse hind paw), Farrington et al. [20] tested the ability of FC5 nanobodies as a drug deliverer. It was shown that FC5 conjugated with opioid peptide Dal could be deployed as a drug delivery shuttle *in vivo* to induce a significant analgesic response in contrast to unconjugated Dal peptide. The FC5 is a nanobody, which selectively recognizes human cerebrovascular endothelial cells (HCEC) and transmigrates across them *in vitro* and across the BBB *in vivo* [33]. The same group later suggested that FC5 binds to a putative  $\alpha$  (2,3)-sialoglycoprotein receptor (Fig. 1A) and is transcytosed *via* clathrin vesicles [5]. The potential of the nanobody FC5 as a shuttling-

nanobody can be used to transfer other therapeutics, e.g. proteins or therapeutic nanobodies through the BBB [43].

Receptor-mediated transcytosis for brain targeting was utilized also by Wang et al. [47]. They showed that a fusion complex of a peptide derived from apolipoprotein E and a model therapeutic protein ( $\alpha$ -L-iduronidase) could be transferred to the brain via binding to the LDL receptor expressed on cells of the BBB. Apolipoprotein E (ApoE) binds to low density lipoprotein receptor-related protein 1 (LRP1) (Fig. 1B) inducing transcytosis, which can be used as a shuttle for therapeutic nanobodies in the future [43].

Another research group studied the transferrin receptor and the insulin receptor (Fig. 1C) in receptor-mediated transcytosis of small molecule drugs and therapeutic proteins [11, 52]. Both receptors can be found on the luminal membrane of brain capillary endothelial cells. These results indicate that triggering transcytosis through nanobodies targeting these receptors could also be a promising alternative to ligand-based delivery of drugs to the brain [51, 52]. Molecular Trojan horse by fusing the therapeutic proteins to the monoclonal antibodies (MAb) against human insulin or transferrin receptor have been demonstrated as an efficient strategy for the delivery of therapeutic protein to the brain [11].

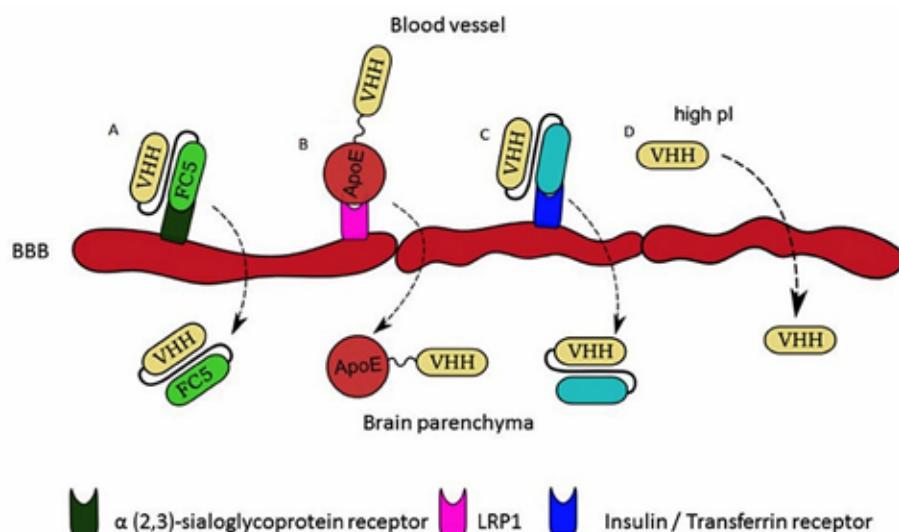


**Fig. 1. Ways of transport of nanobodies across the BBB**

- (A) Nanobody FC5 binding to  $\alpha$ (2,3)-sialoglycoprotein receptor can be used as a drug deliverer for other nanobodies;
  - (B) Transcytosis induced by the binding of Apolipoprotein E (ApoE) to low density lipoprotein receptor-related protein 1 (LRP1);
  - (C) Transcytosis triggered by nanobody against Insulin/Transferrin receptor;
  - (D) Spontaneous crossing of nanobodies with high isoelectric point through the BBB
- Source: An original drawing

Other studies reported that nanobodies with a high isoelectric point (pI)~9,5 [26, 33] spontaneously cross the BBB (Fig. 1D). Such nanobodies easily gain access to the brain and even penetrate cells and bind to intracellular proteins. In a mouse study, Li et al. [26] used a recombinant nanobody E9 (pI = 9.4) directed against glial fibrillary acidic protein (GFAP), a specific marker of astrocytes. This nanobody crossed the BBB *in vivo*, diffused into the brain tissue, and was able to bind to intracellularly expressed GFAP in astrocytes. The FC5 nanobody described above has a basic pI 9.2 which might contribute to its transcytosis into the brain parenchyma [43].

There are other possible routes of transport used in other therapeutics, which were not tested yet with nanobodies. Gaillard et al. [21] have tested the use of CRM197, a non-toxic mutant of diphtheria toxin, as a targeting vector for drug delivery to the brain. CRM197 was tested for its brain delivery potential as it has been shown to endocytose after binding the membrane-bound precursor of heparin binding epidermal growth factor-like growth factor (HB-EGF), also known as the diphtheria toxin receptor.

## CONCLUSIONS

Conventional antibodies are unable to spontaneously cross the BBB, due to the Fc-receptor mediated efflux to the blood. Because of that, novel approaches of therapy of neurodiseases or neuroinfections have been researched. Nanobodies are a promising alternative to conventional antibodies and other CNS therapeutics, given the lack of an Fc-part and recognition of unique or hidden epitopes, which gives them a possibility to succeed where conventional antibodies commonly fail. Thanks to their unique features, such as small size while preserving antigen binding capacity, the recognition of hidden epitopes and the ability to penetrate through biological barriers, they appear to be ideal candidates for therapeutic purposes. Several possible routes for nanobody translocation through the BBB have been already described and tested. Furthermore, there are other successful ways of transport of therapeutics through the BBB, which have not been tested with nanobodies yet. In addition to their therapeutic function, nanobodies can also be used as a drug delivery shuttle, given their ability to trigger a receptor-mediated transcytosis. Despite all of the advantages of the therapeutic use of nanobodies, their

translocation across the BBB and successful utilization in the treatment of neurodiseases is not yet thoroughly researched.

## ACKNOWLEDGEMENTS

*This study was supported by APVV-14-0218 and INFEK-TZOON (Center of excellence for infections in animals and zoonoses, ITMS code: 26220120002, co-financed from the European structural funds) for support of this study.*

## REFERENCES

1. **Abbott, N.J., Friedman, A., 2012:** Overview and introduction: The blood-brain barrier in health and disease. *Epilepsia*, 53, 1–6.
2. **Abbott, N.J., 1992:** Comparative physiology of the blood-brain barrier. In **Bradbury, M. W. B. (Ed.):** *Physiology and Pharmacology of the Blood-Brain Barrier*, Springer Berlin Heidelberg, 371–396.
3. **Abbott, N.J., Patabendige, A. A. K., Dolman, D. E. M., Yusof, S. R., Begley, D. J., 2010:** Structure and function of the blood-brain barrier. *Neurobiol. Dis.*, 37, 13–25.
4. **Abbott, N.J., Ronnback, L., Hansson, E., 2006:** Astrocyte-endothelial interactions at the blood-brain barrier. *Nat. Rev. Neurosci.*, 7, 41–53.
5. **Abulrob, A., Sprong, H., Van Bergen, E., Henegouwen, P., Stanimirovic, D., 2005:** The blood-brain barrier transmigration single domain antibody: Mechanisms of transport and antigenic epitopes in human brain endothelial cells. *J. Neurochem.*, 95, 1201–1214.
6. **Balda, M. S., Matter, K., 2009:** Tight junctions and the regulation of gene expression. *Biochem. Biophys. Acta*, 1788, 761–767.
7. **Begley, D. J., Brightman, M. W., 2003:** Structural and functional aspects of the blood-brain barrier. *Prog. Drug Res.*, 61, 39–78.
8. **Begley, D. J., 2004:** ABC transporters and the blood-brain barrier. *Curr. Pharm. Des.*, 10, 1295–1312.
9. **Begley, D. J., 2004:** Delivery of therapeutic agents to the central nervous system: the problems and the possibilities. *Pharmacol. Ther.*, 104, 29–45.
10. **Bernacki, J., Dobrowolska, A., Nierwinska, K., Malecki, A., 2008:** Physiology and pharmacological role of the blood-brain barrier. *Pharmacol. Rep.*, 60, 600–622.

11. **Boado, R. J., Hui, E. K. W., Lu, J. Z., Pardridge, W. M., 2012:** Glycemic control and chronic dosing of Rhesus monkeys with a fusion protein of iduronidase and a monoclonal antibody against the human insulin receptor. *Drug Metabolism and Disposition*, 40, 2021—2025.
12. **Carman, C. V., Springer, T. A., 2008:** Trans-cellular migration: cell-cell contacts get intimate. *Current Opinion in Cell Biology*, 20, 533—540.
13. **Charles, A. Janeway, J., Travers, P., Walport, M., Shlomchik, M. J., 2001:** The structure of a typical antibody molecule. In *Immunobiology, the Immune System in Health and Disease*, 5th edition., Garland Science Publishing, New York, 600 pp.
14. **Clark, D. E., 2003:** In silico prediction of blood-brain barrier permeation. *Drug Discovery Today*, 8, 927—933.
15. **Comor, L., Dolinska, S., Bhide, K., Pulzova, L., Jiménez-Munguía, I., Bencurova, E., et al., 2017:** Joining the *in vitro* immunization of alpaca lymphocytes and phage display: rapid and cost effective pipeline for sdAb synthesis. *Microb. Cell Fact.*, 16,
16. **Cooper, P. R., Ciambrone, G. J., Kliwinski, C. M., Maze, E., Johnson, L., et al., 2013:** Efflux of monoclonal antibodies from rat brain by neonatal Fc receptor. *Brain Res.*, 1534, 13—21.
17. **Dauchy, S., Miller, F., Couraud, P. O., Weaver, R. J., Weksler, B., Romero, I. A., et al., 2009:** Expression and transcriptional regulation of ABC transporters and cytochromes P450 in hCMEC/D3 human cerebral microvascular endothelial cells. *Biochem. Pharmacol.*, 77, 897—909.
18. **Elgert, K. D., 2009:** *Immunology: Understanding the immune system*, 2nd edn., Wiley-Blackwell, New Jersey, 726.
19. **Engelhardt, B., Wolburg, H., 2004:** Mini-review: Transendothelial migration of leukocytes: through the front door or around the side of the house? *Eur. J. Immunol.*, 34, 2955—2963.
20. **Farrington, G. K., Caram-Salas, N., Haqqani, A. S., Brunette, E., Eldredge, J., Pepinsky, B., et al., 2014:** A novel platform for engineering blood-brain barrier-crossing bispecific biologics. *FASEB J.*, 28, 4764—4778.
21. **Gaillard, P. J., Brink, A., de Boer, A. G., 2005:** Diphtheria toxin receptor-targeted brain drug delivery. *Int. Congr. Ser.*, 1277, 185—198.
22. **Ghassabeh, G. H., Muyldermans, S., Saerens, D., 2010:** Nanobodies, single-domain antigen-binding fragments of camelid heavy-chain antibodies. In **Shire, S. J., Gombotz, W., Bechtold-Peters, K., Andya, J. (Eds.):** *Current Trends in Monoclonal Antibody Development and Manufacturing*. Springer New York, 29—48.
23. **Gingrich, M. B., Traynelis, S. F., 2000:** Serine proteases and brain damage - is there a link? *Trends Neurosci.*, 23, 399—407.
24. **Hamers-Casterman, C., Atarhouch, T., Muyldermans, S., Robinson, G., Hammers, C., Bajyana Songa, E., et al., 1993:** Naturally occurring antibodies devoid of light chains. *Nature*, 363, 446—8.
25. **Jain, K. K., 2012:** Nanobiotechnology-based strategies for crossing the blood-brain barrier. *Nanomedicine*, 7, 1225—1233.
26. **Li, T., Bourgeois, J. P., Celli, S., Glacial, F., Le Sourd, A. M., Mecheri, S., et al., 2012:** Cell-penetrating anti-GFAP VHH and corresponding fluorescent fusion protein VHH-GFP spontaneously cross the blood-brain barrier and specifically recognize astrocytes: application to brain imaging. *FASEB J.*, 26, 3969—3979.
27. **Lim, D. A., Huang, Y.-C., Alvarez-Buylla, A., 2007:** The adult neural stem cell niche: lessons for future neural cell replacement strategies. *Neurosurg. Clin. N. Am.*, 18, 81—92, ix.
28. **Liu, X., Tu, M., Kelly, R. S., Chen, C., Smith, B. J., 2004:** Development of a computational approach to predict blood-brain barrier permeability. *Drug Metab. Dispos.*, 32, 132—139.
29. **McManus, S., Riechmann, L., 1991:** Use of 2D NMR, protein engineering, and molecular modelling to study the hapten-binding site of an antibody Fv fragment against 2-phenyloxazolone. *Biochemistry*, 30, 5851—5857.
30. **Milenic, D. E., Yokota, T., Filipula, D. R., Finkelman, A. J., Dodd, S. W., Wood, J. F., et al., 1991:** Construction, binding properties, metabolism, and tumour targeting of a single-chain Fv derived from the pancarcinoma monoclonal antibody CC49. *Cancer Res.*, 51, 6363—6371.
31. **Mitic, L. L., Van Itallie, C. M., Anderson, J. M., 2000:** Molecular physiology and pathophysiology of tight junctions I. Tight junction structure and function: lessons from mutant animals and proteins. *Am. J. Physiol. Gastrointest. Liver Physiol.*, 279, G250—254.
32. **Muoio, V., Persson, P. B., Sendeski, M. M., 2014:** The neurovascular unit - concept review. *Acta Physiol.*, 210, 790—798.
33. **Muruganandam, A., Tanha, J., Narang, S., Stanimirovic, D., 2002:** Selection of phage-displayed llama single-domain antibodies that transmigrate across human blood-brain barrier endothelium. *FASEB J.*, 16, 240—242.
34. **Muyldermans, S., 2013:** Nanobodies: natural single-domain antibodies. *Annu. Rev. Biochem.*, 82, 775—797.
35. **Nadal, A., Fuentes, E., Pastor, J., McNaughton, P. A., 1995:** Plasma albumin is a potent trigger of calcium signals and DNA synthesis in astrocytes. *Proc. Natl. Acad. Sci. USA*, 92, 1426—1430.

36. Nag, S., Begley, D. J., 2005: Blood brain barrier, exchange of metabolites and gases. In Kalimo, H. (Ed.): *Pathology and Genetics: Cerebrovascular Diseases*. ISN Neuropath. Press, 22—29.
37. Nakagawa, S., Deli, M. A., Kawaguchi, H., Shimizudani, T., Shimono, T., Kittel, A., et al., 2009: A new blood-brain barrier model using primary rat brain endothelial cells, pericytes and astrocytes. *Neurochem. Int.*, 54, 253—263.
38. Padlan, E. A., 1994: Anatomy of the antibody molecule. *Mol. Immunol.*, 31, 169—217.
39. Pardridge, W. M., 2012: Drug transport across the blood-brain barrier. *J. Cereb. Blood Flow Metab.*, 32, 1959—1972.
40. Porter, R. R., 1973: Structural studies of immunoglobulins. *Science*, 180, 713—716.
41. Rennels, M. L., Gregory, T. F., Fujimoto, K., 1983: Innervation of capillaries by local neurons in the cat hypothalamus: A light microscopic study with horseradish peroxidase. *J. Cereb. Blood Flow Metab.*, 3, 535—542.
42. Riechmann, L., Cavanagh, J., McManus, S., 1991: Uniform labelling of a recombinant antibody Fv-fragment with <sup>15</sup>N and <sup>13</sup>C for heteronuclear NMR spectroscopy. *FEBS Lett.*, 287, 185—188.
43. Rissiek, B., Koch-Nolte, F., Magnus, T., 2014: Nanobodies as modulators of inflammation: potential applications for acute brain injury. *Front. Cell. Neurosci.*, 8, 344.
44. Saunders, N. R., Liddelow, S. A., Dziegielewska, K. M., 2012: Barrier mechanisms in the developing brain. *Front. Pharmacol.*, 3, 46.
45. Smith, Q. R., Rapoport, S. I., 1986: Cerebrovascular permeability coefficients to sodium, potassium, and chloride. *J. Neurochem.*, 46, 1732—42.
46. Utsumi, S., Karush, F., 1964: The subunits of purified rabbit antibody. *Biochemistry*, 3, 1329—1338.
47. Wang, D., El-Amouri, S. S., Dai, M., Kuan, C. Y., Hui, D. Y., Brady, R. O., et al., 2013: Engineering a lysosomal enzyme with a derivative of receptor-binding domain of apoE enables delivery across the blood-brain barrier. *Proc. Natl. Acad. Sci. USA*, 110, 2999—3004.
48. Wolburg, H., Lippoldt, A., 2002: Tight junctions of the blood-brain barrier: development, composition and regulation. *Vascul. Pharmacol.*, 38, 323—337.
49. Wolburg, H., Noell, S., Mack, A., Wolburg-Buchholz, K., Fallier-Becker, P., 2009: Brain endothelial cells and the gliovascular complex. *Cell Tissue Res.*, 335, 75—96.
50. Wolburg, H., Wolburg-Buchholz, K., Engelhardt, B., 2005: Diapedesis of mononuclear cells across cerebral venules during experimental autoimmune encephalomyelitis leaves tight junctions intact. *Acta Neuropathol.*, 109, 181—190.
51. Wu, A. M., Senter, P. D., 2005: Arming antibodies: prospects and challenges for immunoconjugates. *Nat. Biotechnol.*, 23, 1137—1146.
52. Xiao, G., Gan, L.-S., 2013: Receptor-mediated endocytosis and brain delivery of therapeutic biologics. *Int. J. Cell Biol.*, 2013, 14.
53. Yokota, T., Milenic, D. E., Whitlow, M., Schlom, J., 1992: Rapid tumor penetration of a single-chain Fv and comparison with other immunoglobulin forms. *Cancer Res.*, 52, 3402—3408.

Received December 4, 2017

Accepted January 26, 2018



## CONTRIBUTION OF PILI OF *S. PNEUMONIAE* IN THE ONSET OF MENINGITIS

Jiménez-Munguía, I.<sup>1</sup>, Pulzová, L.<sup>1</sup>, Bhide, K.<sup>1</sup>, Čomor, Ľ.<sup>1</sup>, Káňová, E.<sup>1</sup>  
Tomečková, Z.<sup>1</sup>; Širochmanová, I.<sup>1</sup>, Bhide, M.<sup>1,2</sup>

<sup>1</sup>Laboratory of Biomedical Microbiology and Immunology  
University of Veterinary Medicine and Pharmacy, Kosice

<sup>2</sup>Institute of Neuroimmunology of the Slovak Academy of Science, Bratislava,  
Slovakia

sire.jm@hotmail.com

### ABSTRACT

**Bacterial meningitis is a devastating worldwide disease. Half of the survivors of meningitis remain with permanent neurological sequelae. The pathogenesis of meningitis is based on a complex host-pathogen interaction. *Streptococcus pneumoniae* is a life-threatening neuroinvasive pathogen that asymptotically colonizes the upper respiratory tract. Adherence of pneumococci to the host epithelium is a prerequisite in the onset of streptococcal infections; such adherence is favored by the formation of bacterial pili. In this article, we will describe the pneumococcal pili and its contribution to the onset of meningitis.**

**Key words:** meningitis; pili; *S. pneumoniae*

### INTRODUCTION

*Streptococcus pneumoniae* is a Gram-positive bacteria and one of the most common etiological agents of bacte-

rial meningitis which is associated with high mortality and morbidity [30]. Pneumococci asymptotically colonize the human nasopharynx in up to 40% of adults [19]. The infectivity of this pathogen and the development of protective immunity is poorly described in the current literature [25]. Meningitis-causing *S. pneumoniae* possess a set of antigenic structures, such as the cell wall components (i. e. teichoic acids, surface-associated proteins, adhesins and pili) that contribute to the bacterial invasion of the host epithelial lining [15].

In order to secure attachment on to host tissues, *S. pneumoniae* use adhesins normally located on its surface or at the end of long hair-like structures called pili [26]. Some strains of this pathogenic bacteria form pili, which play a role in biofilm formation, a characteristic life-style of the bacteria constituting the oral flora and are involved in primary colonization [5]. Pili are encoded within pathogenicity islands and differ among Gram-positive and Gram-negative bacteria. In the case of Gram-positive bacteria, protein subunits are covalently linked, chaperons are not required for assembly and tlp protein is not needed to initiate the formation of the pilus structure [26].

## Pili of Gram-positive bacteria

Pili are long proteinaceous structures implicated in many functions such as adhesion to host cells, biofilm formation, DNA uptake and immune evasion. These structures were identified for the first time in the Gram-positive bacteria *Corynebacterium diphtheria*, and later in many others, such as *S. pneumoniae* [5]. The pili of Gram-positive bacteria are made of covalently linked pilins forming a string of beads of approximately 3 nm in diameter and various lengths ranging from 0.1 to 5 μm, although individual single pili of 9.5 nm diameter have been observed from cryo-EM on *S. pneumoniae* TIGR4 preparations [10].

The cell wall of Gram-positive bacteria is a surface structure, which promotes interactions with its environment and provides physical cell integrity [17]. The forma-

tion of pili initiates at the plasma membrane in which the transpeptidase enzymes are located, and continues to the cell wall, where proteins are anchored to form hair-like structures. Via transpeptidation, sortases A, B, D and E anchor surface proteins to the cell wall by recognizing the conserved C-terminal LPxTG motif, meanwhile sortase C links proteins for the pili assembly (Figure 1)[5]. Cell wall decorators (i.e. all the chemical structures attached to the cell wall such as proteins) provide bacterial envelopes with species- and strain-specific properties. All of these structures, including the bacterial pili, contribute to bacterial virulence, or favor interactions with the host immune systems [17]. Specifically, the pili of *S. pneumoniae* becomes a key element that perform multiple functions during bacterial life cycles, such as host cell invasion, biofilm forma-

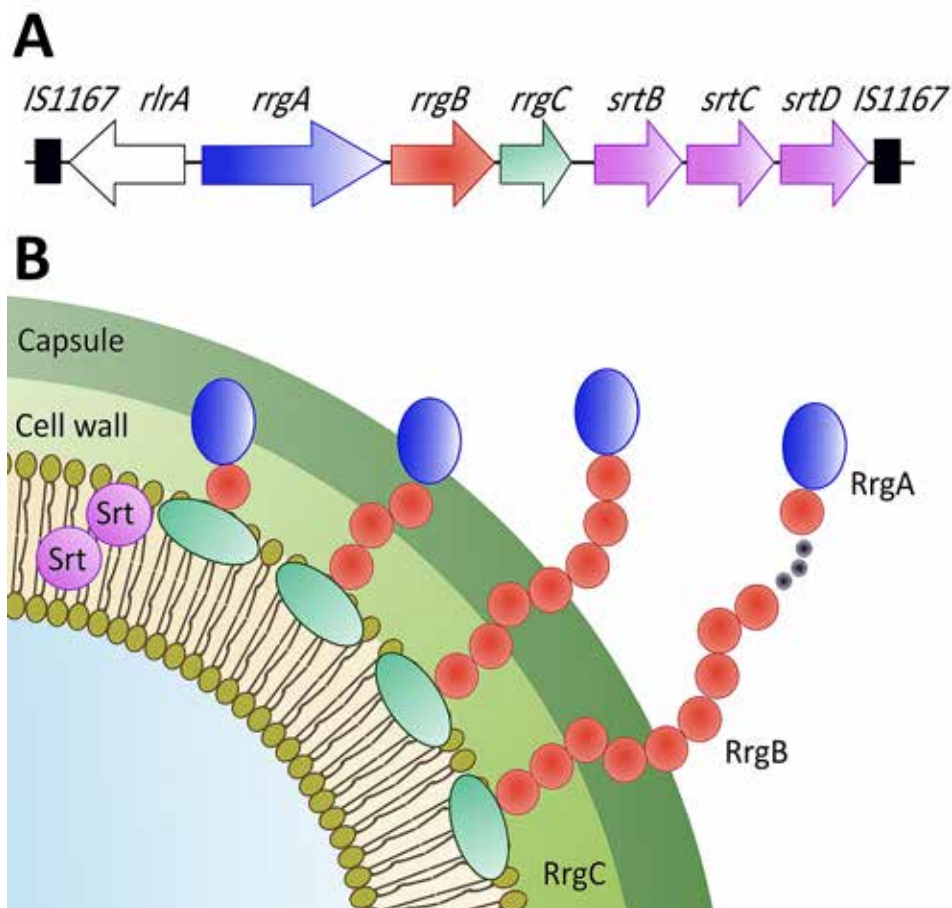


**Fig. 1.** Pili of *S. pneumoniae*

A) Organization of gene clusters encoding pili in the pathogenic strain *S. pneumoniae* TIGR4. Encoding genes for the following proteins are represented as arrows: sortases (violet), major pilin protein RrgB (orange), minor pilin proteins RrgA (blue) and RrgC (green). White arrow represents gene flanking the cluster; B) Biogenesis of pili of *S. pneumoniae* TIGR4. Sortases (green circles), located in the plasma membrane are responsible for anchoring pili to the cell wall. Anchor adhesin RrgC is shown as green oval, major pilin subunit RrgB is coloured in orange and minor adhesion RrgA is located in the tip of pili (blue oval). Figure adapted from Hilleringmann et al., 2009; Scott, Zähler, 2006 [26, 11]

tion, cell aggregation, DNA transfer and twitching motility [11].

### **Assembly of pilus in *Streptococcus pneumoniae***

*S. pneumoniae* produces pili protruding from the bacterial cell surface. This structure is not always visible in all the cells from the same population [3]. Pili are composed of covalently linked pilin subunits. Each subunit has a LPxTG motif required for the covalent attachment to other pilin subunits and it is thought to ultimately be linked to the cell wall peptidoglycan by the housekeeping sortase A [1]. The sortase recognition motif LPxTG is included in the cell wall sorting signal (CWSS) region, together with a transmembrane anchor and a positively charged cytoplasmic tail [8]. The sortase-mediated pilus assembly was first demonstrated in *C. diphtheria*. The pilus assembly is performed on the bacterial surface once pilins are secreted across the plasma membrane via the Sec-dependent pathway. The nascent pilins are anchored in the membrane by its hydrophobic domain of the CWSS [5]. Transpeptidase enzymes responsible to link pilin subunits in *S. pneumoniae* are the sortases SrtC-1, SrtC-2, and SrtC-3 [8]. The pilus backbone is formed in a head-to-tail manner by the polymerization of the backbone pilin subunits, in which a lysine of the pilin motif of one subunit forms a covalent isopeptide bond with a threonine residue in the LPxTG of the next subunit.

The last step is carried out by the sortase A, in which the mature filament is covalently linked to the peptidoglycan precursor lipid II, leading to the covalent attachment of the pilus to the cell wall. Additionally, one or two accessory pilins are integrated into individual pili. Minor pilin 1 containing the LPxTG motif are first integrated into the pilus, serving as pilus polymerization initiators and they are preferentially located at the pilus tip; meanwhile the Minor pilin 2 is often found at the base of the pilus and serves as an anchor [5].

### **Structure of pili of *Streptococcus pneumoniae***

*S. pneumoniae* expresses two types of pili. Pilus-1, encoded by pilus islet 1, is composed of a backbone subunit RrgB and two ancillary proteins, RrgA and RrgC (Figure 1). Pilus-2 is encoded by the pilus islet 2 and is composed of a pitB backbone subunit [1, 11]. The genes required for pilus production are located in a 12 Kb pathogenicity island (the rlrA islet) [27]. The pilus-1 expressed by *S. pneumoniae* is composed of one major (RrgB) and two minor (RrgA

and RrgC) structural proteins. Filaments are formed by a single string of RrgB monomers, which are elongated with RrgA and RrgC according to their putative roles as adhesion and anchor to the cell wall surface, respectively (Figure 1) [10]. Moreover, a genomic region of *S. pneumoniae* codes for a second functional pilus. This region is composed of five genes, two of them coding for putative LPxTG-type surface-anchored proteins (pitB and pitA), the latter containing a stop codon, one gene encoding a signal peptidase-related product (sipA), and two genes coding products displaying similarity to sortases (srtG1 and srtG2) [1]. PitB is suggested to be the most probable backbone of the fimbria containing stabilizing intramolecular isopeptide bonds and PitA, a putative ancillary protein [31].

### **Biological functions of bacterial pili**

Bacterial pili are considered as surface-exposed virulence factors [14]. These structures appear crucial for the initiation of bacterial colonization inside the host and are involved in adhesion, recognition of host cell receptors, biofilm formation and evasion from the innate immune system, all of which contribute to infection [5]. The role of pili in adherence has been demonstrated in several Gram-positive bacteria such as *C. renale* and *S. agalactiae*, which adhere to kidney or to human lung epithelial cells [7, 12]. *S. agalactiae* expresses a pili composed of three structural subunits (PilA, PilB and PilC), of which PilB is the major backbone protein; PilA is an adhesive protein located at the tip of the pilus (AP-1), and PilC (AP-2) acts as pilus anchors [7].

In regard to *S. pneumoniae*, RrgB is the shaft protein and two accessory proteins, RrgA and RrgC, act as an adhesin and anchor, respectively [11]. Both PilA and RrgA adhesins exhibit a von Willebrand adhesion domain (VWA), which is important for their cell binding properties [14]. VWA-containing proteins are widely distributed among archae, bacteria and eukaryotes [23]. This domain found in eukaryotes is involved in interactions with the extracellular matrix (ECM) [28]. Likewise, some bacterial surface proteins specifically interact with extracellular matrix components such as fibronectin, fibrinogen, collagen, and heparin-related polysaccharides [22]. Similarly, RrgA has been shown to bind in a dose-dependent manner to the ECM compounds (e.g. fibrinogen, fibronectin, laminin and collagen I) and to recognize different receptors on their target cells [10, 14]. Collagen-binding Microbial

Surface Components Recognizing Adhesive Matrix Molecule (MSCRAMMs) represents a major class of adhesins contributing to host colonization. Pilus-associated adhesins often belong to the MSCRAMMs family, suggesting the importance of pili in bacterial adhesion to the extracellular matrix [5]. It has been demonstrated that there is markedly less adherence to human respiratory epithelial cells when the gene encoding for the RrgA pilin subunit of *S. pneumoniae* TIGR4 has been deleted [21].

Concerning the biofilm formation, the 3D-biofilm structure begins with a primary attachment of the bacterial surface. Then, interactions among bacteria are strengthened by long pilus structures that contribute to an irreversible attachment. Regularly, during infections *S. pneumoniae* exists in a sessile biofilm rather than in a planktonic form, except during sepsis or meningitis [13, 22]. Specifically, it has been established the contribution of RrgA in biofilm formation once insertions into *rrgA* gene, encoding the PI-1 pilus adhesion, abrogated biofilm formation [20].

On the other hand, pili have also been related to the host immune responses modulation. Piliated strains of *S. pneumoniae* triggered higher pro-inflammatory TNF- $\alpha$  and IL-6 responses compared to the non-piliated counterpart during systemic infections. Finally, another pili-related function is the contribution to colonization. Pneumococci expressing pI-1 displayed advantages on colonization of the respiratory tract in mice after intranasal challenge in comparison to non-piliated TIGR4 mutant which had shown less virulence in the murine models of colonization, pneumonia and bacteraemia. Particularly, *S. pneumoniae* TIGR4 pilus-associated RrgA is critical for the colonization of the upper respiratory tract in mice [21].

#### **Colonization and neuroinvasion of *S. pneumoniae***

*S. pneumoniae* colonizes the nasopharynx degrading the mucus viscosity by ex-olygoidases such as neuraminidase A (NanA),  $\beta$ -galactosidase (BgaA), N-acetylglucosaminidase (StrH), and neuraminidase B (NanB), which allows the pneumococci to persist in the airways [20]. It is believed that pneumococcal meningitis is acquired via this colonization, followed by bacteraemia and invasion of the Central Nervous System (CNS) [4]. Recent studies have reported that a high degree of bacteraemia is necessary but at times may not be sufficient enough for developing meningitis. Moreover, microbial binding to microvascular endothelial cells (BMEC), and invasion in this cell type is a

prerequisite for the penetration of the blood-brain barrier (BBB). Alternatively, other routes of bacterial entry into the CNS have been associated with pneumococci. Such routes include spreading from contiguous sources of infection, or to enter into the CNS through a non-hematogenous route after intranasal inoculation in experimental animals or otitis media [9].

Pathogens causing meningitis share a common strategy to move from the mucosa into the brain through the blood stream. Many bacteria bind to extracellular matrix proteins (e.g. laminin, collagen or fibronectin), which facilitate the initial attachment preceding the actual invasion [16]. *S. pneumoniae* is thought to enter the CNS by crossing the BBB or the blood-cerebrospinal fluid (CSF) barrier by local tissue damage or by transcytosis through BMEC [6]. In order to enter the CNS, pneumococci possess an armory of virulence factors including surface proteins, polysaccharide capsule and cell wall components for invasion [16]. The capsule is a major virulence determinant due to its anti-phagocytic activity. Some surface-exposed proteins such as pneumococcal surface protein A (PspA) and C (PspC) are the best characterized as choline-binding proteins. PspA interferes with complement activation while PspC interacts with human immunoglobulin A and with the polymeric immunoglobulin receptors, showing also anti-phagocytic properties due to its capability to bind to complement C3 [18].

Pneumococci have the ability to bind to certain receptors located on the plasma membrane of epithelial and endothelial cells. This receptor-mediated binding facilitates bacterial translocation and the bacterial invasion through the human cell layers mice [21]. The binding of bacterial adhesins to specific host cell receptors may lead to a signal transduction resulting in tight bacterial attachment or internalization via host cells invasion [16]. Pneumococci could take advantage of an increased expression of cell adhesion molecules, generated during inflammation as a response of cell migration, attach to the platelet-activating factor (PAF) receptor and cross the BBB by transcellular mechanisms [24]. Once pneumococci enter the CNS, the brain's resident macrophages act as key effectors of initial innate immunity clearing the bacteria and recruiting peripheral blood cells to the site of infections [18]. Replication of pneumococci inside the subarachnoid space, simultaneously occurs with the release of bacterial products such as peptidoglycans, which are highly immunogenic and in-

crease the inflammatory response. The initial pneumococcus sensing in the CNS is performed by Toll-like 2, 4 and 9 receptors which recognize peptidoglycan, pneumolysin, and CpG in the bacterial DNA, respectively [29].

### Role of *S. pneumoniae* pili in meningitis

Pneumococcal meningitis is characterized by a high mortality rate (20–30%) due to complications derived from an excessive immune response as well as damage by the pathogen itself. These complications include brain edema, cerebral ischemia and increased intracranial pressure [16]. Expression of the pili is related with the pathogenicity of the pneumococci. Thirty percent of the *S. pneumoniae* strains, isolated from clinical environments are piliated and contain the *rlrA* genetic element [14].

The contribution of *S. pneumoniae* pili in meningitis has not been completely described. Pathogens-causing meningitis possess small size and this feature may facilitate their migration through the BBB. Pneumococci grow forming chains and sometimes they are found as individual cocci. Chain formation is thought to favor adherence to the epithelium [2]. In 2016, Iovino et al. described the advantages that pili-expressing *S. pneumoniae* possess for the brain entry; mice infected with piliated *S. pneumoniae* TIGR4 had approximately 80% more pneumococci in the brain than mice infected with a non-piliated strain. The ability to enter the brain was also evaluated using TIGR4 $\Delta$ rrgA and TIGR4 $\Delta$ rrgBC mutants, suggesting that RrgA allows bacterial binding to the BBB endothelium, and thereby promotes the entry of pneumococci into the brain. Despite whether or not *S. pneumoniae* forms either chains or biofilms in the majority of infections during meningitis, individual cells have been observed inside the brain more frequent than in the bloodstream. This fact suggests that even if the fraction of single cocci in circulation is low, they continuously seed the brain endothelium during infections [21].

### CONCLUSIONS

In conclusion, bacterial pili play different roles during infections. Meningitis caused by pathogenic bacteria such as *S. pneumoniae* have been widely studied but the detailed mechanisms about how the bacteria enter into the brain still remain unknown. Pili in Gram-positive bacteria are well characterized but their interplay with the CNS, spe-

cifically with cells from the neurovascular unit, needs to be investigated in order to decipher its contribution in the development of meningitis.

### ACKNOWLEDGEMENTS

The study was supported by APVV-14-0218 and INFEK-TZOOM (Center of excellence for infections in animals and zoonoses, ITMS code: 26220120002, co-financed from the European structural funds) for support of this study.

### REFERENCES

1. **Bagnoli, F., Moschioni, M., Donati, C., Dimitrovska, V., Ferlenghi, I., Facciotti, C., et al., 2008:** A second pilus type in *Streptococcus pneumoniae* is prevalent in emerging serotypes and mediates adhesion to host cells. *J. Bacteriol.*, 190, 5480–5492.
2. **Barichello, T., Generoso, J.S., Collodel, A., Moreira, A.P., Almeida, S.M. De., 2012:** Pathophysiology of acute meningitis caused by *Streptococcus pneumoniae* and adjunctive therapy approaches. *Arquivos de neuro-psiquiatria*, 70, 366–372. <http://www.ncbi.nlm.nih.gov/pubmed/22618789>.
3. **Barocchi, M. A., Ries, J., Zogaj, X., Hemsley, C., Albiger, B., Kanth, A., et al., 2006:** A pneumococcal pilus influences virulence and host inflammatory responses. In *Proc. Natl. Acad. Sci. USA*. 103, 2857–2862. <http://www.pubmedcentral.nih.gov/articlerender.fcgi?artid=1368962&tool=pmcentrez&rendertype=abstract> (4 March 2015).
4. **Burnaugh, A. M., Frantz, L. J. and King, S. J., 2008:** Growth of *Streptococcus pneumoniae* on human glycoconjugates is dependent upon the sequential activity of bacterial exoglycosidases. *J. Bacteriol.*, 190, 221–230.
5. **Danne, C., Dramsi, S., 2012:** Pili of Gram-positive bacteria: Roles in host colonization. *Research in Microbiology*, 163, 645–658. <http://dx.doi.org/10.1016/j.resmic.2012.10.012>.
6. **Doran, K.S., Fulde, M., Gratz, N., Kim, B.J., Nau, R., Prasadarao, N., et al., 2016:** Host-pathogen interactions in bacterial meningitis. *Acta Neuropathologica*, 131, 185–209.
7. **Dramsi, S., Caliot, E., Bonne, I., Guadagnini, S., Prévost, M. C., Kojadinovic, M., et al., 2006:** Assembly and role of pili in group B streptococci. *Molecular Microbiology*, 60, 1401–1413.
8. **El Mortaji, L., Fenel, D., Vernet, T., Di Guilmi, A.M., 2012:** Association of RrgA and RrgC into the *Streptococcus*

- pneumoniae* pilus by sortases C-2 and C-3. *Biochemistry*, 51, 342–352.
9. Gurung, M., Moon, D. C., Choi, C. W., Lee, J. H., Bae, Y. C., Kim, J., et al., 2011: *Staphylococcus aureus* produces membrane-derived vesicles that induce host cell death. *PLoS ONE*, 6, 1–8.
  10. Hilleringmann, M., Giusti, F., Baudner, B. C., Masignani, V., Covacci, A., Rappuoli, R., et al., 2008: Pneumococcal pili are composed of protofilaments exposing adhesive clusters of Rrg A. *PLoS Pathogens*, 4, e1000026.
  11. Hilleringmann, M., Ringler, P., Müller, S. A., De Angelis, G., Rappuoli, R., Ferlenghi, I., et al., 2009: Molecular architecture of *Streptococcus pneumoniae* TIGR4 pili. *The EMBO Journal*, 28, 3921–3930. <http://emboj.embopress.org/cgi/doi/10.1038/emboj.2009.360>.
  12. Honda, E., Yanagawa, R., 1978: Pili-mediated attachment of *Corynebacterium renale* to mucous membrane of urinary bladder of mice. *Am. J. Vet. Res.*, 39, 155–158.
  13. Iovino, F., Hammarlöf, D. L., Garriss, G., Brovall, S., Nanapaneni, P., Henriques-Normark, B., 2016: Pneumococcal meningitis is promoted by single cocci expressing pilus adhesin RrgA. *J. Clin. Invest.*, 126, 2821–2826.
  14. Izoré, T., Contreras-Martel, C., El Mortaji, L., Manzano, C., Terrasse, R., Vernet, T., et al., 2010: Structural basis of host cell recognition by the pilus adhesin from *Streptococcus pneumoniae*. *Structure*, 18, 106–115.
  15. Jayaraman, R., 2011: Phase variation and adaptation in bacteria: A ‘Red Queen’s Race’. *Current Science*, 100, 1163–1171.
  16. Kim, K. S., 2008: Mechanisms of microbial traversal of the blood-brain barrier. *Nature reviews. Microbiology*, 6, 625–34. <http://dx.doi.org/10.1038/nrmicro1952> (23 March 2016).
  17. Marraffini, L. A., DeDent, A. C., Schneewind, O., 2006: Sortases and the art of anchoring proteins to the envelopes of Gram-positive bacteria. *Microbiol. Mol. Biol. Rev.*, 70, 192–221. <http://mmbr.asm.org/cgi/doi/10.1128/MMBR.70.1.192-221.2006>.
  18. Meli, D. N., Christen, S., Leib, S. L., Täuber, M. G., 2002: Current concepts in the pathogenesis of meningitis caused by *Streptococcus pneumoniae*. *Cur. Opin. Infect. Dis.*, 15, 253–257. <http://www.ncbi.nlm.nih.gov/pubmed/12015459> (15 January 2016).
  19. Mook-Kanamori, B. B., Geldhoff, M., Der, T. Van, van der Poll, T. B., van de Eek, D., 2011: Pathogenesis and pathophysiology of pneumococcal meningitis. *Clin. Microbiol. Rev.*, 24, 557–591.
  20. Muñoz-Elías, E. J., Marcano, J., Camilli, A., 2008: Isolation of *Streptococcus pneumoniae* biofilm mutants and their characterization during nasopharyngeal colonization. *Infect. Immun.*, 76, 5049–5061.
  21. Nelson, A. L., Ries, J., Bagnoli, F., Dahlberg, S., Fälker, S., Rounioja, S., et al., 2007: RrgA is a pilus-associated adhesin in *Streptococcus pneumoniae*. *Mol. Microbiol.*, 66, 329–340.
  22. Oggioni, M. R., Trappetti, C., Kadioglu, A., Cassone, M., Iannelli, F., Ricci, S., et al., 2006: Switch from planktonic to sessile life: A major event in pneumococcal pathogenesis. *Mol. Microbiol.*, 61, 1196–1210.
  23. Ponting, C. P., Aravind, L., Schultz, J., Bork, P., Koonin, E. V., 1999: Eukaryotic signalling domain homologues in archaea and bacteria. Ancient ancestry and horizontal gene transfer. *J. Mol. Biol.*, 289, 729–745. <http://linkinghub.elsevier.com/retrieve/pii/S0022283699928279>.
  24. Ricci, S., Gerlini, A., Pammolli, A., Chiavolini, D., Braione, V., Tripodi, S. A., et al., 2013: Contribution of different pneumococcal virulence factors to experimental meningitis in mice. *BMC Infect. Dis.*, 13, 444. <http://www.pubmedcentral.nih.gov/articlerender.fcgi?artid=3848944&tool=pmcentrez&rendertype=abstract>.
  25. Scheld, W. M., Whitley, R. J., Marra, C. M., 2004: *Infections of the Central Nervous System*. 1st edn., Williams & Wilkins, China, 353 pp.
  26. Scott, J. R., Zähler, D., 2006: Pili with strong attachments: Gram-positive bacteria do it differently. *Mol. Microbiol.*, 62, 320–330.
  27. Spraggon, G., Koesema, E., Scarselli, M., Malito, E., Biagini, M., Norais, N., et al., 2010: Supramolecular organization of the repetitive backbone unit of the *Streptococcus pneumoniae* pilus. *PLoS ONE*, 5, e10919.
  28. Springer, T. A., 2006: Complement and the multifaceted functions of VWA and integrin I domains. *Structure*, 14, 1611–161.
  29. Tuomanen, E. I., 1996: Molecular and cellular mechanisms of pneumococcal meningitis. *Ann. NY Acad. Sci.*, 797, 42–52.
  30. Van de Beek, D., Brouwer, M., Hasbun, R., Koedel, U., Whitney, C. G., Wijdicks, E., 2016: Community-acquired bacterial meningitis. *Nat. Rev. Dis. Primers*, 2, 1–20. <http://www.nature.com/articles/nrdp201674>.
  31. Zähler, D., Gandhi, A. R., Stuchlik, O., Reed, M., Pohl, J., Stephens, D. S., 2011: Pilus backbone protein PitB of *Streptococcus pneumoniae* contains stabilizing intramolecular isopeptide bonds. *Biochem. Biophys. Res. Comm.*, 409, 526–531.

Received December 4, 2017

Accepted February 8, 2018